

PALEOBIOLOGY AND TAPHONOMY OF EXCEPTIONALLY PRESERVED PUTATIVE
MACROALGAE FROM THE EDIACARAN ZUUN-ARTS BIOTA, ZAVKHAN PROVINCE,
MONGOLIA

by

Keenan Hassell

A Thesis Submitted in
Partial Fulfillment of the
Requirements for the Degree of

Master of Science

in Geosciences

at

The University of Wisconsin-Milwaukee

May 2018

ABSTRACT

PALEOBIOLOGY AND TAPHONOMY OF EXCEPTIONALLY PRESERVED PUTATIVE MACROALGAE FROM THE EDIACARAN ZUUN-ARTS BIOTA, ZAVKHAN PROVINCE, MONGOLIA

by

Keenan Hassell

The University of Wisconsin-Milwaukee, 2018
Under the Supervision of Professor Stephen Q. Dornbos

The first unequivocal evidence of complex multicellular life appears in exceptionally preserved Ediacaran (635-541 Ma) fossil deposits. The newly discovered Ediacaran Burgess Shale-type (BST) Zuun-Arts Biota of Zavkhan Province, Mongolia, contains putative macroalgae fossils. Morphological measurements of 821 individual specimens including length, width, and branching angle obtained using ImageJ software were used to calculate morphological parameters including median thallus length (16.75 mm), filament width (0.50 mm), branching angle (63.63°), and surface area/volume ratio (8.19 mm^{-1}). The Zuun-Arts biota contains fossils of six distinct morphotypes: non-branching, dichotomous branching, monopodial branching, fan-shaped, shrub-like, and small non-branching, all morphologies are similar to macroalgae from the Ediacaran Lantian and Miaohu biotas. Morphological and taphonomic data rule out a non-macroalgae affinity, and SEM-EDS data indicate that the Zuun-Arts fossils are preserved as aluminosilicate and carbon films. Results indicate that the Zuun-Arts fossils are macroalgae preserved as aluminosilicate mineral films.

© Copyright by Keenan Hassell, 2018
All Rights Reserved

TABLE OF CONTENTS

I. INTRODUCTION.....	1
II. BACKGROUND.....	3
Functional morphology in modern macroalgae.....	3
Applying functional morphology to the fossil record.....	8
The Proterozoic macroalgae fossil record.....	10
The Lantian biota.....	11
The Miaohe biota.....	13
The Zuun-Arts biota.....	14
Burgess Shale-type taphonomy.....	17
III. GEOLOGIC SETTING.....	20
IV. METHODS.....	27
Morphology.....	27
Scanning electron microscopy.....	28
X-ray diffraction.....	30
V. RESULTS.....	31
Morphology.....	31
Small non-branching morphology.....	31
Shrub-like morphology.....	31
Non-branching morphology.....	38
Monopodial branching morphology.....	38

Dichotomously branching morphology.....	38
Fan-shaped morphology.....	39
Scanning electron microscopy.....	39
X-ray diffraction.....	43
VI. DISCUSSION.....	49
Morphology.....	49
Comparison of the Zuun-Arts biota with other Ediacaran BST deposits.....	54
Scanning electron microscopy.....	58
X-ray diffraction.....	61
VII. CONCLUSIONS.....	63
VIII. REFERENCES.....	66
IX. APPENDICES.....	70
Appendix A: SEM-EDS maps.....	70
Appendix B: SEM-EDS maps C and Al overlay.....	74
Appendix C: SEM-EDS line scans.....	76
Appendix D: Morphological measurements of non-branching thalli.....	81
Appendix E: Morphological measurements of dichotomously branching thalli.....	96
Appendix F: Morphological measurements of monopodial branching thalli.....	98
Appendix G: Morphological measurements of fan-like thalli.....	99
Appendix H: Morphological measurements of small non-branching thalli.....	100
Appendix I: Morphological measurements of shrub-like thalli.....	101
Appendix J: XRD patterns.....	102

LIST OF FIGURES

Figure 1. Stratigraphic column of the Zuun-Arts Formation.....	15
Figure 2. BST early diagenesis model.....	19
Figure 3. SEM- 15 KeV accelerating velocity.....	21
Figure 4. SEM- 5 KeV accelerating velocity	22
Figure 5. Location map.....	23
Figure 6. Geochemical data.....	26
Figure 7. SEM-Sample orientation.....	29
Figure 8. Photographs of the Zuun-Arts fossils.....	32
Figure 9. Illustrations of the Zuun-Arts fossils.....	33
Figure 10. Length plot-small morphologies	34
Figure 11. Surface area/volume plot- small morphologies	35
Figure 12. Length plot- large morphologies	36
Figure 13. Surface area/volume plot- large morphologies.....	37
Figure 14. Relative abundance of Zuun-Arts morphologies.....	40
Figure 15. SEM-EDS maps.....	41

Figure 16. SEM-EDS C and Al overlay map.....	42
Figure 17. SEM-EDS line scan.....	44
Figure 18. SEM-BSE images.....	46
Figure 19. XRD results.....	47
Figure 20. XRD results with ethyl glycol.....	48
Figure 21. SEM-BSE comparison of Zuun-Arts fossils with graptolites.....	51
Figure 22. Length comparison.....	55
Figure 23. Surface area-volume comparison.....	56
Figure 24. Alternative early diagenesis model.....	60
Figure 25. Comparison of Zuun-Arts fossils with other Ediacaran macroalgae.....	64

LIST OF ABBREVIATIONS

BST	Burgess Shale-Type
BSE	Backscattered Electron
EDS	Energy Dispersive X-ray Spectroscopy
FFG	Functional Form Group
SEM	Scanning Electron Microscope
SE	Secondary Electron
XRD	X-Ray Diffraction
Ma	Million Years Ago
Ga	Billion Years Ago

ACKNOWLEDGEMENTS

First, I would first like to thank my thesis advisor Dr. Stephen Dornbos for his guidance throughout this process, and for allowing me to further explore my interest in Ediacaran paleontology. I would also like to thank Dr. Lindsay McHenry and Dr. Margaret Fraiser for serving on my thesis committee. In addition, I would like to thank Dr. Lindsay McHenry for guiding me through the X-ray diffraction component of this project, and Dr. Heather Owen from the UWM electron microscopy laboratory for her support on my scanning electron microscopy work. Lastly, I would like to thank my parents for their unwavering support and encouragement throughout my academic career.

Introduction

The Ediacaran Period stretches from 635 Ma to 542 Ma and is characterized by important paleobiological and paleoenvironmental changes. This period between the end of the Snowball Earth glaciations and the beginning of the Cambrian Period shows the first unequivocal complex animal life, and may hold the key to a better understanding of the origins of multicellular life (Xiao et al., 2008). The fossil record indicates a soft-bodied Ediacaran biota appearing as early as 575 Ma and persisting until around 541 Ma, at the beginning of the Cambrian Period (Xiao et al., 2008). Interpretations of these organisms have been controversial, and their phylogenetic affinities are still not entirely understood. Paleontologists first tried to shoehorn the Ediacaran organisms into Paleozoic phyla, however more recent studies suggest that many of these organisms belong to an extinct kingdom level taxon known as the rangeomorphs (Seilacher, 1992; Narbonne, 2005). The Ediacaran biota is characterized by rangeomorphs and erniettomorphs, but also includes microbial colonies, algae, fungi, protists and stem-group bilaterians and other metazoans (Narbonne, 2005).

The Ediacaran Period also contains fossil deposits of exceptional quality, known as Lagerstätten (Wang et al., 2014). Ediacaran Lagerstätten preserve a variety of soft-bodied organisms including enigmatic forms, putative metazoans, and algae that are not normally preserved, and show a variety of preservation types (Butterfield, 2003). Preservation types include external molds of soft tissue in fine-grained sand stone, carbonaceous compressions, phosphatization, pyritization, and silicification (Wang et al., 2014; Cai et al., 2010, Meyer et al., 2012; Brasier et al., 2011). Deposits that preserve carbonaceous compression fossils in fine-grained marine

siliciclastics, or Burgess Shale-type (BST) deposits, are a specific type of Lagerstätten that does an excellent job of preserving evidence of soft tissue (Wang et al., 2014).

Ediacaran BST deposits are known from around the world, including the recently described Zuun-Arts Biota in the Zavkhan terrane of western Mongolia (Dornbos et al., 2016). The Zavkhan terrane is a Precambrian crustal fragment that was embedded in the core of the central Asian orogenic belt (Smith et al., 2016). During the Ediacaran Period, arc terranes were accreting to the south, causing the Zavkhan terrane to begin subducting beneath the Khantaishir-Dariv arc. This subduction created the foreland basin in which the Zuun-Arts Formation was deposited (Macdonald et al., 2009). The Zuun-Arts Formation is composed of a basal stromatolitic limestone, a thin black shale interval with a cherty phosphorite layer, and then a thick carbonate sequence (Dornbos et al., 2016). The Zuun-Arts Biota is only beginning to be studied, but so far two new species of putative macroalgae, *Chinggiskhaania bifurcata* and *Zuunartsphyton delicatum*, have been identified (Dornbos et al., 2016). Preliminary data suggest they are preserved as aluminosilicate films (Dornbos et al., 2016).

The goal of this project was to test the hypotheses that 1) the Zuun-Arts fossils are indeed macroalgae, and 2) they are preserved as aluminosilicate films. These hypotheses were tested through thorough micro- and macroscopic study and morphometric analysis of Zuun-Arts fossil specimens in combination with scanning electron microscope energy dispersive x-ray spectroscopy (SEM-EDS) and x-ray diffraction (XRD) analysis. Learning more about the morphology, preservation, and the paleoenvironmental conditions under which these

exceptional fossils were preserved will provide a better understanding of early multicellular life in the Ediacaran.

Background

Functional morphology in modern macroalgae

BST macroalgae fossils preserve only the exterior morphology of the the organism and can look similar to other types of fossils, so establishing a macroalgae affinity can be difficult (Xunlai et al., 1999). Most notably, macroalgae fossils can look similar to burrow fossils, although they can be distinguished from burrows by their flattened form, carbonaceous composition, clearly defined margins, jagged endings, and non-disturbance of adjacent sediment, all of which burrow fossils lack (Miller, 2007; Osgood, 1970). Macroalgae fossils can look similar to graptolite fossils as well, however in scanning electron microscope backscatter (SEM-BSE) images, graptolite fusellae are clearly visible, while macroalgae lack these structures (Tang et al., 2017; Muscente and Xiao, 2015). Lastly, large bacterial sheaths produced by photosynthetic eukaryotes can look morphologically similar to non-branching tubular forms of macroalgae in the fossil record, however these macroalgae are an order of magnitude larger than the largest known bacterium with a similar morphology (LoDuca et al, 2017).

Once a macroalgae affinity has been determined for a fossil, the biggest obstacle is a lack of any genetic information required for proper taxonomic classification (Xunlai et al., 1999). In some cases, 3-dimensional preservation of a thallus may provide additional information about the internal structure, however such preservation is rare. In most cases the only information available is gross thallus morphology, so this is the criteria used in the classification of ancient

macroalgae (Wang et al., 2014). Due to the role of morphology in classification, understanding the functional morphology of macroalgae is crucial for classifying and understanding their evolutionary history (Xiao et al., 2002).

Although many Proterozoic and Cambrian macroalgae have no direct modern ancestors, they likely filled some of the same ecological roles as modern macroalgae. Extensive research has been done in order to understand the functional morphology of modern macroalgae, and much of this can be applied to ancient macroalgae as well (LoDuca and Behringer, 2009).

Littler and Littler (1980) published an extensive study examining the cost/benefit of various aspects of modern macroalgae morphology to ecological interactions and physiological function. The evolution of features such as environmental hardiness, defense against predation, and interference with competition were considered in terms of the energetic cost, material commitment, and possible incompatibility with basic physiological processes for each feature. Community succession was examined experimentally by clearing and sterilizing an area of seafloor and observing which macroalgae species appeared over 12 months. Based on this experiment, macroalgae were divided into two main groups: opportunistic forms and late successional/climax forms (Littler and Littler, 1980).

The first macroalgae to appear in the cleared areas are opportunistic forms, which are rapid colonizers with a simple thallus morphology and high surface area to volume ratio.

Opportunistic thalli are characterized by rapid growth, high reproductive capacity, and a high and uniform distribution of nutrient value (caloric density) across the entire thallus. These algae maintain the same morphology throughout their life cycle, and avoid predation by having an

unpredictable spatial and temporal distribution. This life style allows opportunistic macroalgae to rapidly invade and cover newly exposed areas of seafloor. Since the thallus is made almost entirely of photosynthetic tissue, these algae are highly productive, allowing them to rapidly replace any tissue lost to herbivorous predators. Although opportunistic algae are well adapted for rapid colonization, many aspects of their morphology and life cycle prevent them from long-term domination of their ecosystems. Although reproduction rates are high, mortality rates for reproductive bodies are also high. Once later successional forms of taller, more complex macroalgae begin to invade, opportunistic forms cannot adequately compete for light and other resources (Littler and Littler, 1980).

Late successional macroalgae appear after opportunistic forms have established a community, and often push them out of the area. In general, late successional forms have a lower surface area to volume ratio, grow slower, have a more structurally differentiated thallus, and have a lower reproductive capacity than opportunistic forms. Although reproductive rates are lower, mortality rates in reproductive bodies are also lower, and larger size and structural differentiation of the thallus allows late successional forms to better compete for light. An overall toughness of the thallus combined with other morphological and chemical characteristics act as defense mechanisms against herbivorous predators (Littler and Littler, 1980).

Both of these morphologies provide advantages to macroalgae in terms of predation defense and light acquisition. Below is a summary of adaptations leading to these advantageous morphological features, some of which should be observable in the fossil record.

Morphological characteristics increasing productivity

The morphology of macroalgae is the most important control of photosynthetic efficiency (Littler and Littler, 1980). Studies of modern macroalgae have found that sheet-like and finely branched morphologies result in the highest rates of photosynthetic productivity.

Photosynthetic cells in macroalgae are concentrated in the outer tissue layer, so thalli with higher surface area to volume ratios will have more photosynthetic cells, and will therefore have a higher rate of photosynthetic productivity. In sheet-like forms, a higher surface area to volume ratio is achieved through folding of the thallus, and fine branching increases this ratio by decreasing branch volume and increasing surface area. In addition to increasing rates of photosynthesis, these thin morphologies have larger cells, which minimizes internal self-shading by non-photosynthetic wall components (Littler, 1979).

Defense mechanisms

Macroalgae employ a variety of morphological and non-morphological strategies in order to protect themselves from herbivorous predation (Littler and Littler, 1980). Defense mechanisms fall into two broad categories: non-coexistence and coexistence (Iken, 2012). Non-coexistence strategies are non-morphological strategies that reduce the number and frequency of macroalgae-herbivore interactions (Iken, 2012). This is achieved through strategic temporal and spatial occurrences of macroalgae. Taxa using non-coexistence strategies live in locations that are not easily accessible to predators, or during seasons when herbivorous predators are not present. For example, some forms of brown algae are only susceptible to predation during early

life cycle stages. These algae reproduce during seasons when herbivores are not in the area.

Once large numbers of predators arrive, many of these macroalgae will be in the adult stage of their life cycle, so predation is thwarted (Markel and DeWeede, 1998).

Spatial and temporal defenses are often not an option, so macroalgae have evolved several morphological features for defense against predation (Iken, 2012). Producing high numbers of fleshy, lateral branches was an important morphological innovation leading to an increased resistance to predation. Filaments can be easily grazed upon, but the high number of lateral branches, along with the low cost of replacing damaged lateral branches, results in little impact on photosynthetic capacity (Iken, 2012; Van Alstyne, 1989). Littler and Littler (1980) also observed a morphological trend leading to thalli with a tough central axis containing the reproductive bodies. The development of a tough central axis with numerous soft lateral branches allows macroalgae to survive in environments with high populations of herbivorous predators (Iken, 2012; Littler and Littler, 1980).

Based on this functional morphology study, Littler and Arnold (1982) established six functional form groups (FFGs). FFG 1 consists of thin tubular and sheet-like thalli, FFG 2 consists of delicately- branched thalli, FFG 3 consists of coarsely-branched thalli, FFG 4 consists of thalli composed of thick blades and branches, FFG 5 consists of articulated calcareous thalli, and FFG 6 consists of encrusting thalli. These functional form groups fall on a spectrum of photosynthetic productivity, environmental hardness, and resistance to predation. The tubular and sheet-like morphologies in FFG 1 have the highest photosynthetic productivity due to their high surface area-volume ratio and lack of branches, which reduces self shading. Although FFG 1 is highly

productive, thalli have little to no ability to resist harsh environmental conditions or herbivorous predation. From FFG 1 to FFG 6, photosynthetic productivity decreases at a steady rate (Littler and Littler, 1980; Littler and Arnold, 1982).

Thalli in FFG 6 are the least photosynthetically productive, but have the greatest environmental hardiness and ability to resist herbivorous predation. These thalli have the most robust morphologies and highest degree of structural differentiation, allowing them to protect chloroplasts and reproductive structures inside a tough thallus when not in use (LoDuca, 2017). The robust morphologies of FFG 6 thalli also account for their low photosynthetic productivity, since the ratio of photosynthetic to non-photosynthetic tissue is much lower than in FFG 1 (Littler and Arnold, 1982).

Modern macroalgae have developed numerous morphological features which increase their photosynthetic efficiency and ability to defend themselves against predation (Littler and Littler, 1980). Although evidence of some features, such as chemical defenses and non-coexistence strategies, cannot be observed in the fossil record, trends towards some morphological strategies should be observable.

Applying the functional form group concept to the fossil record

Due to the limitations associated with classifying ancient macroalgae, classification is based on morphogroups, which are groups of fossils with similar morphological features. LoDuca et al. (2017) performed a detailed survey of all known BST deposits containing macroalgae from the Cambrian, Ordovician, and Silurian periods and calculated canopy height, maximum length and surface area for all thalli. Based on these morphological data, nine morphogroups were

established for the early Paleozoic: tubiform, ribbon-like, spherical, delicately dichotomously branching, coarsely dichotomously branching, stoloniform, frondose, simple monopodial, and complex monopodial. Morphogroups were then assigned to a functional form group based on Littler and Littler (1980). The tubiform, ribbon-like, spherical, and frondose morphogroups were assigned to FFG 1, delicately dichotomously branching and stoloniform morphogroups were assigned in FFG 2, the simple monopodial morphogroup was assigned to FFG 2.5, complex monopodial and most of the coarsely dichotomously branched morphogroups were assigned to FFG 3, and one specimen from the coarsely dichotomously branched morphogroup was assigned to FFG 4 (LoDuca et al., 2017).

LoDuca et al. (2017) found several trends in the evolution of macroalgae thallus morphology from the Cambrian through Silurian periods. First of all, there is a trend of increasing complexity of morphogroups. The Cambrian Period was dominated by the simplest tubiform and delicately dichotomously branching morphogroups. In the Ordovician Period, the tubiform morphogroup disappears, the delicate dichotomously branching morphogroup becomes less common, and the monopodial branching morphogroup becomes dominant. The Silurian macroalgae record is similar to the Ordovician, however the ratio of monopodial to delicately dichotomously branching morphogroups is slightly higher (LoDuca et al., 2017).

A similar pattern is seen in functional form groups, with the Cambrian Period dominated by FFG 1 and FFG 2. In the Ordovician, FFG 1 becomes less common, FFG 2 and FFG 2.5 become the most common, and FFG 3 first appears. The Silurian Period is similar to the Ordovician, with FFG 2.5 and FFG 3 being the most common. The Silurian Period also contains one example of a FFG

4 specimen. Based on these trends in morphogroups and functional form groups, there appears to be a general trend towards increasing complexity in macroalgae thalli from the Cambrian to the Silurian, with a major diversification occurring during the Ordovician radiation. This trend from highly efficient, delicate morphogroups to less efficient, hardier morphogroups was likely driven primarily by the evolution of herbivorous predation (LoDuca et al., 2017). In order to better understand the early Paleozoic evolutionary trends seen in the fossil record of macroalgae, a better understanding of Proterozoic macroalgae is required, especially during the Ediacaran Period.

The Proterozoic fossil record of macroalgae

Macroalgae underwent a major diversification event during the Ediacaran Period, however macroalgae such as *Grypania* have been found in rocks as old 1.8-2.0 Ga (Han and Runnegar, 1992). Other putative Paleoproterozoic macroalgae include the spherical to cylindrical forms of *Churia*, *Ellipsophysa*, and *Tawuia* from 1.7-1.8 Ga rocks in North China (Zhu et al., 2000).

Although these putative Paleoproterozoic macroalgae are small and simple, some early morphological advances can be seen even at this time, including the development of stipe morphology and possibly the earliest holdfast structures (Xiao and Dong, 2006).

Mesoproterozoic macroalgae include spherical, ellipsoidal, tomaculate and cylindrical thallus morphologies as well as more complex discoidal holdfasts and transverse annulations (Xiao and Dong, 2006). Ediacaran BST deposits containing abundant macroalgae fossils include the Lantian biota of southern Anhui Province, China, the Miaohe biota in the terminal Doushantuo Formation at Miaohe in Hubei Province, China, and the Zuun-Arts biota of western Mongolia.

The Lantian Biota

The Lantian Biota of southern Anhui Province, China, is the oldest known Ediacaran BST deposit containing macroalgae (Yuan et al., 2011). This biota represents a slope basinal depositional environment within the photic zone, and is regarded as the oldest fossil assemblage containing macroscopic and morphologically complex life (Yuan et al., 2011).

Two formations are present at this location; the Lantian Formation, which correlates with the 635-551 Ma Doushantuo Formation based on $\delta^{13}\text{C}$ chemostratigraphy, and the Piyuancun Formation, which correlates with the 551-542 Ma Dengying Formation in the Yangtze Gorges area (Xunlai et al., 1999). The stratigraphic column consists of 1.8 m of dolostone cap carbonate, 35 m of finely laminated, fossiliferous black shale, a 34 m unit of dolostone interbedded with mudstone and ribbon rock, and 20 m of black silty mudstone (Yuan et al., 2002). The lower shale unit contains the Lantian biota fossils, and its age has been constrained to 579-565 Ma based on U-Pb radiometric dating (Condon et al., 2016). Fossils here are exceptionally preserved as carbonaceous compressions in black shale and are up to 40 mm in length. Several enigmatic forms are present here, including a cone shaped thallus with a globose holdfast and a splay of filaments at the top, a conical thallus with a fusiform inner body, and a thin stalk with a cylindrical thallus and a dark axial trace. Interpretations of these fossils remain controversial due to a lack of modern analogues for comparison (Yuan et al., 2011). Different morphologies have been interpreted as macroalgae, Cnidarians, bilaterian worm-like organisms, and bilaterian metazoans (Xiao et al., 2002). Regardless of the taxonomic

affinities of these fossils, the presence of macroeukaryotes suggests that some amount of free oxygen must have been present in the environment while these organisms were alive (Yuan et al., 2011).

The Lantian Biota also contains a diverse assemblage of megascopic, non-calcareous macroalgae ranging from 10-100 mm in length and 0.1-20 mm in width. Many of these specimens have holdfasts and include ribbon-like and dichotomous branching morphologies (Xunlai et al., 1999). Several morphotypes have been identified from the Lantian Biota macroalgae including thin and thick dichotomous and ribbon-like branching, fan shaped thalli with dichotomous branching, broom shaped thalli with all branches attached to a single basal structure, spherical/elliptical forms, and a variety of tube and cone shaped morphologies composed of many filaments attached to a basal structure. Septation is not common, but some forms have septated filaments. Filament branching as well as disc/globose holdfasts found in most specimens suggest that these were erect, benthic macroalgae (Xunlai et al., 1999).

The Lantian Biota macroalgae are preserved as carbonaceous compressions, often associated with densely packed, framboidal pyrite (Wang et al., 2014; Yuan et al., 2011). The presence of pyrite in these fossils can be used to interpret the redox history of the basin. Pyrite framboids form in anoxic conditions, but the presence of macroeukaryotes suggest that there must have been some free oxygen present in the water. Wang et al. (2014) proposed a cyclical redox model to explain this apparent dichotomy by suggesting that there was a flux in oxygen levels between when the organisms were alive and when they died: the basin was largely anoxic, punctuated by brief oxic episodes. During oxic intervals, the chemocline was below the water-

sediment interface and macroalgae lived in oxic waters within the photic zone. When oxic intervals ended, the chemocline shifted up into the water column, killing the algae (Wang et al., 2014). Algal remains were buried in fine-grained siliciclastics, where they were preserved as carbonaceous compressions and acted as localized substrates for large pyrite framboids to form on. This led to primary preservation as carbonaceous compressions with some late stage Pyritization (Gabbott et al., 2004).

The Miaohu Biota

The other major Ediacaran BST deposit is the Miaohu Biota from the terminal Doushantuo Formation at Miaohu in Hubei Province, China (Xiao et al., 2002). The Doushantuo Formation at this location is about 200 m thick, and is composed of extremely finely laminated, organic rich shale and cherty carbonates deposited in a quiet subtidal environment, likely within a restricted basin (Wang et al., 1998; Ding et al., 1996). Fossils are within a 2 m thick interval in the upper shale member (Xiao et al., 2002).

Several distinct morphologies have been identified in the Miaohu Biota, most are multicellular algae (Xiao et al., 2002). Most algal specimens have holdfasts and dichotomous branching, and some have reproductive structures preserved (Zhang et al., 1989). Morphologies include spherical cell-like vesicles, cylindrical forms with monopodial branching, unbranching cylindrical thalli, straight/zigzag central axis with dichotomous branching (some with several successive dichotomies), and ribbon-like thalli with or without branching and fan or dumbbell-shaped thalli composed of a bundle of filaments. Branching and the presence of basal attachment structures in most morphologies suggest an erect, benthic life habit (Xiao et al., 2002).

Miaohe Biota fossils are preserved primarily as carbonaceous compressions in fine-grained marine siliciclastic sediments (Xiao et al., 2002). Like the Lantian Biota, Miaohe carbonaceous compressions are often associated with framboidal pyrite, or cavities left by framboids that have weathered out (Wang et al., 2014). The presence of pyrite framboids suggests an environmental model similar to that of the Lantian Biota in which organisms lived during oxic episodes in a largely anoxic basin, and were preserved through carbonization and late-stage pyritization. Although the Lantian and Miaohe Biotas are over 600 km apart, they are both composed primarily of macroalgae preserved through carbonization and late-stage pyritization, suggesting that anoxic conditions were wide spread in this basin (Wang et al., 2014).

The Zuun-Arts Biota

The recently discovered Zuun-Arts biota is a late Ediacaran BST deposit in the Zuun-Arts Formation of Zavkhan Province, western Mongolia (Dornbos et al., 2016). The absolute age of the Zuun-Arts biota is unclear, however it lies beneath the oldest indisputable trace fossils in the region (~555 Ma) (Macdonald, 2011), and is therefore likely younger than the Miaohe Biota (Zhu et al., 2013). The stratigraphic sequence of the Zuun-Arts formation consists of a basal stromatolitic limestone followed by a shale interval, a cherty phosphorite unit, and a thick carbonate succession (Figure 1). Fossils are preserved in a roughly 40 cm thick black shale interval. The Zuun-Arts Formation represents a transgressive lag deposit and has an unclear age relationship with the Lantian and Miaohe Biotas, although it may correlate with the terminal Doushantuo Formation at Miaohe (Dornbos et al., 2016).

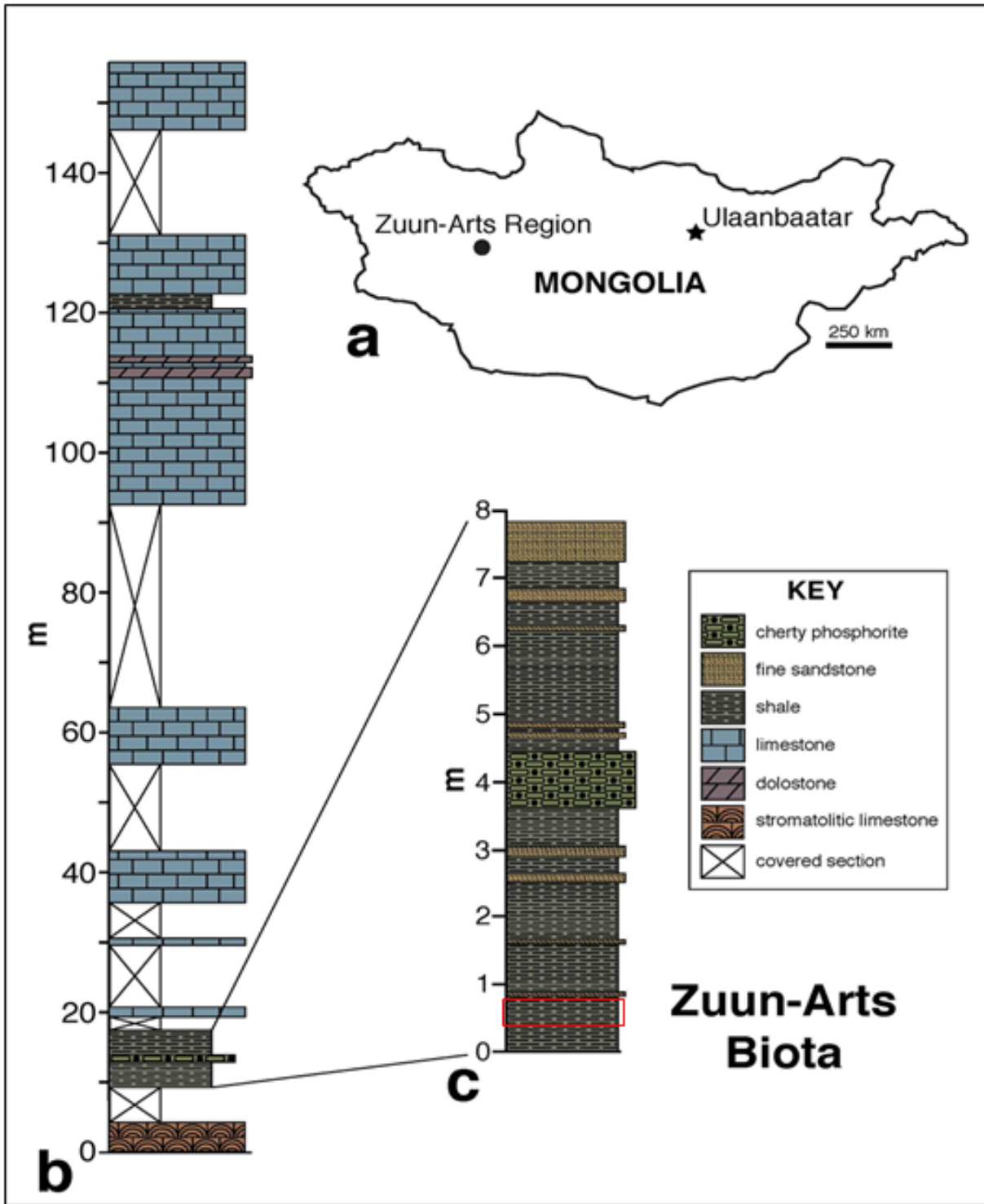


Figure 1. The stratigraphic context of the Zuun-Arts Biota. A) Regional map of Mongolia showing the location of the Zuun-Arts region. B) Stratigraphic column of the Zuun-Arts Formation. C) Detailed stratigraphic column of the Zuun-Arts Formation at the location of the Zuun-Arts biota. Modified from Dornbos et al. (2016).

Preliminary study of the Zuun-Arts Biota indicates two species of probable eukaryotic macroalgae (Dornbos et al., 2016). *Chinggiskhaania bifurcata* consists of thin filaments that lack transverse longitudinal ornamentation, are gently curving, and rarely branch. Filaments have fine length-wise lineations, no consistent distal tapering, and diverge at 43°-85°, with a mean branching angle of 63°. These specimens are mostly fragmentary, but one well-preserved specimen shows four filaments that are not densely grouped. *Chinggiskhaania bifurcata* is not entirely analogous to any other known Ediacaran macroalgae, but it most closely resembles *Doushantophyton* from the Miaohu Biota and *Huangshanophyton* from the Lantian biota (Dornbos et al., 2016). The other probable macroalgae species found in the Zuun-Arts biota is *Zuunartsphyton delicatum*, which is known from three specimens. *Zuunartsphyton delicatum* exhibits a shrub-like morphology less than 3 mm in diameter, composed of tightly curling filaments lacking branching and longitudinal divisions or ornamentation. Attachment structures are unknown, and *Zuunartsphyton delicatum* does not appear to closely resemble any specimens from the Lantian or Miaohu Biotas (Dornbos et al., 2016).

Preliminary SEM-EDS data show that filaments have high concentrations of Al and Si relative to other elements, and that Si is not enriched relative to the matrix (Dornbos et al., 2016). Carbon is locally concentrated in portions of specimens. These results are consistent with preservation as aluminosilicate clay mineral films. The presence of locally concentrated carbon suggests that these organisms were originally preserved as carbonaceous compressions, and were diagenetically altered to aluminosilicate mineral films. One specimen shows a concentration of Fe in a zone with a high C concentration, and SEM analysis reveals the presence of framboidal minerals consistent with pyrite. As in the Lantian and Miaohu Biotas, it appears that late-stage

pyrite formation occurred as a result of sulfate reduction during the decay of filaments, however aluminosilicate clay mineral preservation contrasts with the carbonaceous compressions fossils in the Lantian and Miaohu Biotas, as well as most other Ediacaran and Cambrian BST deposits (Dornbos et al., 2016).

Burgess Shale-type taphonomy

BST preservation is a unique taphonomic pathway that leads to 2-dimensional preservation of soft tissue as a film of carbon and/or aluminosilicate mineral films with a thickness on the scale of microns (Orr et al., 2009; Briggs and Williams, 1981). This rare taphonomic window is largely limited to the Ediacaran- early Ordovician Periods (~ 545-480 Ma) (Van Roy et al., 2010). The BST preservation pathway begins when a soft-bodied organism is buried in anoxic mud very soon after death, which isolates delicate morphological features and seals out heterotrophic microbes (Marshall, 1976). The carcass then begins to degrade, leaving behind only a thin film of organic carbon. Two primary models attempt to explain when aluminosilicate films form during fossil diagenesis, and both have implications for how organisms should appear in the fossil record (Orr et al., 2009; Butterfield et al., 2007).

Orr et al. (2009) proposed an early diagenesis model in which aluminosilicate layers form on the decaying organism shortly after burial. In this model, the decaying carcass acts as a substrate for the accumulation of colloids or the precipitation of authigenic clays (Orr et al., 2009; Orr et al., 1998). Once the carcass decays, aluminosilicate clay that precipitates on the original C film. Over time, the rock containing the fossil is subjected to regional metamorphism, which alters the clay to a coherent aluminosilicate film. This model would result in a fossil film composed of

three layers: a layer of C in the middle with layers of Al above and below, or an Al layer in the middle with C layers above and below (Figure 2) (Orr et al., 2009; Orr et al., 1998).

Butterfield et al. (2007) suggests an alternative late diagenesis origin of aluminosilicate films. In this model, the diagenetic process also begins with an organism being buried in anoxic mud, decaying, and leaving behind a carbon film. The role of clay in early diagenesis and the formation of aluminosilicate films, however, differ considerably from the early diagenesis model. In the late diagenesis model, clay minerals in the sediment absorb degradative enzymes due to their large surface area and high cation exchange capacity, indefinitely delaying the decay process (Butterfield, 1990; Thang, 1979). The formation of aluminosilicate films does not require a pre-existing mineral phase (Butterfield et al., 2007), as shown by the replacement and/or overgrowth of organic-walled graptolite fossils by aluminosilicate films as a result of metamorphism (Underwood, 1992). Thus, clay plays a vital role in preservation, but does not form the aluminosilicate film. The late diagenesis model should result in fossils composed primarily of aluminum, possibly with areas of elevated carbon concentrations (Butterfield, 2007; Orr et al., 2009).

Scanning electron microscopy

SEM-EDS elemental mapping has become a common tool for paleontologists trying to understand how BST fossils form (e.g. Loydell, 2004; Huggett et al, 2000; Moore and Liberman,

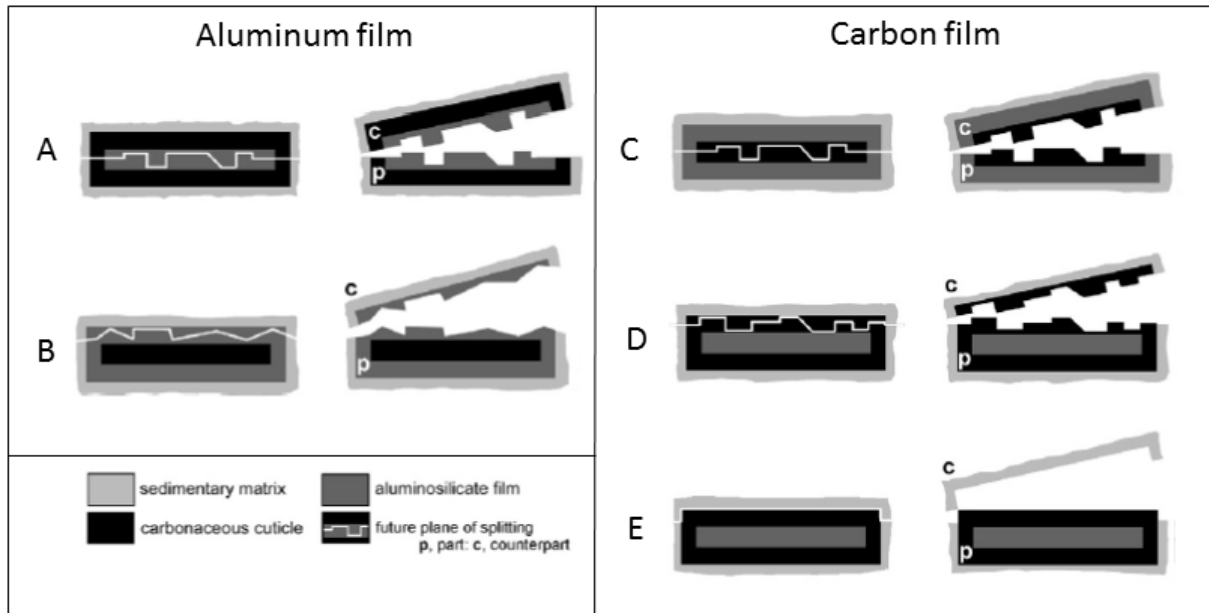


Figure 2. A summary of the early taphonomic model for BST preservation. A-B result in Al films. A) Al inside, C outside, plane of plitting through the Al layer. B) C inside, Al outside, plane of splitting through the Al layer. C-D result in C films. C) C inside, Al outside, plane of splitting through the C layer. D) Al inside, C outside, plane of splitting through the C layer. E) Al inside, C outside, plane of splitting through the sedimentary matrix. Modified from Orr et al. (2009).

2009). Although EDS analysis can provide a wealth of information about the composition of fossils, determining the appropriate SEM parameters, especially accelerating voltage, can be difficult (Orr et al., 2009). BST fossils are extremely thin, often having a thickness of 0.05 μm or less, creating a challenge in EDS analysis. EDS works best at a high accelerating voltage, which creates a large interaction volume, extending far below the fossil of interest and into the rock containing the fossil. Orr et al. (2009) addressed this problem using Electron Flight Simulator software to generate interaction volumes for rocks with C films 2.5 μm , 0.175 μm and 0.15 μm thick at 15 keV (Figure 3), and 0.05 μm , 0.03 μm and 0.02 μm thick at 5 keV (Figure 4). For the 15 keV accelerating voltage, the interaction volume extended far beneath the C film of interest. The 2.5 μm film showed up clearly, the 0.175 μm film was faint but visible, and the 0.15 μm film was not seen at all in the spectrum. The large interaction volume associated with a 15 keV accelerating voltage extended so far into the rock that the signals from the C films were washed out. At the 5 keV accelerating voltage, the 0.05 μm , 0.03 μm and 0.02 μm C films were all detectable in the spectrum. Since the 5 keV accelerating voltage produces a much smaller interaction volume than 15 keV, more of the signal came from the film and there was less background noise from the rock, resulting in an increase in resolution (Orr et al., 2009).

Geologic Setting

The Zuun-Arts Formation is located in the Zavkhan terrane of Western Mongolia, a Precambrian crustal fragment embedded in the core of the central Asian orogenic belt (Fig. 5) (Kroner et al.,

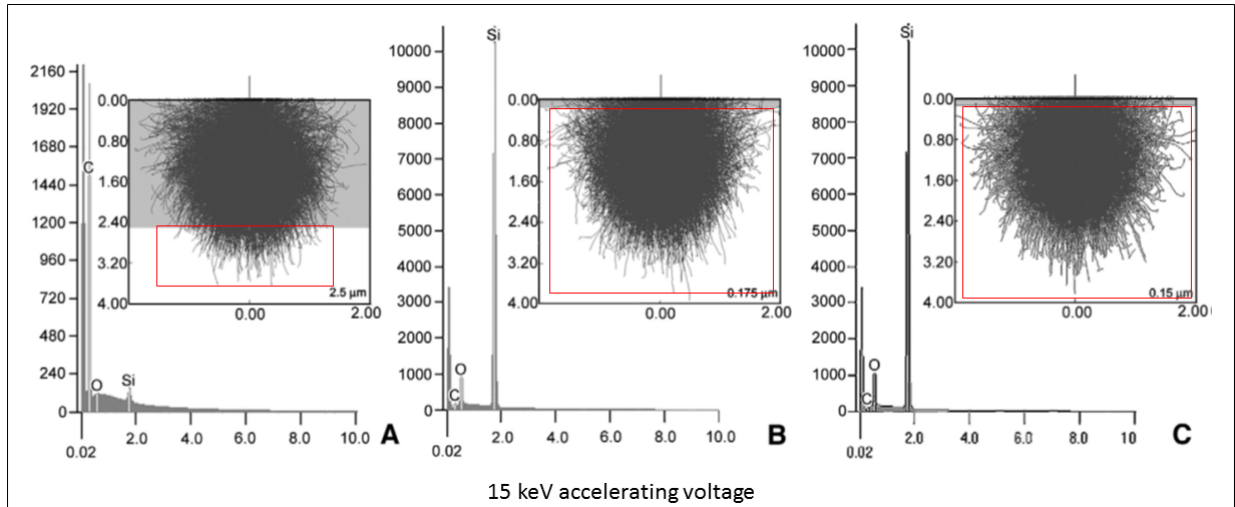


Figure 3. Simulated interaction volume of a 15 keV accelerating voltage in shale containing carbon films of various thicknesses. A) 2.5 μm thick carbon films, note the large carbon peak in the spectrum. B) 0.175 μm thick carbon films, note the subtle but still distinguishable carbon peak in the spectrum. C) 0.15 μm thick carbon film, the carbon peak is not distinguishable in the spectrum. Red boxes show the portion of the interaction volume penetrating into the matrix beneath the fossil. Modified from Orr et al. (2009).

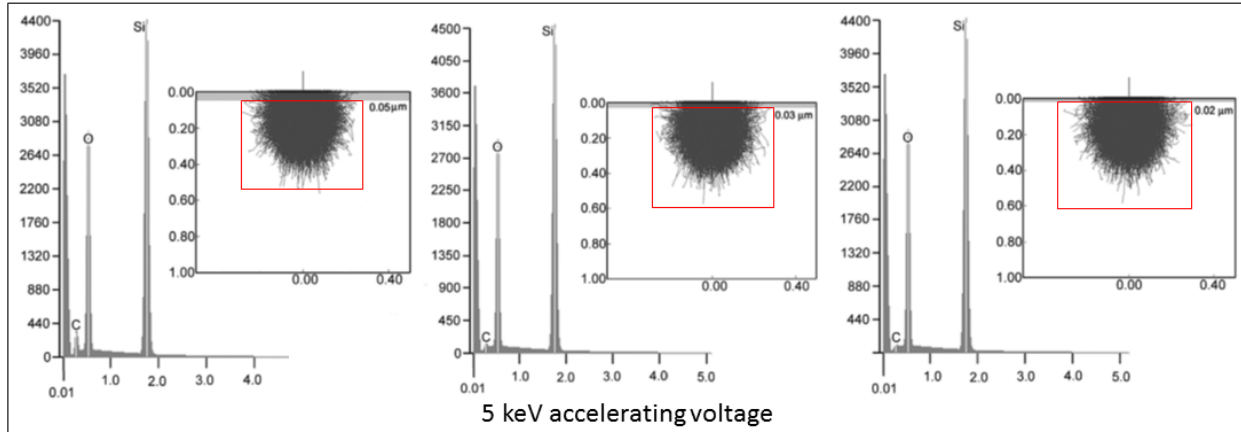


Figure 4. Simulated interaction volumes for a 5 keV accelerating voltage in shale containing carbon films of various thicknesses. A) 0.05 μm thick carbon film, note the distinct carbon spike on the spectrum. B) 0.03 μm thick carbon films, note the distinct carbon spike on the spectrum. C) 0.02 μm thick carbon film, although the carbon speak is smaller, it is distinguishable in the spectrum. Red boxes show the portion of the interaction volume penetrating the matrix beneath the fossil. Modified from Orr et al. (2009).

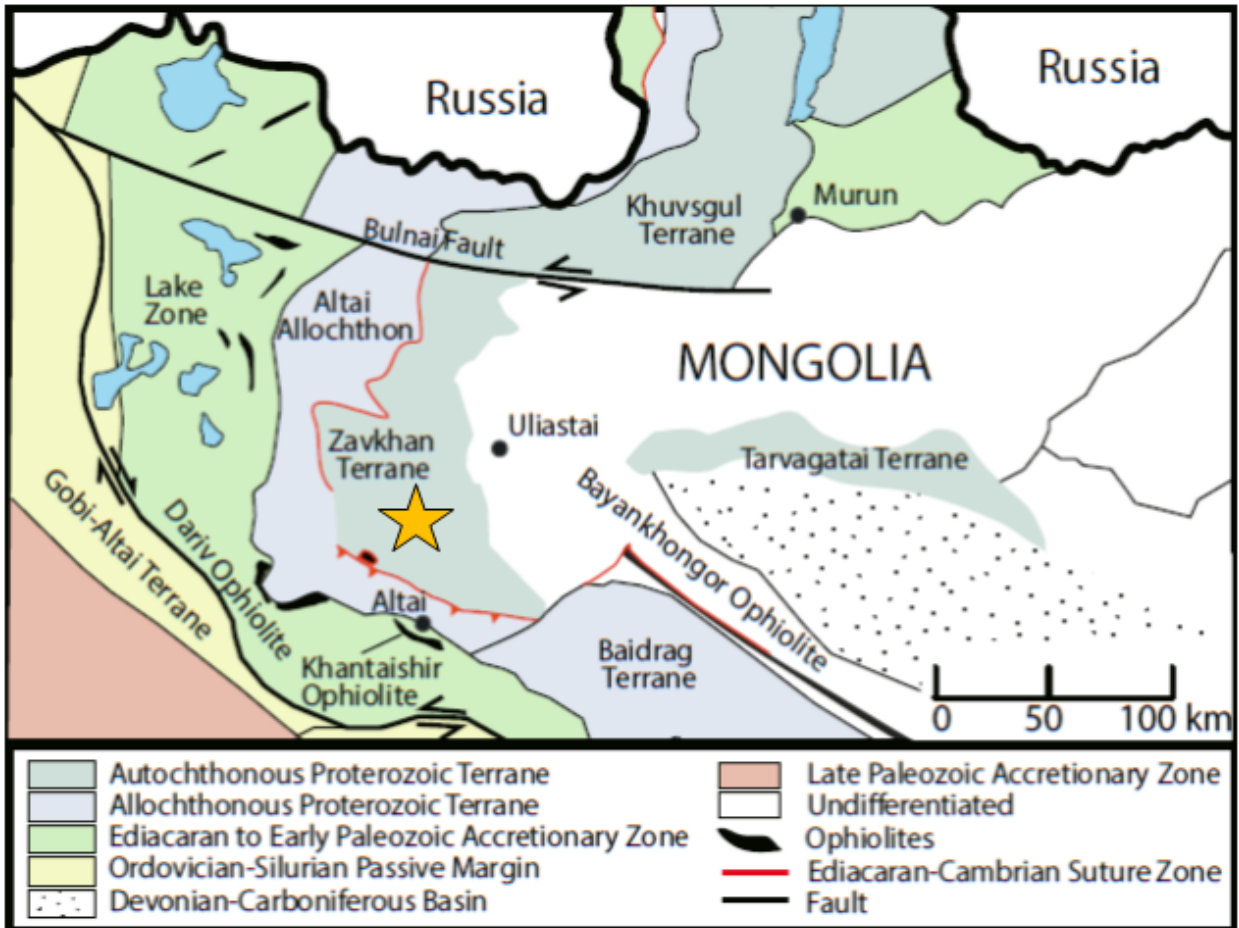


Figure 5. Regional map showing the location of the Zavkhan Terrane. The orange star marks the region of the Zuun-Arts biota. Modified from Smith et al. (2016).

2010). Accretion of arc terranes occurred to the south of the Zavkhan terrane from the late Ediacaran through the Ordovician Period. The late Ordovician and Silurian Periods are marked by extensional magmatism and basin formation. The Zavkhan terrane was buckled during the arrival of North China from the early Devonian through the Permian Period (Kroner et al., 2010).

Cryogenian stratigraphy in the Zavkhan terrane begins with 773.3-803.4 Ma felsic igneous rocks containing ~755 Ma granitic intrusions (Macdonald et al., 2009). The Zavkhan Formation is then overlain by synrift and passive margin deposits. The Zuun-Arts Formation is within the Tsagaan Oloom Group, which contains two Cryogenian glacial deposits. The first is the Maikhan-Uul Formation, which is a Sturtian age diamictite (717-660 Ma) and the Taishie Formation, which is composed of Sturtian cap carbonates and interglacial strata (Bold et al., 2006). These are overlain by the Khongor Formation, which has been correlated to Marinoan glacial deposits. The Ol Formation, which is correlative with 635 Ma basal Ediacaran cap carbonates, overlies the Khongor Formation. The Ol Formation is overlain by the early Ediacaran Shuurgat Formation, which consists of 100-500 m of carbonates, and is unconformably overlain by the late Ediacaran Zuun-Arts Formation (Bold et al., 2006). The Zuun-Arts Formation was deposited in the Zavkhan basin. The age of continental arc volcanism, position of the accretionary wedge and ophiolites on the northern margin of the Khantayshir-Dariv arc, and north vergent thrusting in the accretionary zone all indicate that the Zavkhan basin was created through the subduction of the Zavkhan terrane beneath the Khantayshir-Dariv arc (Macdonald et al., 2009).

Chemostratigraphy of $\delta^{13}\text{C}$ isotopic data has been used to interpret the environmental conditions present within the Tsagaan Oloom Group, including the Zuun-Arts Formation (Fig. 6) (Macdonald et al., 2009). $\delta^{13}\text{C}$ values in the Maikhan diamictites are moderately negative, and increase to +8‰ in the overlying Tayshir Formation. $\delta^{13}\text{C}$ then plummets abruptly from +8‰ to -7.5‰ during the third transgression in the Tayshir Formation before returning to +8‰ through the top of the Tayshir Formation (Macdonald et al., 2009). In the OI Formation, the $\delta^{13}\text{C}$ profile forms a sigmoidal pattern which reaches -6‰ and remains negative throughout the OI Formation and into the beginning of the Ulaan Bulagyn Formation, where $\delta^{13}\text{C}$ abruptly jumps to +3‰ through the top of the Ulaan Bulagyn Formation. The carbon isotopic profile observed in the Ulaan Bulagyn Formation is consistent with a mid-Ediacaran age. The Zuun-Arts Formation overlies the Ulaan Member and has a variable $\delta^{13}\text{C}$ profile, which ranges from +2‰ to -5‰, but is mostly negative. Strontium isotopic data shows a high $^{87}\text{Sr}/^{86}\text{Sr}$ value of 0.7085 in the Zuun-Arts Formation (Figure 6). These strontium isotopic values are consistent with values typically found during the Proterozoic-Phanerozoic transition, indicating a late Ediacaran age for the Zuun-Arts Biota (Bold et al., 2016). This, in addition to the mid-Ediacaran carbon isotopic values in the Ulaan Bulagyn Formation, supports the interpretation that there is a hiatus of about 35 MY between the Zuun-Arts Formation and the underlying Ulaan Bulagyn Formation (Macdonald et al., 2009).

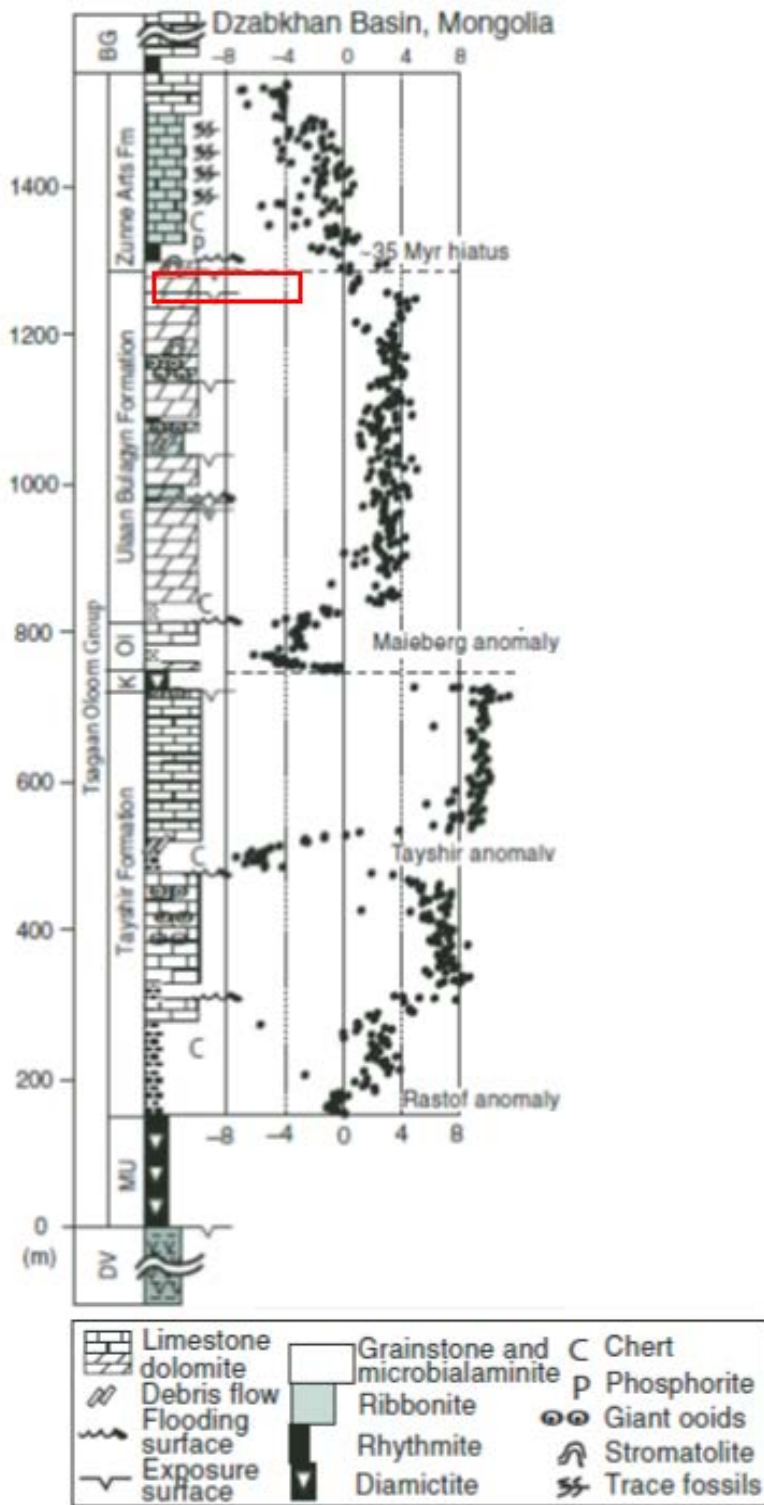


Figure 6. Carbon isotope chemostratigraphy and lithostratigraphy of the Tsagaan Oloom Group. The red box shows the interval containing the Zuun-Arts biota. K-Khongoryn Fm, OI- OI Fm, MU- Maikhan UI Fm, DV- Dzabkhan volcanics. Modified from Macdonald et al. (2009).

Methods

Morphological analysis

Fossils were collected from the Zuun-Arts biota in Zavkhan Province, Mongolia. Fossils were first examined under low magnification using a Leica EZ4D light microscope, and then photographed with a Canon EOS 350D camera under cross-polarized light. ImageJ software was used to take morphological measurements from the photographs. Morphological measurements of 821 individual fossil specimens include length, width and canopy height for all specimens, and branching angle for branching specimens. These morphological measurements were then used to calculate surface area, volume, and surface area/volume ratio. Fossils were modeled as cylinders based on one pair of 3-dimensionally preserved part-counterpart fossils with a tube-like cross section. Surface area, volume, and surface area/volume ratio were calculated as follows:

$$\text{Surface area (SA)} = 2\pi r l + 2\pi r^2$$

$$\text{Volume (V)} = \pi r^2 l$$

$$\text{Surface area/volume ratio (SA/V)} = \frac{SA}{V}$$

where r is the radius of the filament $\left(\frac{\text{filament width}}{2}\right)$ and l is the length of the filament. For specimens with more than one thallus element, total length and width were calculated as the sum of all elements. Median length, width, canopy height, branching angle, and surface area/volume ratio were calculated for all thalli. Canopy height was calculated as the total

distance between the seafloor and the top of the thallus in life. For specimens showing evidence of an erect, benthic lifestyle, canopy height is the total distance from the base of the thallus to the top of the highest thallus element. Specimens lacking evidence of an erect, benthic lifestyle were assumed to be either pelagic or benthic organisms that laid flat on the seafloor. Canopy height for these individuals is the same as width.

To compare the Zuun-Arts fossils to accepted Ediacaran macroalgae, the above measurements and calculations were also performed on fossils from the Lantian and Miaohu biotas. The photos used were obtained from Xiao et al. (2008) and Xunlai et al. (1999).

Scanning electron microscopy

SEM-EDS mapping and line scans were used to examine the elemental composition of 39 *Chinggiskhaania* fossils from the Zuun-Arts biota. All SEM analysis was done on a Hitachi S-4800 scanning electron microscope with a Bruker Quantax ESPRIT energy dispersive x-ray detector in the scanning electron microscopy laboratory at the University of Wisconsin-Milwaukee. Specimens were cut with a rock saw and mounted on a 1-inch stub using carbon glue, and the sides of the sample were painted with colloidal carbon paint to increase conductivity. Fossils were mounted with the long axis of the fossil perpendicular to the beam in order to examine the distribution of elements on the exterior (Figure 7). All specimens were coated with carbon using an Edwards's vacuum coating unit. An accelerating voltage of 10 keV was used for all specimens to produce SEM-EDS maps for O, C, Al, Si and Fe. Line scans were

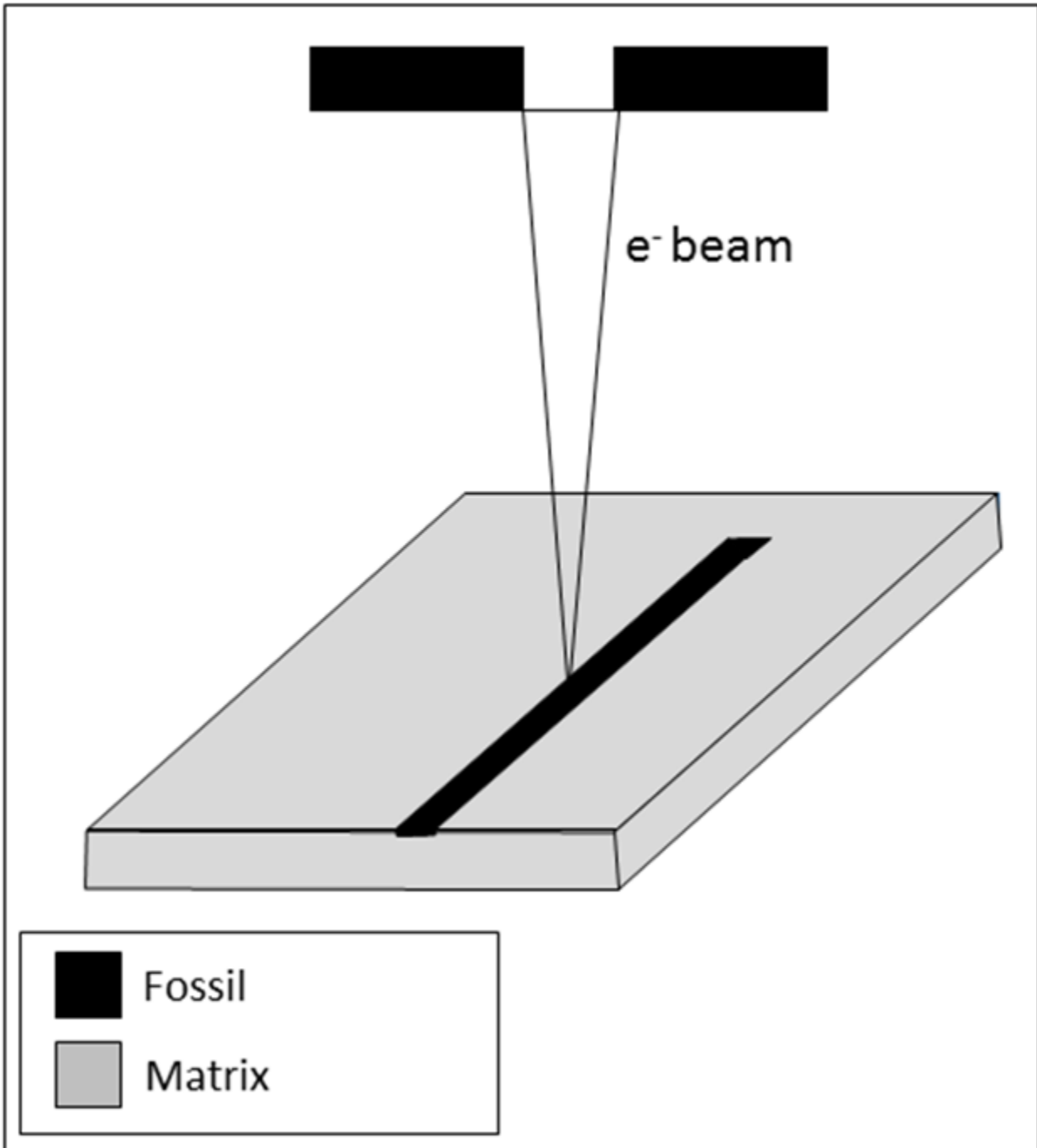


Figure 7. Illustration showing the orientation of fossils with respect to the electron beam. Fossils were mounted perpendicular to the electron beam in order to examine elemental variations across the exterior surface.

also produced for C, Si, and Al. Backscatter images were used to locate the outer margins of fossils before EDS analysis was done.

X-ray diffraction

XRD was used to examine the clay mineral content of the Zuun-Arts shale. Grain size separation was used to segregate the clay size fraction from 6 samples of shale from the Zuun-Arts Formation. For each sample, approximately 10 grams of shale was ground with a mortar and pestle, soaked in deionized water in 200 ml glass beakers overnight, and blended for 3 minutes in a Waring blender. The fine grain fraction was decanted into plastic tubes for centrifugation.

About 30 mg of sodium pyrophosphate dispersing agent was added to each tube, and samples were centrifuged at 750 rpm for 3.3 minutes. The clay size fraction was then decanted into a new tube, and this process was repeated 5-6 times to isolate the clay fraction. To induce flocculation, 2.2 g of CaCl_2 were added to each sample. Samples were left overnight to flocculate, then centrifuged a final time for 3.3 minutes at 750 rpm, concentrating the clay fraction in the bottom of the tube. Sediment free water was removed with a vacuum hose, and the remaining samples were mounted on glass slides.

To test for the presence of montmorillonite, three samples were run a second after adding ethyl glycol to the slides. Samples were run on a Bruker D8 Focus XRD with Diffrac Plus software, and interpretation was done using Diffrac Plus EVA software.

Results

Morphology

Two species of putative macroalgae, *Chinggiskhaania bifurcata* and *Zuunartsphyton delicatum*, have been identified in the Zuun-Arts biota (Figure 8; Figure 9). *Zuunartsphyton delicatum* has a shrub-like morphology. *Chinggiskhaania bifurcata* has four different morphologies: non-branching, single monopodial branching, dichotomous branching, and fan-shaped. A small non-branching morphology has also been identified, but its affinity is unclear.

Small non-branching morphology

The small non-branching morphology is composed of a single, non-branching element less than 4 mm in length, and is often twisted or curved. Thalli have a median length of 2.87 mm (Figure 10), median width of 0.16 mm and a median surface area/volume ratio of 27.4 mm^{-1} (Figure 11).

Zuunartsphyton: Shrub-like morphology

The shrub-like morphology is composed of up to six thin elements twisted tightly together to form a shrub-like thallus. Individual elements have a median length of 3.80 mm (Figure 10) and a median width of 0.27 mm. Elements twist around and overlap one another. The entire thallus has a median surface area/volume ratio of 16.12 mm^{-1} (Figure 11) and a total width of less than 6 mm.

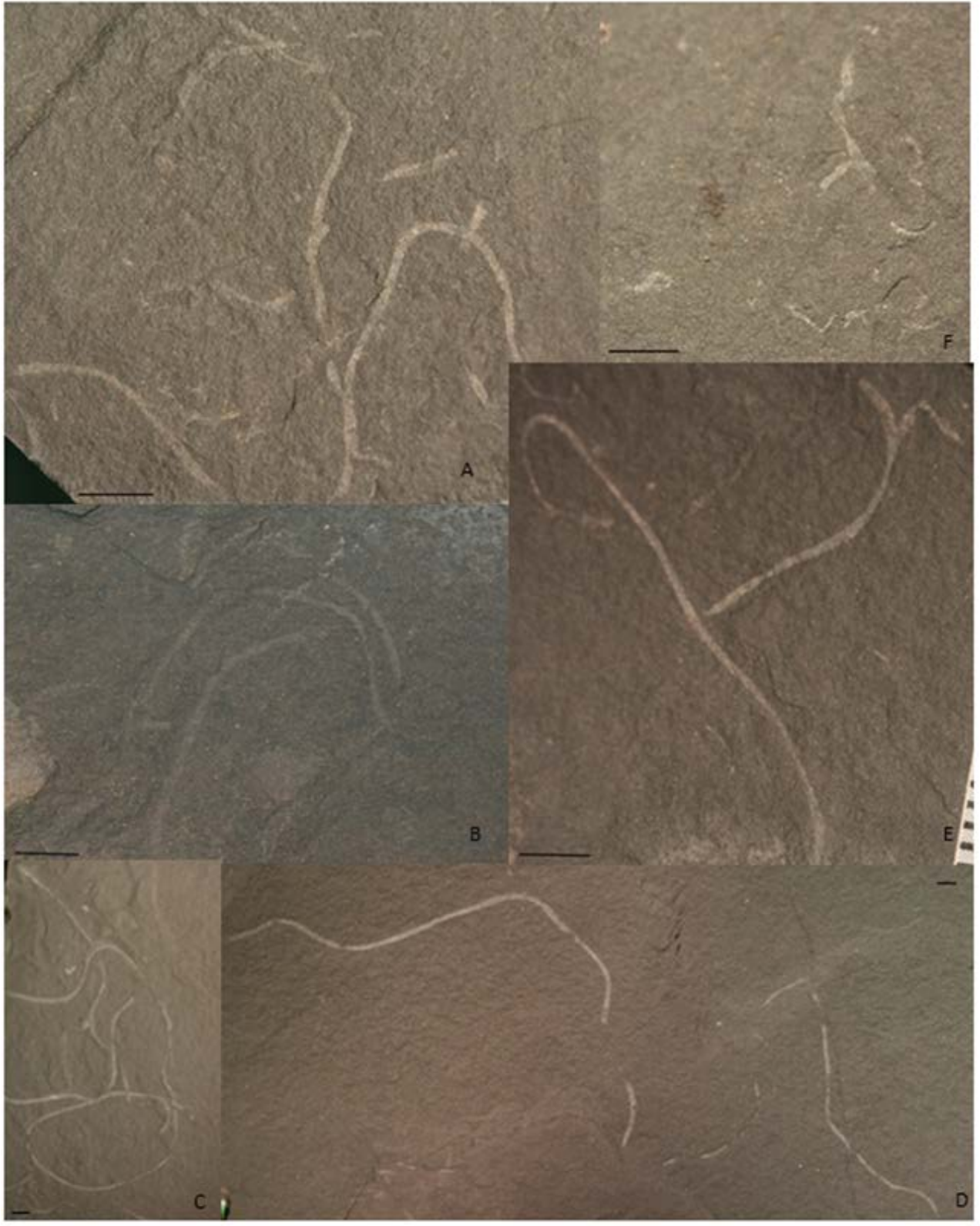


Figure 8. The Zuun-Arts morphologies. A,E) dichotomously branching, B) fan-shaped, C) monopodial branching, D) non-branching, F) shrub-like. Scale bars= 3mm.

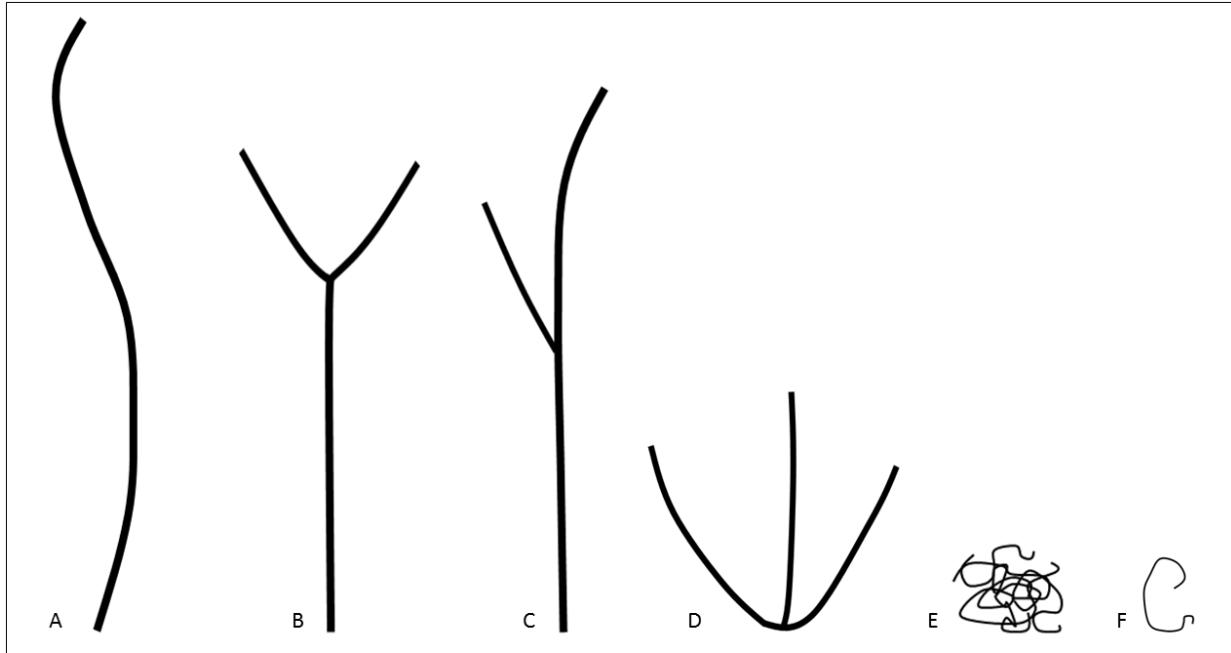


Figure 9. Illustrations of the Zuun-Arts morphologies. A) non-branching, B) dichotomously branching, C) monopodial branching, D) fan-shaped, E) shrub-like, F) small non-branching.

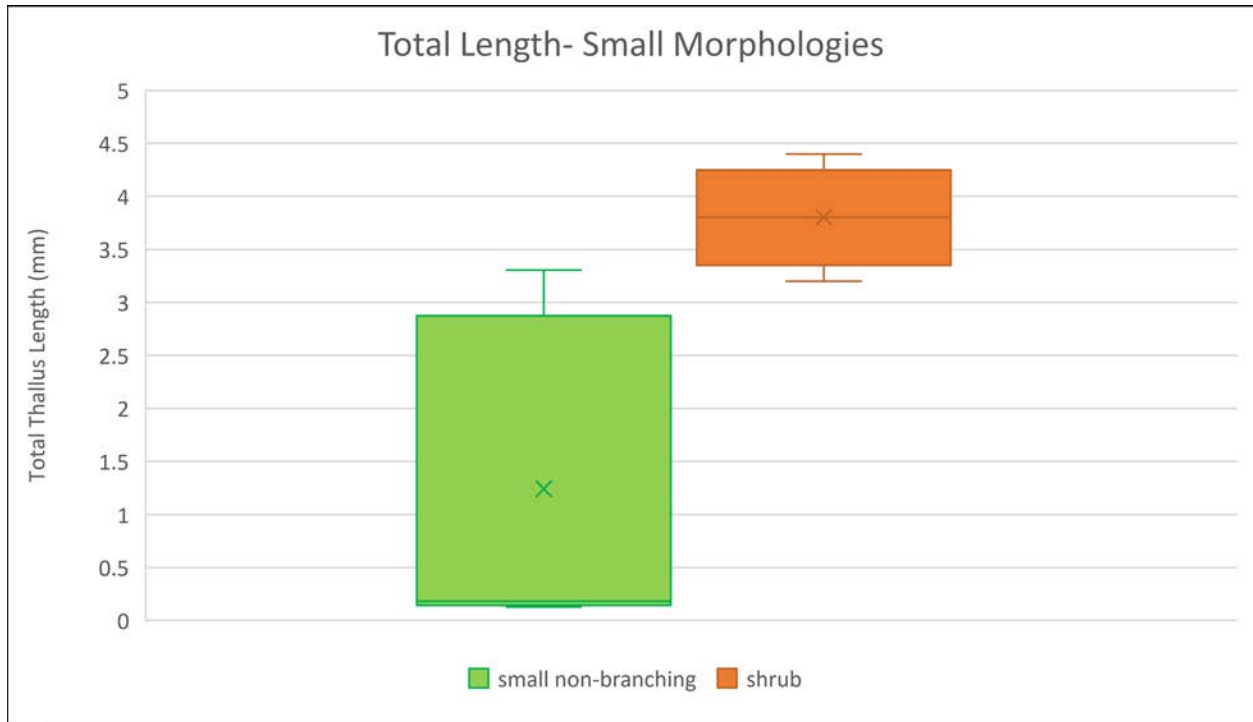


Figure 10. Box and whisker plot showing total thallus length of the small non-branching and shrub-like morphologies. Median value is marked by the middle horizontal bar, mean is indicated with an X.

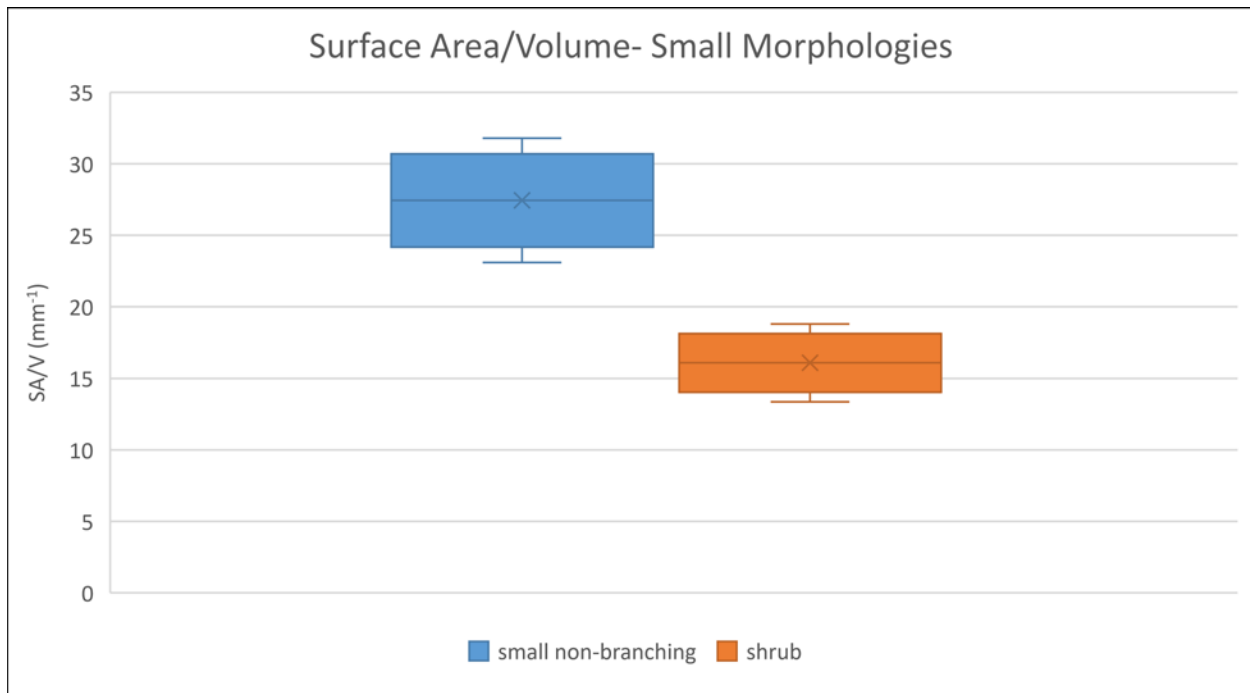


Figure 11. Box and whisker plot showing surface area/volume ratio of the small non-branching and shrub-like morphologies. Median value is marked by the middle horizontal bar, mean is indicated with an X.

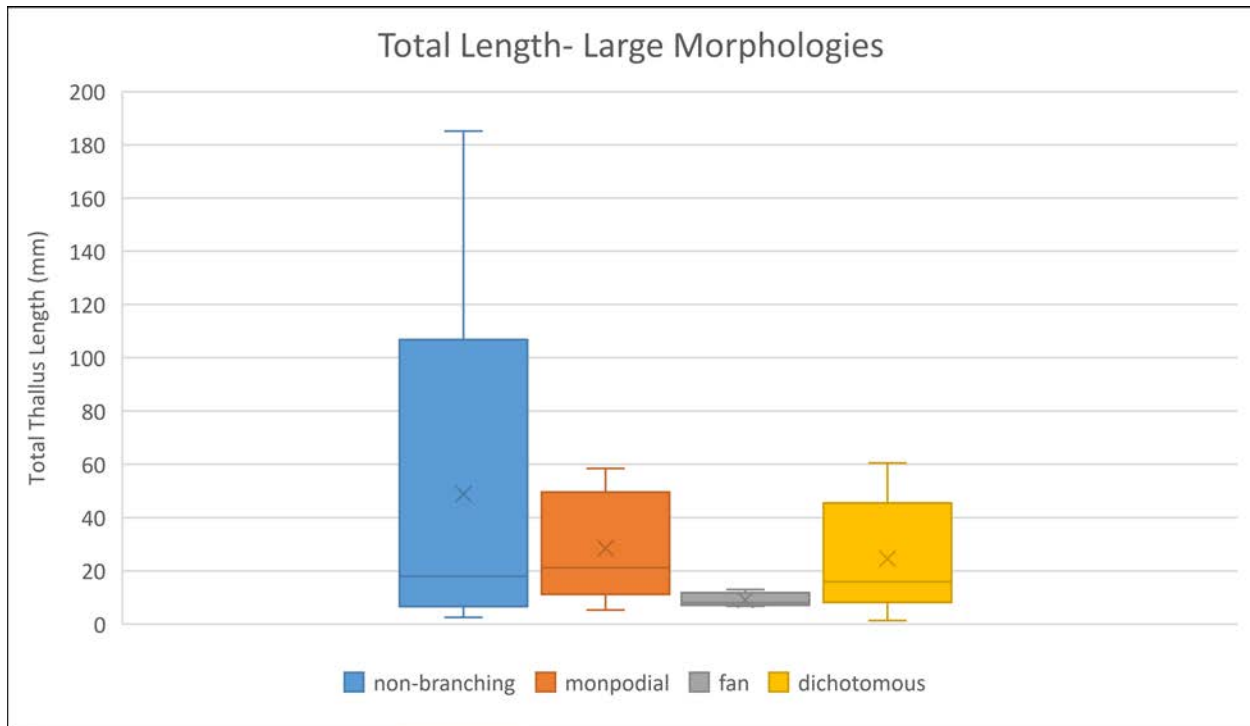


Figure 12. Box and whisker plot showing total thallus length of the non-branching, monopodial, fan-shaped, and dichotomous branching morphologies. Median value is marked by the middle horizontal bar, mean is indicated with an X.

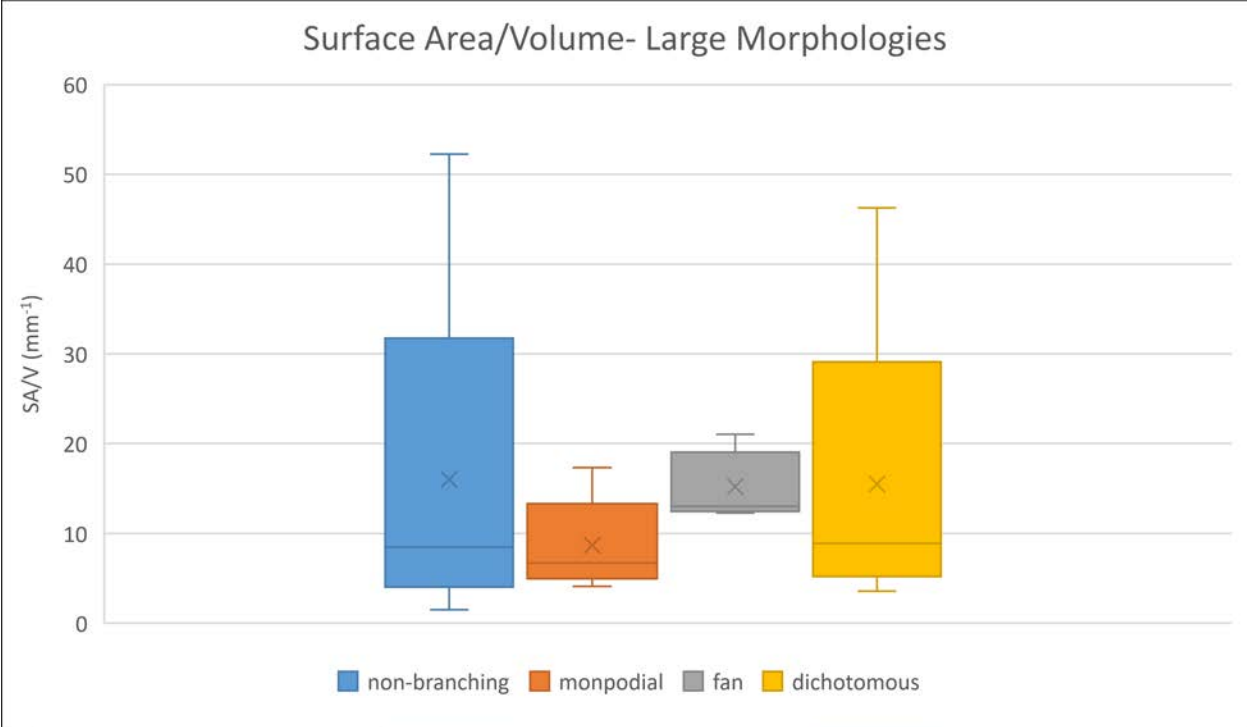


Figure 13. Box and whisker plot showing surface area/volume ratio of the non-branching, monopodial branching, fan-like, and dichotomously branching morphologies. Median value is marked by the middle horizontal bar, mean is indicated with an X.

Chinggiskhaania: Non-branching morphology

The non-branching morphology is composed of a single, non-branching element with a median length of 17.9 mm (Figure 12), a median width of 0.48 mm, and a median surface area/volume ratio of 8.47 mm⁻¹ (Figure 13). Non-branching fossils are found straight, slightly curved, or twisted, and often overlap each other on slabs containing multiple fossils. Non-branching fossils lack any evidence of basal attachment structures, transverse lineations, or distal tapering in width across the thallus.

Chinggiskhaania: Single monopodial branching morphology

The single monopodial branching morphology is composed of a central element running the entire length of the thallus and 1-2 secondary elements branching off the central axis in a monopodial fashion. The central element is straight or slightly curved and has a median length of 17.0 mm (Figure 12) and median width of 0.57 mm. Secondary elements have a median length of 5.10 mm, median width of 0.39 mm and a median branching angle of 50°. Thalli have an overall median canopy height of 17.0 mm, and surface area/volume ratio of 6.70 mm⁻¹ (Figure 13).

Chinggiskhaania: Dichotomously branching morphology

The dichotomous branching morphology consists of one primary element and two dichotomously branching secondary elements. Primary elements have a median length of 10.7 mm (Figure 12) and median width of 0.44 mm. Secondary elements have a median length of 8.66, median width of 0.45 mm, and a median branching angle of 60.4°. Thalli have an overall

median canopy height of 15.0 and median surface area/volume ratio of 8.89 mm⁻¹ (Figure 13).

All thalli have only one level of branching (1 primary element and 2 secondary elements).

Chinggiskhaania: Fan-shaped morphology

The fan shaped morphology is composed of 2-3 primary elements that come together in a fan shape. Individual elements have a median length of 8.084 mm (Figure 12) and median width of 0.31 mm. Thalli have an overall canopy height of 8.08 mm and median surface area/volume ratio of 13.0 mm⁻¹ (Figure 13).

Of the 821 individual fossils examined, the non-branching morphology is the most dominant with 761 specimens (92.7 %). Branching morphologies are the most abundant after non-branching with 39 dichotomously branching (4.8 %) and 14 monopodial branching (1.7 %) samples. There are only 3 fossils with a fan morphology (0.4 %), 2 with a small non-branching morphology (0.2 %) and 2 with a shrub-like morphology (0.2 %) (Figure 14).

Scanning electron microscopy

The results of EDS mapping show no variation in Fe and O concentrations between fossils and the surrounding matrix. There is, however, variation in C, Al and Si concentrations (Figure 15).

All fossils have increased concentrations of Al and are depleted in Si compared to the matrix.

Some fossils are composed entirely of Al, but most contain some amount of C (Figure 16). Some fossils have high concentrations of C around the margins and Al with little to no C in the center, however most have areas of elevated carbon throughout. Areas of the fossil with

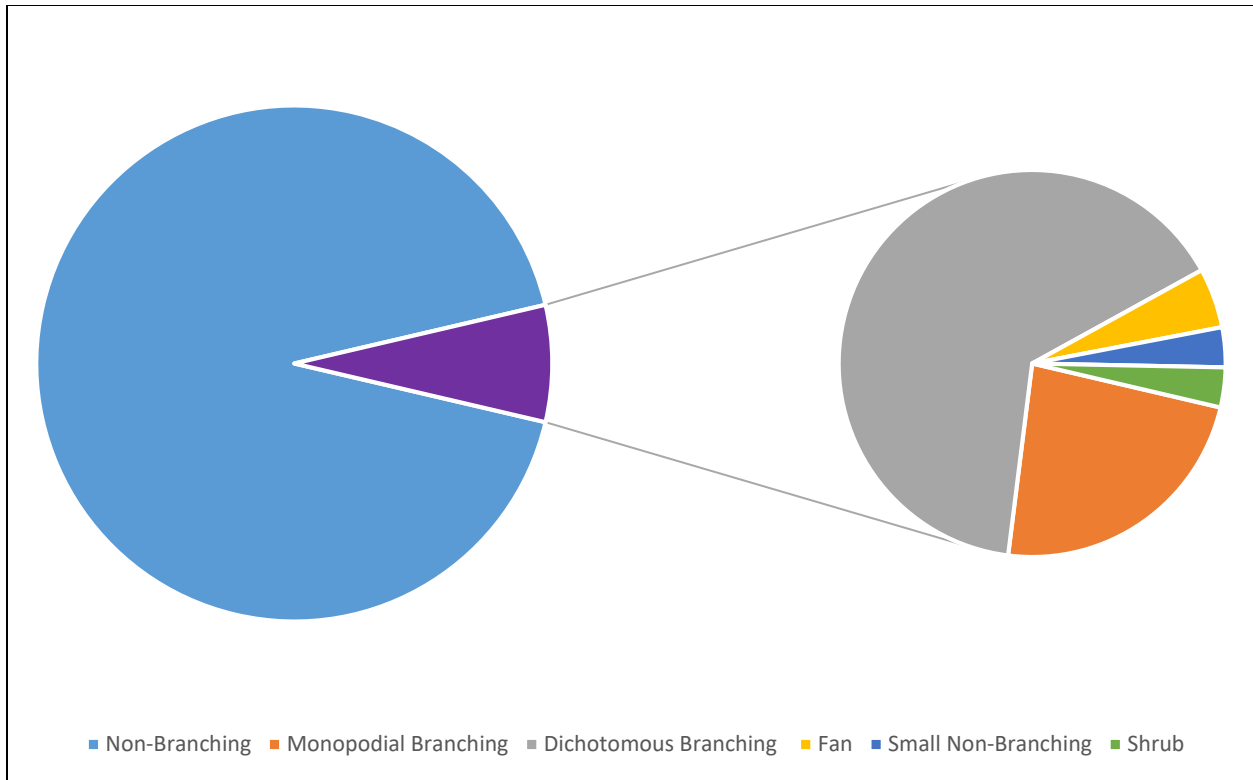


Figure 14. Pie chart showing the relative abundance of different morphologies in the Zuun-Arts biota. The non-branching morphology makes up 93% of the biota, with all other morphologies making up the remaining 7%.

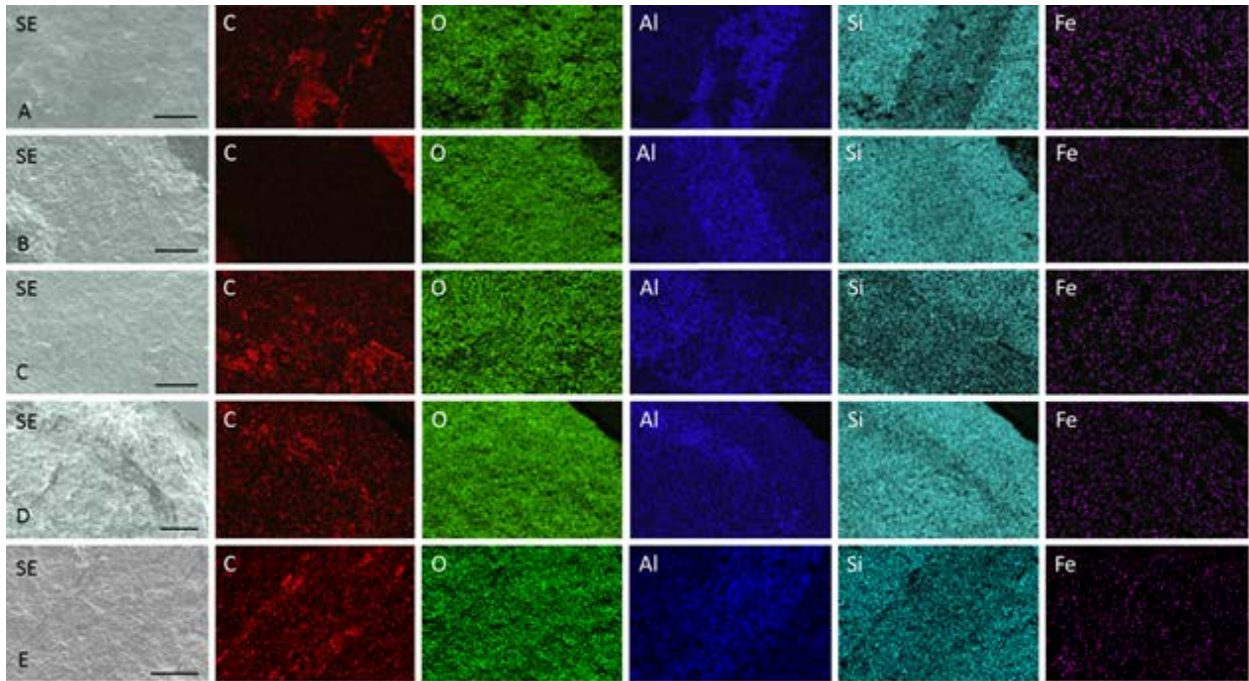


Figure 15. Selected SEM-EDS maps of 5 fossils and surrounding matrix. A) Note high C and Al concentrations and Si depletion throughout the fossil. Scale bar = 300 μm , final magnification = 90x. B) Note high Al concentration and Si depletion within the fossil and the total absence of C within the fossil. Scale bar = 300 μm , final magnification = 90 x. C) Note high C concentrations along the margins of and within the fossil and high Al concentrations and Si depletion throughout. Scale bar = 300 μm , final magnification = 90 x. D) Note high C and Al concentrations and Si depletion throughout the fossil. Scale bar = 400 μm , final magnification = 50 x. E) Note high C concentrations along the margins and high Al and Si depletion throughout the fossil. Scale bar = 200 μm , final magnification = 130 x.

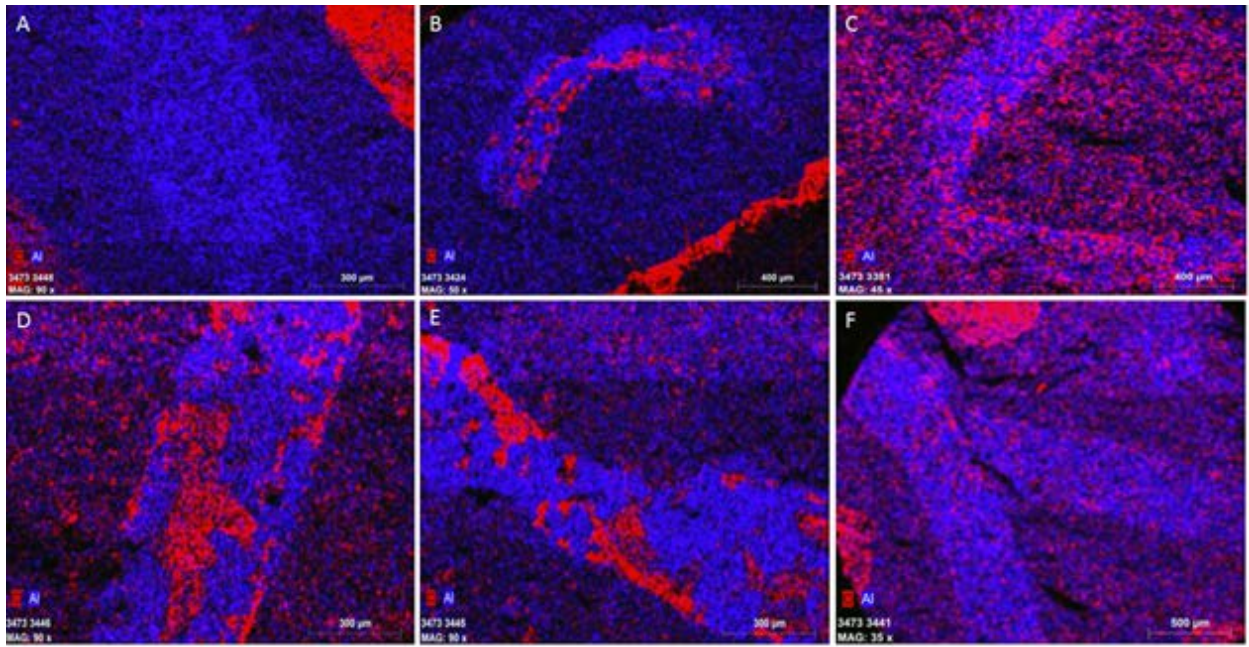


Figure 16. EDS maps of fossils and surrounding matrix showing concentrations of C and Al. Areas of the fossils have elevated concentrations of C or Al, but never both.

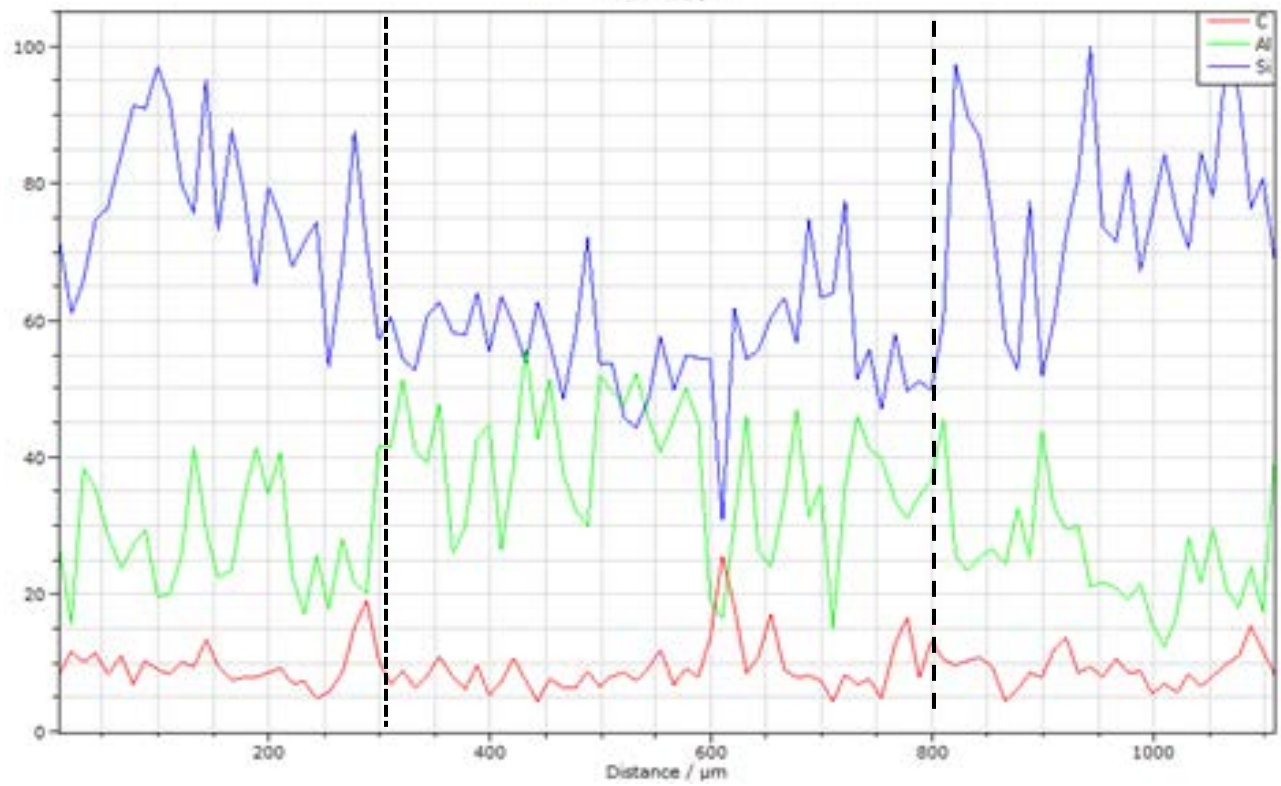
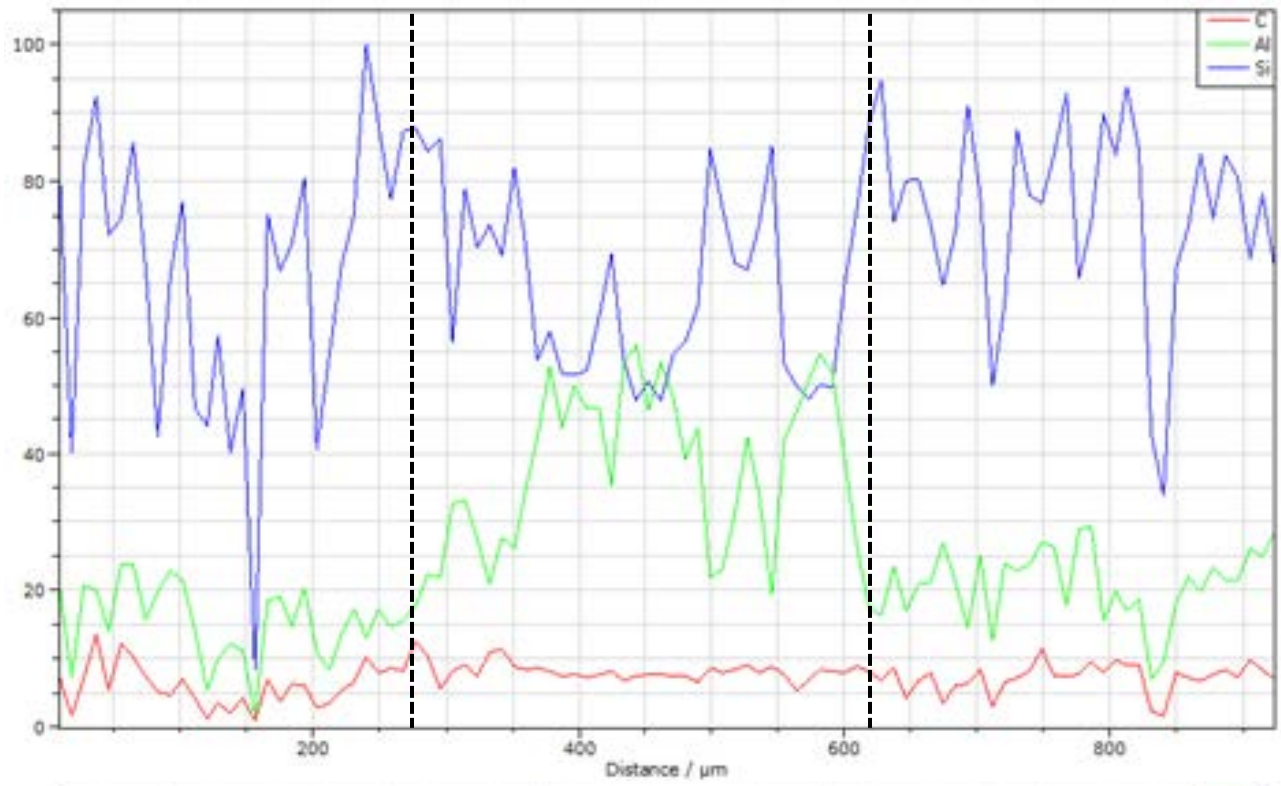
high Al concentrations are depleted in C, and areas of high C concentrations are depleted in Al. All fossils are depleted in Si regardless of the distribution of Al and C.

The relationship between C, Al, and Si is especially clear in line scans run perpendicular to the long axis of the fossils (Figure 17). In most specimens, Si concentrations are initially high in the matrix, decline sharply when the line passes over the fossil, then increase again when the line passes over the fossil and back into the matrix on the opposite side. Al concentrations show the opposite pattern: Al is relatively low in the matrix, increases sharply within the fossil, and then declines in the matrix on the opposite side. Similar to the elemental maps, line scans show variable C concentrations within the fossils, but are consistently low in the matrix. In specimens containing carbon within the fossil, spikes in C correspond to decreases in Al.

In backscatter images of the Zuun-Arts fossils, areas with high C concentrations appear as conspicuous black to brown spots, and areas of high Al concentrations are not visible (Figure 18).

X-ray diffraction

XRD patterns for all samples have large 2θ peaks around 9, 18, 21, and 27, although there is some variation between samples (Figure 19). For the three samples run with ethyl glycol, there is no difference in XRD patterns with and without ethyl glycol (Figure 20). In addition, there is no major difference in XRD patterns between samples from the fossil bearing and non-fossil bearing intervals.



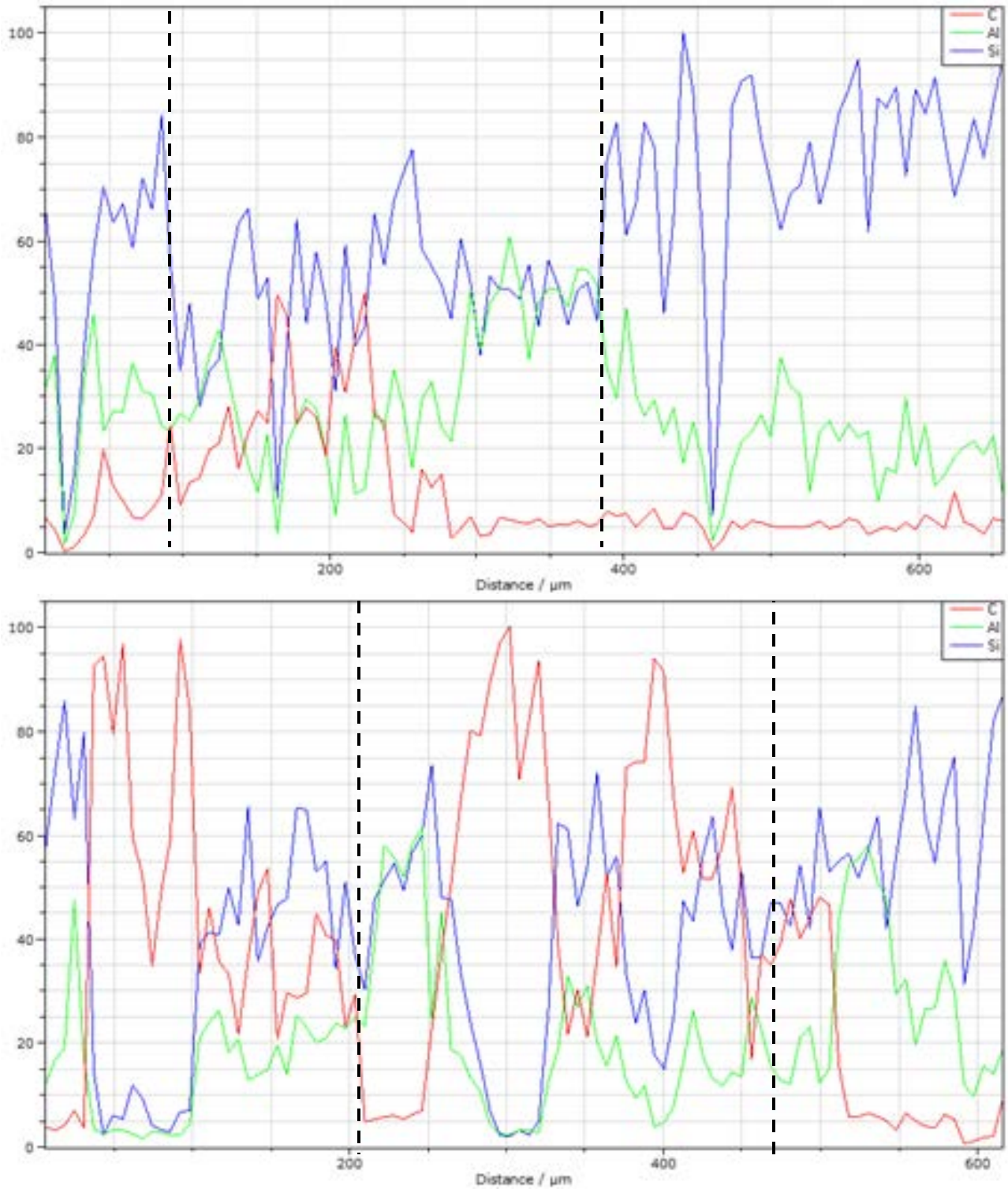


Figure 17. Line scans run across the width of fossils, including a small amount of matrix on either side. Fossil margins are marked by vertical dashed lines. Fossils containing C also have large carbon peaks within the fossil. Line scan distance vary from 600 μm to 1,000 μm (see individual graphs).

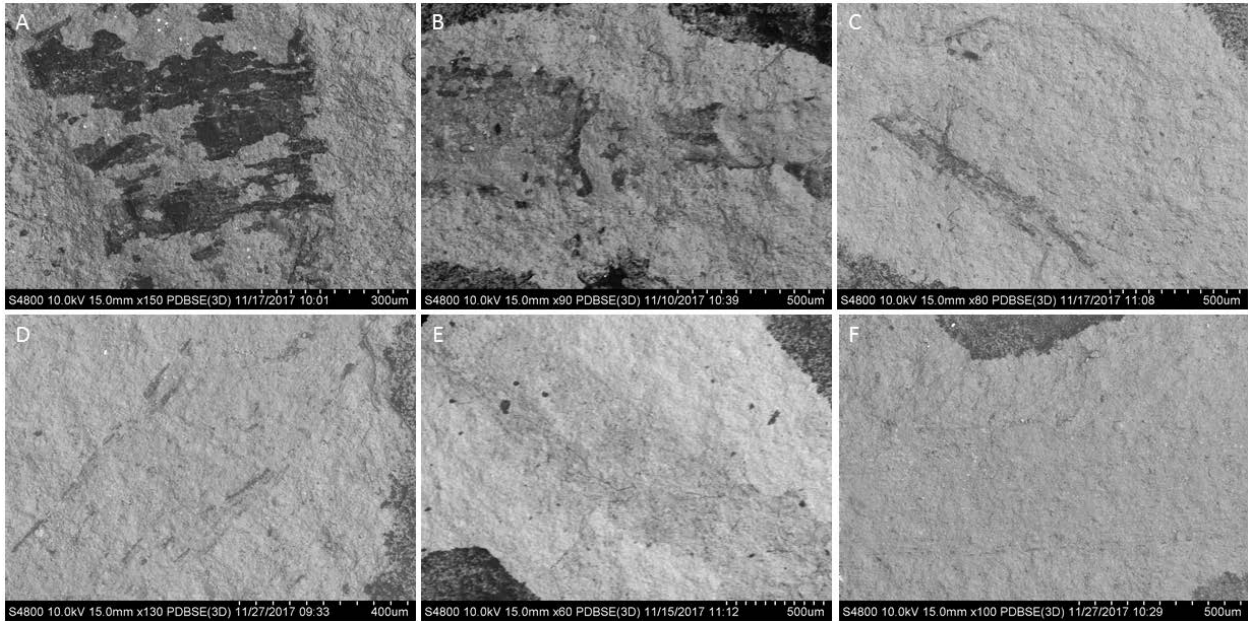


Figure 18. Backscatter images of fossils and surrounding matrix. Dark areas indicate high C concentrations, areas with high Al concentrations are indistinguishable from the surrounding material. Fossils containing high C concentrations (A-C) are clearly seen in BSE mode, fossils composed primarily of aluminum (D-E) show little to no contrast against the matrix. All images were taken at an accelerating voltage of 10 keV, see individual images for scale and final magnification.

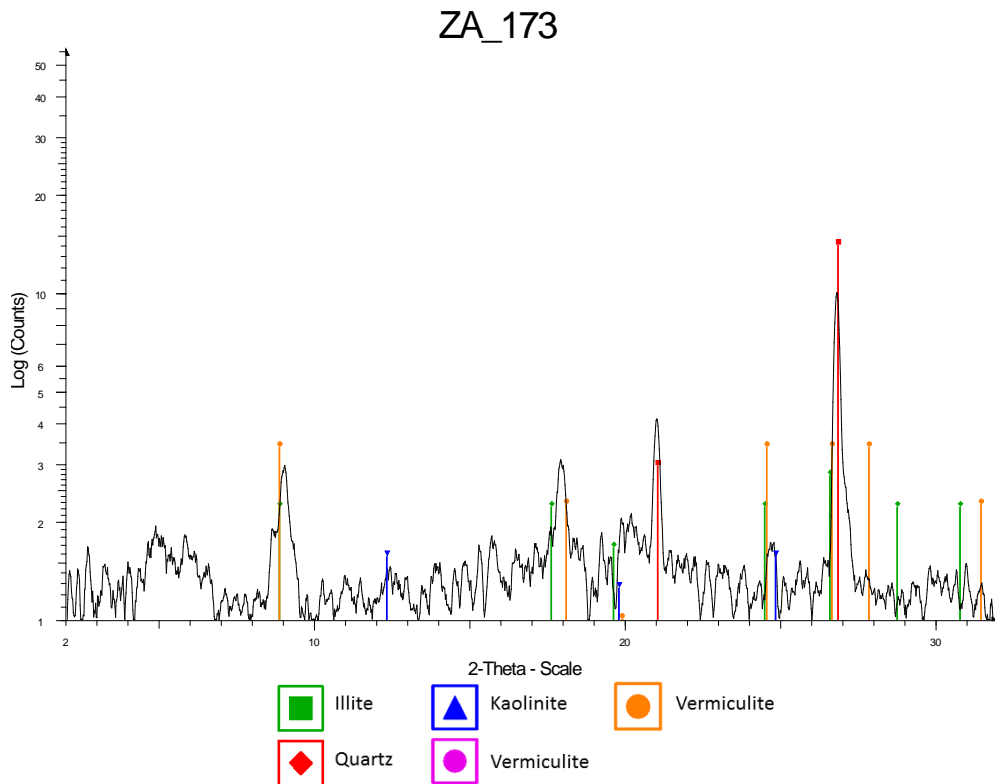
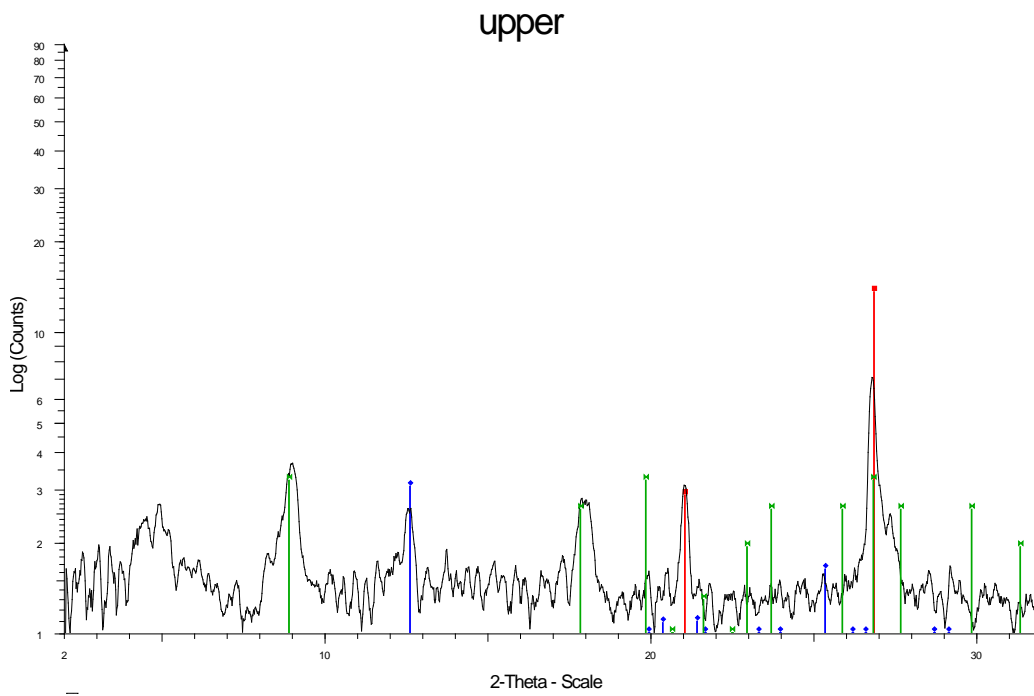


Figure 19. Clay fraction XRD patterns for samples from non-fossil bearing shale (upper) and fossil bearing shale (ZA_173) from the Zuun-Arts Formation. Notice the similarity of the two.

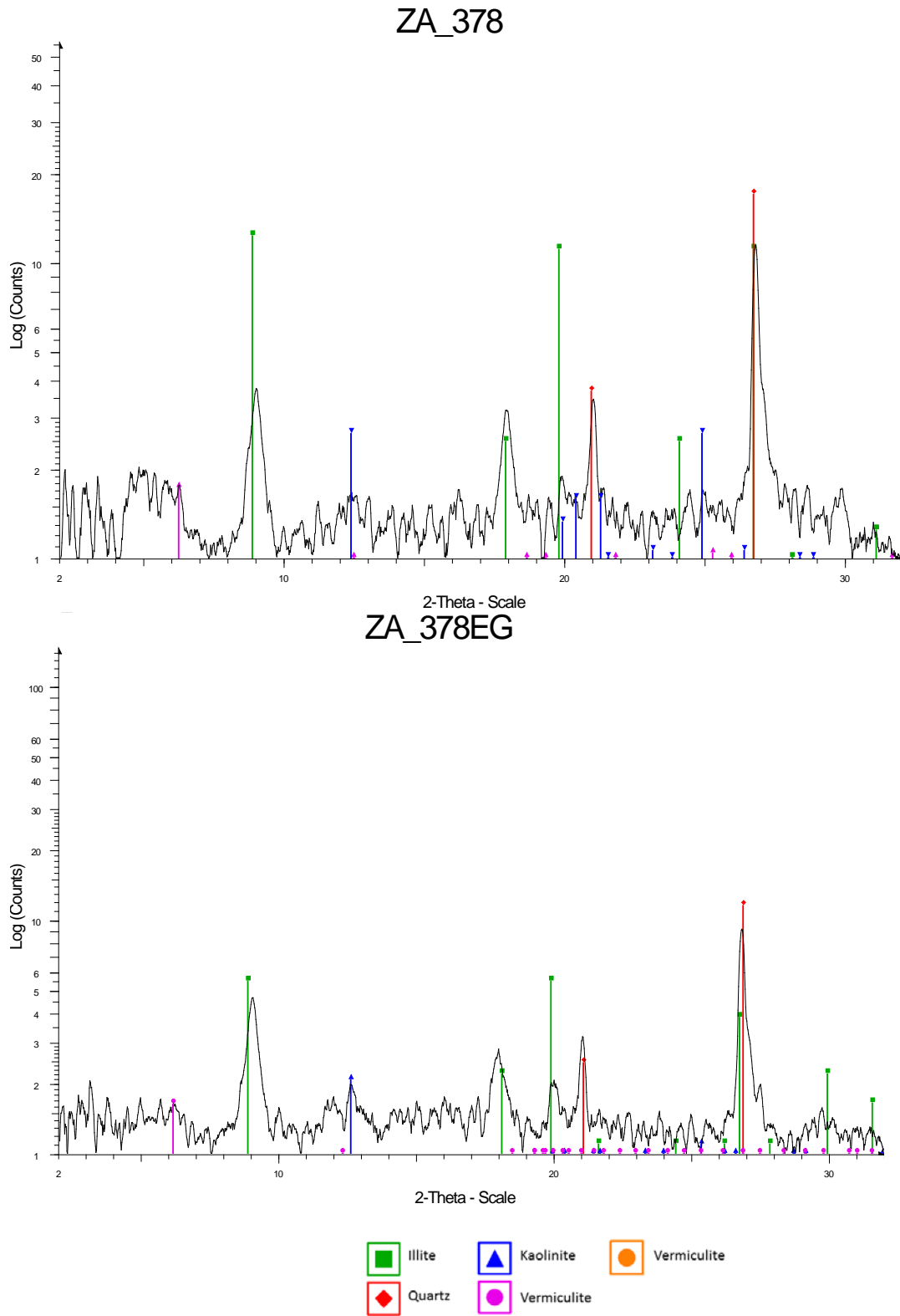


Figure 20. Clay fraction XRD patterns for a sample run without ethyl glycol (ZA_378) and with ethyl glycol (XA_378EG). The similarity of samples run with and without ethyl glycol indicates a lack of smectite.

Discussion

Morphology

Many body and trace fossils can have an ambiguous, tubular morphology similar to macroalgae, so a detailed morphological analysis is necessary to determine if the Zuun-Arts fossils are in fact macroalgae. Fossilized burrows have a tubular, branching morphology formed when an animal digs a burrow that later fills with sediment. The result is a 3-dimensional, often cylindrical fossil that can be distinguished from surrounding sediment by its tubular morphology as well as the burrow margins, which are not always clearly defined (Miller, 2007). In addition, burrows often result in disturbance of the sediment in the surrounding matrix (Cohen, 2009; LoDuca et al., 2017). The Zuun-Arts fossils are preserved as 2-dimensional films and are composed of C and/or Al, they are not 3-dimensional sediment-filled casts. Unlike some burrows, the Zuun-Arts fossils have sharp margins that are easily distinguishable from the surrounding matrix, and there is no evidence of disturbance of the surrounding sediment. All morphological data suggest that the Zuun-Arts fossils are not burrows or any other type of trace fossil.

BST macroalgae fossils can also look similar to hemichordate fossils such as graptolites, since both have a similar gross morphology and are commonly preserved as carbonaceous compressions (Muscente and Xiao, 2015). Although macroalgae and graptolites can appear superficially similar, close examination of the Zuun-Arts fossils under a microscope failed to detect any structural features found in graptolites such as theca or zooids. SEM-BSE imaging also suggests that the Zuun-Arts fossils are not graptolites, since they lack fusellae which would

suggest a hemichordate affinity (Figure 21) (Tang et al., 2017). Detailed morphological examination and SEM-BSE imaging suggest that the Zuun-Arts fossils are not hemichordates.

Another alternative interpretation of the Zuun-Arts fossils is that they are bacterial sheaths preserved as carbonaceous compressions. Some microorganisms living in marine environments attach to submerged substrates and many individuals align in a filamentous arrangement, enclosed by a sheath (LoDuca et al., 2017). Bacterial sheaths have morphologies similar to the non-branching fossils in the Zuun-Arts biota and can be preserved as BST fossils, however the Zuun-Arts fossils are about ten times larger than the largest known bacterial sheaths (LoDuca et al., 2017). The size of the Zuun-Arts fossils alone suggests that they are not bacterial sheaths preserved as carbonaceous compressions.

In addition to ruling out the possibility that the Zuun-Arts fossils are burrows, graptolites or bacterial sheaths, several morphological features including the length, width, and branching are also consistent with a macroalgae interpretation. Most of the Zuun-Arts fossils also bear a morphological resemblance to other types of Ediacaran macroalgae.

The non-branching specimens of *Chinggiskhaania* have a morphology that closely resembles the macroalgae genus *Sinocylindra*, which is common in the Ediacaran Miaohu biota, although *Chinggiskhaania* is generally smaller than most specimens of *Sinocylindra*. *Chinggiskhaania* has a median length of 17.865 mm and a median width of 0.481 mm, while *Sinocylindra* has a median length of 28.33 mm and median width of 0.481 mm (Xiao et al., 2002). Although *Sinocylindra* is larger, two have similar surface area-volume ratios, with *Sinocylindra* having a ratio of 7.77 mm^{-1} and *Chinggiskhaania* having a ratio of 8.47 mm^{-1} .

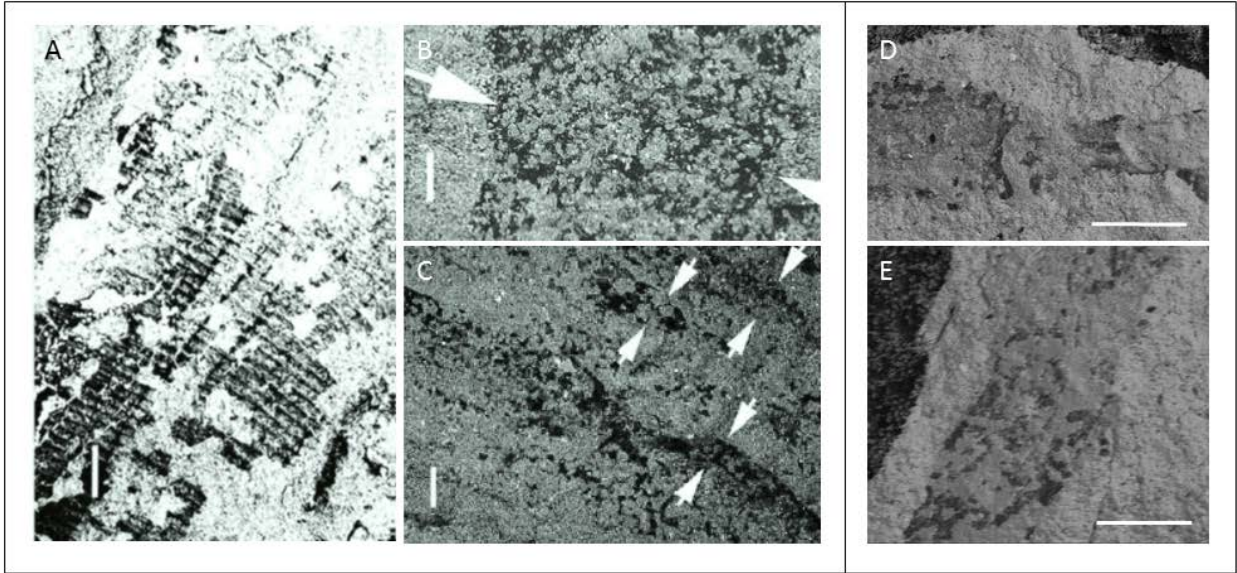


Figure 21. A-C) Backscatter images of (A) BST hemichordate fossil and (B-C) BST macroalgae fossils. Scale bars = 0.2 mm. D-E) BST macroalgae fossils from the Zuun-Arts biota. Scale bars = 0.5mm, final magnification = 90x. Note the transverse bands in A and lack of bands or any other internal structures in B-E. Modified from LoDuca et al. (2017).

The fan-shaped morphology of *Chinggiskhaania* somewhat resembles the Ediacaran macroalgae *Doushantuophyton cometa*, although the *Chinggiskhaania* specimens are much simpler. Fan-shaped *Chinggiskhaania* and *Doushantuophyton cometa* specimens have similar median lengths of 8.084 mm and 11.92 mm, respectively. With a median width of 0.09 mm, *Doushantuophyton cometa* filaments are generally much thinner than *Chinggiskhaania* filaments, which have a median width of 0.311 mm (Xunlai et al., 1999). The two also differ with respect to surface area-volume ratio and number of filaments. *Doushantuophyton cometa* has a SA/V of 44.61 mm⁻¹ and about 40 filaments on average (Xunlai et al., 1999), *Chinggiskhaania* has a SA/V of 13.016 mm⁻¹ and only 3 filaments. Based on these morphological data it is unclear whether the fan-shaped *Chinggiskhaania* morphology has any direct relationship to *Doushantuophyton cometa*. Although the fan-shaped morphology is much simpler than *Doushantuophyton cometa*, the general morphological resemblance at least indicates that this morphology is consistent with a macroalgae interpretation.

The dichotomously branching morphology of *Chinggiskhaania* bears a general morphological resemblance to the Ediacaran macroalgae *Doushantophyton rigidium*. The dichotomous branching form of *Chinggiskhaania* and *Doushantophyton rigidium* both have a similar morphology consisting of a primary element that terminates in two dichotomous branches, and similar heights of 14.988 mm and 15.28 mm, respectively. *Chinggiskhaania* has a median width of 0.438 mm, has only 2 branches, and has a surface area-volume ratio of 8.891 mm⁻¹, while *Doushantophyton rigidium* has a median width of 0.09 mm, has up to 6 branches, and has a surface area-volume ratio of 44.58 mm⁻¹ (Xiao et al., 2002). Based on the number of branches and surface area-volume ratio, it appears that *Doushantophyton rigidium* is more complex than

the dichotomously branching *Chinggiskhaania* specimens. Overall, *Chinggiskhaania* does have a morphology generally similar to that of *Doushantophyton rigidium*, indicating that *Chinggiskhaania* has a macroalgae affinity.

The single monopodial morphology of *Chinggiskhaania* resembles a simpler version of *Doushantophyton quyuanii*, which is composed of a central axis with 6 or more monopodial branches. The monopodial *Chinggiskhaania* has a median height of 16.96 mm and *Doushantophyton quyuanii* has a median height of 8.69 mm, and *Chinggiskhaania* has only 1-2 monopodial branches. *Doushantophyton quyuanii* also has a greater surface area-volume ratio of 33.49 mm⁻¹ (Xunlai et al., 1999), compared to *Chinggiskhaania*, which has a ratio of 6.704 mm⁻¹. The monopodial branching morphology of *Chinggiskhaania* is morphologically similar to *Doushantophyton quyuanii*, but is simpler in terms of the number of branches and surface area-volume ratio.

The shrub-like thallus of *Zuunartsphyton* is morphologically similar to the Ediacaran macroalgae *Glomulus filamentous*, which consists of a number of fine filaments twisted together into a colony. The shrub morphology of *Zuunartsphyton* consists of about 6 filaments forming a colony with a total width of 3.80 mm, while *Glomulus filamentous* consists of about 10 filaments forming a colony with a total width of 5 mm (Xiao et al., 2002).

The small non-branching morphology of *Zuunartsphyton* does not resemble any known form of macroalgae from the Ediacaran or early Paleozoic. Although it is possible that the small non-branching form represents a novel morphology, it is more likely that these specimens are fragments or an earlier life cycle stage of *Chinggiskhaania*. Reproductive bodies are not

preserved in the Zuun-Arts fossils, so it is not possible to know with certainty how these organisms reproduced or what earlier life cycle stages would have looked like. The results of this morphological analysis indicate that the Zuun-Arts fossils are not trace fossils, graptolites or bacterial sheaths and that they bear a strong morphological resemblance to other Ediacaran macroalgae, supporting the hypothesis that these fossils are indeed macroalgae.

Comparison of the Zuun-Arts biota with other Ediacaran BST deposits

Lagerstätten are not common in the Ediacaran, and those that do occur often do not contain BST preservation, but when BST preservation is present, macroalgae fossils are often preserved (Xiao, 2002). Two Ediacaran BST deposits, the Lantian biota and the Miaohe biota, preserve a large number of macroalgae with a variety of morphologies (Xunlai et al., 1999; Xiao et al., 2002). Compared to the Lantian and Miaohe biotas, the Zuun-Arts fossils are morphologically simple, and the biota as a whole is low in diversity, although the Zuun-Arts fossils do have length (Figure 22) and surface area-volume ratios similar to macroalgae in the Lantian and Miaohe biotas (Figure 23). The Lantian biota contains 13 macroalgae morphotypes (Xunlai et al., 1999) and the Miaohe biota contains 23 (Xiao et al., 2002), while the Zuun-Arts contains only 6. The Lantian and Miaohe biotas also include macroalgae with complex morphologies including a variety of complex dichotomous and monopodial branching thalli and tube-shaped thalli, some of which contain rhizoidal holdfasts and septation. The Lantian biota also contains enigmatic fossils that may have a metazoan affinity (Xunlai et al., 1999; Xiao et al., 2002). The Zuun-Arts biota lacks much of the morphological complexity seen in the Lantian and Miaohe biotas, and is morphologically simple even when compared to much older deposits (Han and

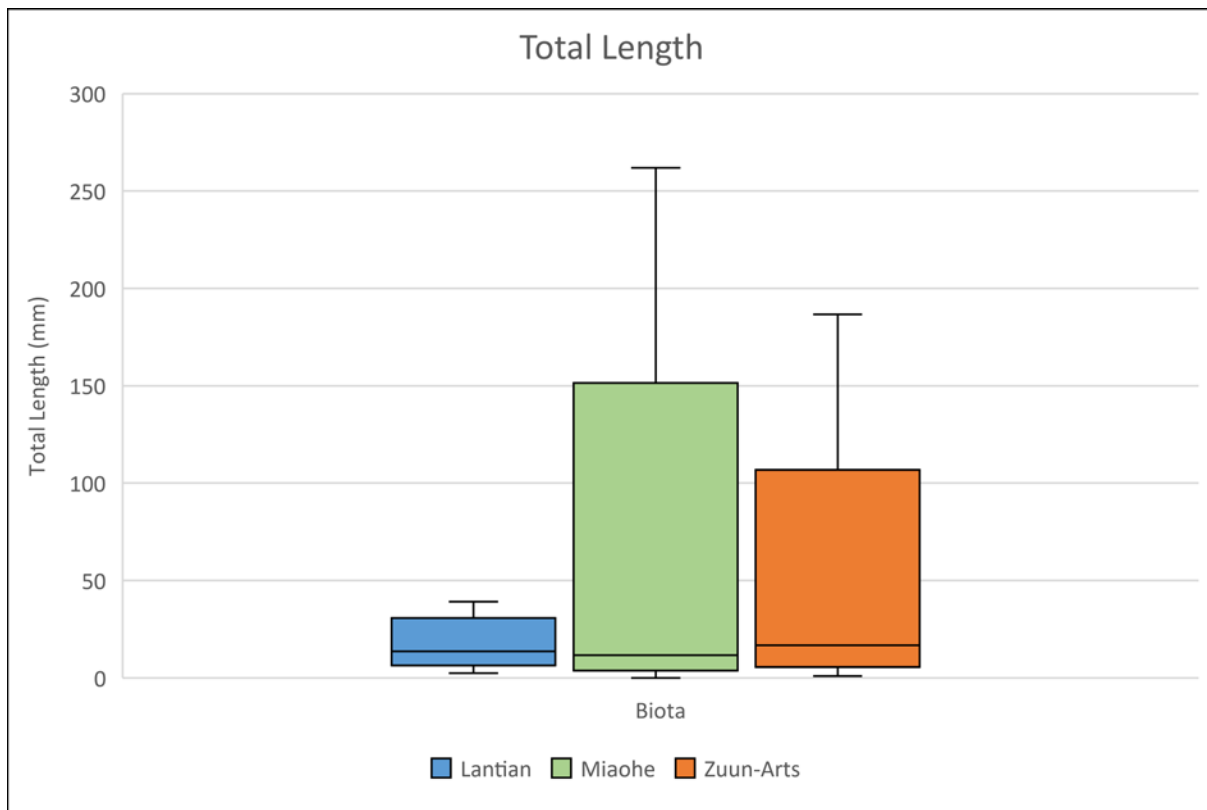


Figure 22. Box and whisker plot showing total length values for macroalgae from the Lantian, Miaohe, and Zuun-Arts biotas. Note how similar the median values are in all three biotas.

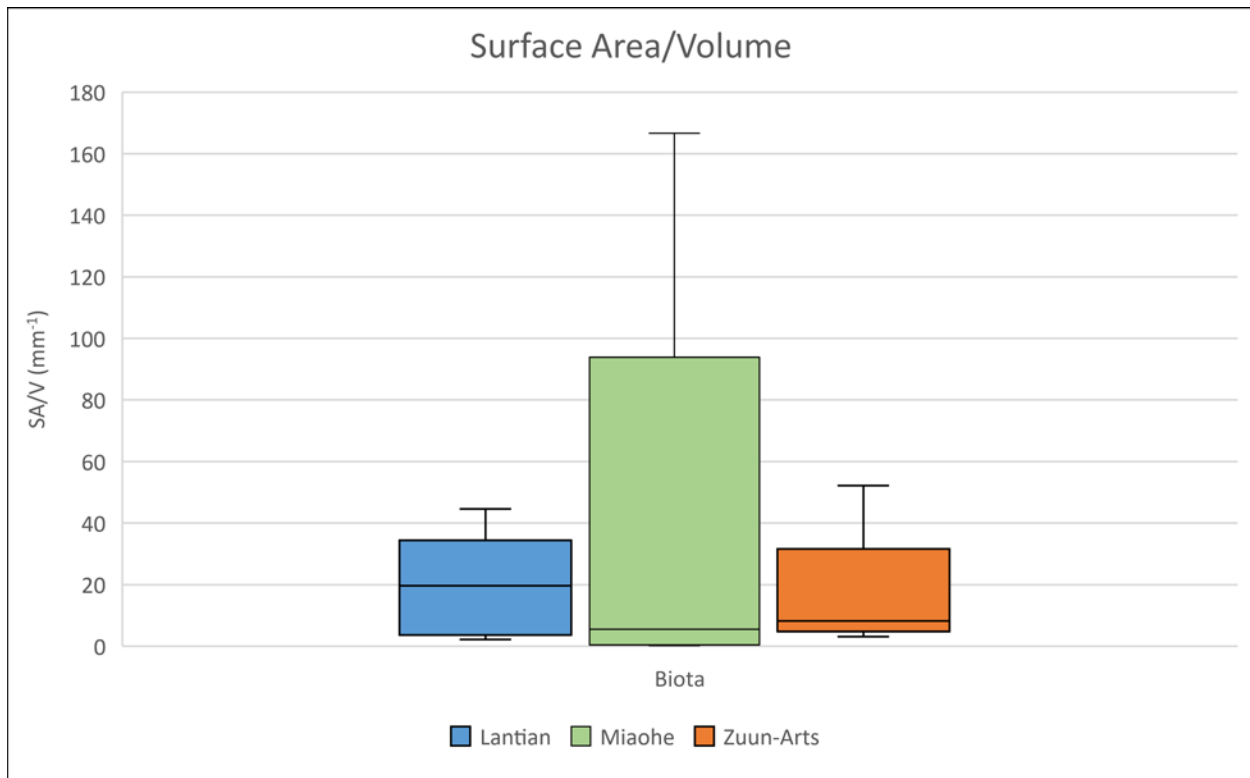


Figure 23. Box and whisker plot showing surface area-volume ratios for macroalgae from the Lantian, Miaohe, and Zuun-Arts biotas. Median surface area-volume ratios for the Zuun-Arts fossils fall in between those for macroalgae from the Lantian and Miaohe biotas.

Runnegar, 1992). Definitive rhizoidal and discoidal holdfasts, annulations, and some degree of structural differentiation dates back to at least the Mesoproterozoic (Xiao and Dong, 2006).

The Zuun-Arts biota is composed entirely of macroalgae belonging to FFG 1 and FFG 2, although over 93% of all specimens are in FFG 1 (non-branching). The Miaohe and Lantian biotas include macroalgae that fall within FFG 1, however most belong the FFG 2 or FFG 2.5. These morphologies indicate that the Zuun-Arts macroalgae are highly photosynthetically productive and lack environmental hardiness and the ability to resist herbivorous predation. Specimens of the genus *Doushantophyton* tend to have higher surface area-volume ratio than specimens of *Chinggiskhaania*, which may suggest that *Doushantophyton* was more photosynthetically efficient than *Chinggiskhaania*, however *Doushantophyton* specimens also tend to have more branches than *Chinggiskhaania*, which could reduce photosynthetic efficiency by increasing self-shading (Xiao and Dong, 2006).

Ediacaran macroalgae as a whole are simple compared to early Paleozoic macroalgae. The simplicity of Ediacaran morphologies should not be surprising, since much of the Paleozoic diversification of thallus morphology was driven by competition for light and adaptation to herbivorous predation (LoDuca et al., 2017; Littler and Littler, 1980). Macroalgae communities were just beginning to form in the Ediacaran, and the low number of individual macroalgae in a given community, especially in the Zuun-Arts biota, suggests there probably was not much competition for light, unlike in the dense, robust communities that formed in the Paleozoic (LoDuca et al., 2017). In addition to competition for light, adaptation to predation has been a major driving force behind macroalgae diversification. Most of the trends in macroalgae

evolution seen in the Phanerozoic, including an increase in surface area-volume ratio, a higher degree of thallus differentiation, the advent of lateral monopodial branching, and an overall increase in thallus toughness, have been driven by herbivorous predation (Littler and Littler, 1980). Although evidence of small-scale herbivorous predation by microscopic organisms may be impossible to detect in the fossil record, there are no known examples of macro-herbivorous predation in the Ediacaran fossil record (LoDuca et al., 2017). The lack of predation and competition for light in Ediacaran macroalgae communities may explain the simplicity of thallus morphology. Structural differentiation comes with an enormous energy cost, so it makes sense that macroalgae facing little competition or predation pressure would not expend the energy required to develop more complex thallus morphologies. Ediacaran macroalgae are morphologically simple, highly photosynthetically efficient, and seem to be very well equipped for life in the Ediacaran.

Scanning electron microscopy

The SEM-EDS results indicate BST preservation as Al and sometimes C-rich films. These results are consistent with the SEM-EDS results from Dornbos et al. (2016), which indicate that the Zuun-Arts fossils are preserved primarily as aluminosilicate mineral films with some areas of elevated C content. Overall, these results support the second major hypothesis of this project, that the Zuun-Arts fossils are preserved through BST preservation as aluminosilicate mineral films.

Although the goal of this project was not to evaluate the different models for the formation of BST fossils, the SEM-EDS data obtained may provide some new insight into the process. SEM-

EDS data for the Zuun-Arts fossils does not necessarily provide support for or against the early diagenesis or late diagenesis models outlined earlier, but it may have implications for some aspects of these models.

The early diagenesis model proposed by Orr et al. (2009) suggests a variety of ways that authogenic clay films can form in early diagenesis, as well as several models of how the elemental composition of fossils may appear based on the way the fossil splits into part and counterpart (Figure 2). In the early diagenesis model, the aluminosilicate film can form on the outside or inside of the cuticle, resulting in an a film composed of an internal C layer with Al above and below it, or an internal Al layer with C above and below it. Orr et al. (2009) also suggest that, when the fossil is split into part and counter-part, the split will happen preferentially through the C layer, the Al layer, or through the sediment encasing the fossil. In all cases, this model proposes that the splitting plane is confined to a single layer of the fossil, which should result in a fossil with a homogenous elemental composition.

SEM-EDS results clearly show that some of the Zuun-Arts fossils are composed of Al and C, which seems to be inconsistent with the early diagenesis model. These results do not disprove the early diagenesis model as a mechanism for BST preservation, but do suggest that the model of how fossils split into part and counterpart may need to be revisited. It is possible that BST films do form in the way proposed in the early diagenesis model, but that the splitting plane is not always confined to a single layer of the film. Many of the Zuun-Arts fossils are composed mostly of Al, which is consistent with the splitting plane being confined to a single layer. The

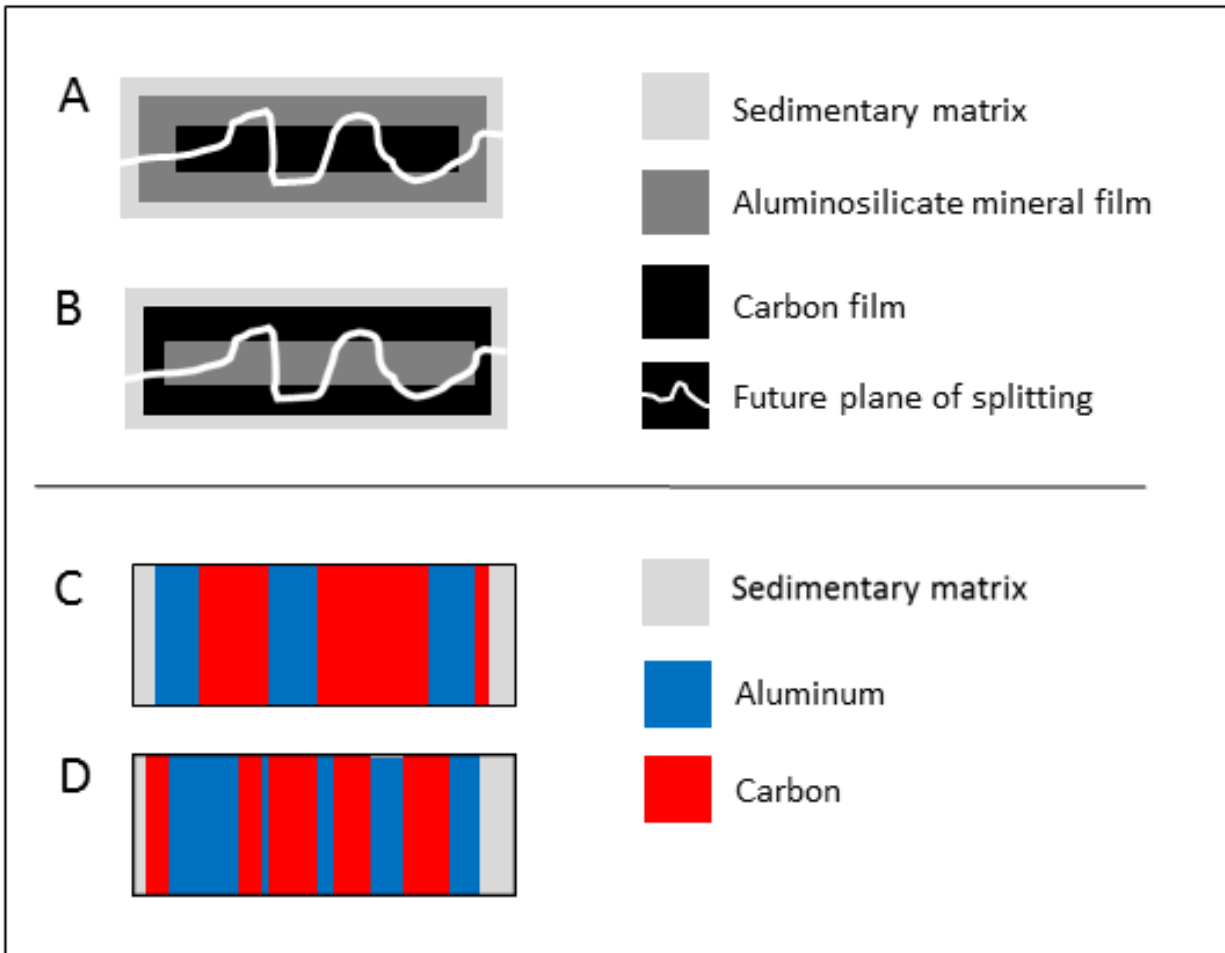


Figure 24. One possible alternative to the splitting paths proposed in the early diagenesis model for the formation of BST fossils. A-B) cross section view of a zig-zag splitting path breaking through C and Al layers. C-D) the theoretical SEM-EDS map pattern created by the zig-zag splitting paths shown in A and B. This provides a potential explanation for the SEM-EDS map patterns seen in the Zuun-Arts fossils that does not necessarily conflict with the early diagenesis model.

Zuun-Arts fossils containing Al and C may represent instances where the splitting plane was not confined to one layer, leading to a fossil showing Al and C in SEM-EDS (Figure 24).

The SEM-EDS results from the Zuun-Arts fossils are generally consistent with the late diagenesis model for BST fossil formation proposed by Butterfield et al. (2007). This model proposes that BST films are originally composed of organic C left behind by the organism in early diagenesis, and that the original C film is gradually overprinted by aluminosilicate minerals in later diagenesis as a result of low-grade regional metamorphism. Over time, this process should lead to a film composed entirely of aluminum. This taphonomic model may be able to explain why some of Zuun-Arts fossils contained C and Al; the original C films had not been completely overprinted by Al yet when regional metamorphism ended. However, it does seem odd that there would be any variation in the composition of fossils if regional metamorphism were the primary control of Al overprinting, since all of the Zuun-Arts fossils are from the same location, and have gone through the same diagenetic history. Overall, the SEM-EDS data from the Zuun-Arts fossils are generally consistent with both the early diagenesis and late diagenesis models, although they do raise minor concerns with both.

X-ray diffraction

Prominent 2θ peaks around 18 and 21 in XRD patterns can be accounted for by quartz in all samples. Besides quartz, the largest 2θ peaks in most samples can be accounted for by illite. XRD results indicate that the clay size fraction of the Zuun-Arts shale is composed primarily of quartz and illite, although most samples contain additional minerals. In several samples,

kaolinite, muscovite, and possibly glauconite and vermiculite can account for many of the smaller peaks.

Interestingly, there appears to be little to no montmorillonite in any of the samples. Some samples have one or two 2θ peaks that match montmorillonite peaks, but none have the large, low angle peaks that are diagnostic of montmorillonite. In addition, in samples re-run with ethylene glycol, XRD patterns with and without ethylene glycol are essentially identical. Smectite will absorb ethylene glycol, causing the XRD pattern to shift to the right (Moore and Reynolds, 1997). If the clay fraction contained montmorillonite, such a shift would have occurred after ethylene glycol was added to the slides, but this is not the case. It is possible that montmorillonite was present in early diagenesis and has since altered to illite. This process of alteration usually results in mixed layer illite-montmorillonite clays, however XRD analysis did not show any evidence of mixed layer illite-montmorillonite clay.

Butterfield (1990) suggested that smectite may be important in the BST preservation process due to its ability to absorb degradative enzymes, delaying soft tissue decay. The lack of montmorillonite in the Zuun-Arts fossil bearing shale suggests that smectite is not necessary for BST preservation to occur, although it may be beneficial when present. In addition, the similarity of the clay fraction in the fossil bearing and non-fossil bearing intervals of the Zuun-Arts Formation suggests that variation in clay mineral content cannot explain the lack of fossils in the non-fossil bearing intervals. Despite the lack of smectite in the Zuun-Arts Formation, clay minerals still play an important role in the BST preservation process. Even non-swelling clays could absorb degradative enzymes, since they have a large surface area compared to the non-

clay component of the clay sized fraction. In addition, all minerals in the clay fraction play an important role early in the taphonomic process by packing around the organism and sealing out oxygen. If the organism is not sealed tight very soon after death, there is no chance of preservation.

Conclusions

Morphological analysis of *Chinggiskhaania* and *Zuunartsphyton* from the Zuun-Arts biota indicate six different morphologies: unbranching, dichotomously branching, single monopodial branching, fan-shaped, shrub-like and small non-branching. The dichotomously branching, single monopodial branching, and fan-shaped morphologies of *Chinggiskhaania* generally resemble species of the macroalgae *Doushantophyton* and the non-branching morphology resembles *Sinocylindra*, while the shrub-like morphology of *Zuunartsphyton* generally resembles the macroalgae species *Glomulus filamentous* (Figure 25). Morphological measurements including width, length and surface area to volume ratio for the Zuun-Arts fossils are similar to the macroalgae from the Ediacaran Lantian and Miaohe biotas. In addition, morphological and SEM-BSE data indicate that the Zuun-Arts fossils are not hemichordates, trace fossils, or bacterial sheaths. All these data indicate that the Zuun-Arts fossils are indeed macroalgae, supporting the first hypothesis of this project. The Zuun-Arts biota is dominated by the non-branching morphology *Chinggiskhaania*, and lacks much of the macroalgal diversity preserved in the Lantian and Miaohe biotas.

SEM-EDS data show that the Zuun-Arts fossils are preserved as films composed primarily of Al with areas of elevated C concentrations in some fossils. These data are consistent with

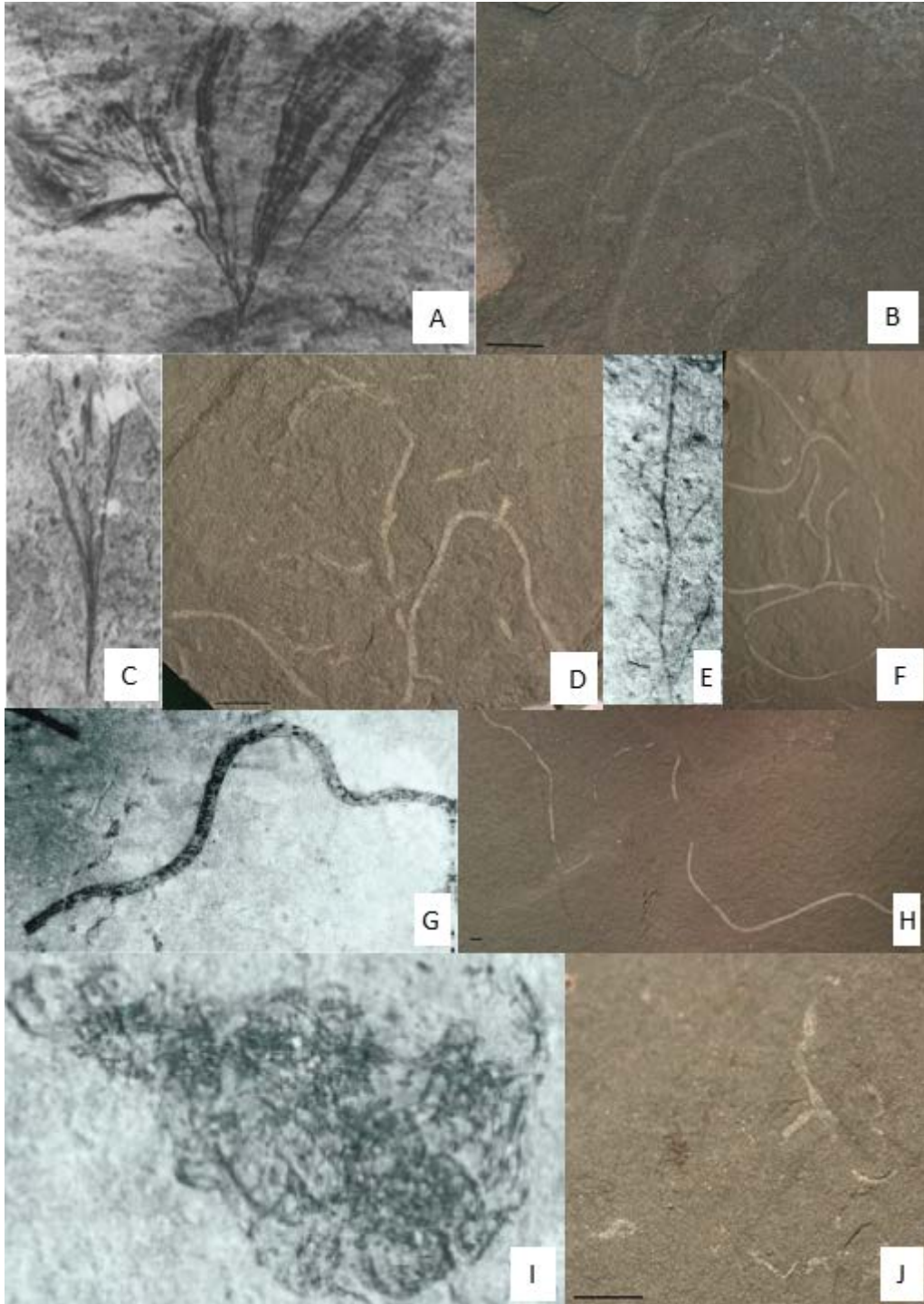


Figure 25. A comparison of the Zuun-Arts fossil morphologies with their closest Ediacaran macroalgae counterparts. A) *Doushantuophyton cometa*, a macroalgae species from the Lantian biota. B) The Zuun-Arts fan-like morphology. C) *Doushantuophyton rigidium* from the Miaohu biota. D) The Zuun-Arts dichotomously branching morphology. E) *Doushantuophyton quyuani* from the Lantian biota. F) The monopodial branching morphology from the Zuun-Arts biota. G) *Sinocylindra sp.* from the Lantian and Miaohu biotas. H) The Zuun-Arts non-branching morphology. I) *Glomulus filamentous* from the Miaohu biota. J) The Zuun-Arts shrub-like morphology. A,E modified from Xunlai et al. (1999); C,G,I modified from Xiao et al. (2002).

preservation through the BST taphonomic pathway as aluminosilicate mineral films, supporting the second hypothesis of this project. Although these data do not definitively prove or disprove any of the models proposed for the formation of BST fossils in general, they do offer insights into how the plane of splitting passes through the fossil when the rock is split into part and counterpart (Figure 20). The similarity in clay mineral content between shale within and outside of the Zuun-Arts biota indicates that the lack of fossils outside of the fossiliferous zone is not due to a lack of swelling clays. In addition, the lack of smectite in the clay fraction of the Zuun-Arts shale indicates that swelling clay is not necessary for BST preservation to occur. Overall, although simple compared to the Lantian and Miaohu biotas, the Zuun-Arts biota does provide a rare view of soft-bodied organisms during an important time in the history of life, and may lead to a more complete understanding of the origins of complex multicellular life.

References

- Bold S., Smith F.E., Rooney D.A., Bowring A.S., Buchwaldt R., Dubas O.F., Ramezani J., Crowley L.J., Schrag P.D., Macdonald A.F. "Neoproterozoic Stratigraphy of the Zavkhan Terrane of Mongolia: the Backbone for Cryogenian and Early Ediacaran Chemostratigraphic Records." *American Journal of Science* (2016): vol. 316, 1-63.
- Brasier, M., Antcliffe, J., Callow, R. "Evolutionary trends in remarkable fossil preservation across the Ediacaran-Cambrian transition and the impact of metazoan mixing." Allison, P., Bottjet, D. *Taphonomy: process and bias through time, second edition*. Dordrecht: Springer, 2011. p. 519-567.
- Briggs, D., Williams, S. "The restoration of flattened fossils." *Lethaia* (1981): v. 14, pg. 157-164.
- Butterfield, J. N. "Exceptional Fossil Preservation and the Cambrian Explosion." *Integrative and Comparative Biology* (2003): vol. 43, 166-177.
- Butterfield, N. "Organic preservation of non-mineralizing organisms and the taphonomy of the Burgess Shale." *Paleobiology* (1990): vol. 16-3, pg. 272-286.
- Butterfield, N., Balthasar, U., Wilson, L. "Fossil diagenesis in the Burgess Shale." *Paleontology* (2007): v. 50-3, pg. 537-543.
- Cai, Y., Hua, H., Xiao, S., Schiffbauer, D., Li, P. "Biostratigraphy of the late Ediacaran pyritized Gaojishan from southern Shaanxi, south China: importance of event deposits." *PALAIOS* (2010): v. 25, pg. 487-506.
- Cohen, P.S., Bradlet, A.H., Knoll, J.P., Grotzinger, S., Jensen, J., Abelson, K., Hand, G., Love, J., Metz, N., McLoughlin, P. "Tubular compression fossils from the Ediacaran Nama Group, Namibia." *Journal of Paleontology* (2009): v. 83-1, pg. 110-122.
- Condon D., Zhu M., Bowring S., Wang W., Yang A., Jin Y. "U-Pb Ages from the Neoproterozoic Doushantuo Formation, China." *Science* (2016): vol. 308, 95-98.
- Ding, L., Li, Z., Hu, Y., Xiao, C., Huang, J. *Sinian Miaohu biota*. Beijing: Geological Publishing House, 1996.
- Dornbos Q.S., Oji T., Kanayama A., Gonchigdorj S. "A new Burgess Shale-type Deposit from the Ediacaran of Western Mongolia." *Scientific Reports* (2016): 6:243438, 1-5.
- Gabbott E.S., Xian-guang H., Norry J.M., Siveter J.D. "Preservation of Early Cambrian Animals of the Chengjiang Biota." *Geology* (2004): vol. 32, no. 10, 901-904.
- Han T., Runnegar B. "Megascopic eukaryotic algae from the 2.1-billion-year-old Negaunee iron-formation, Michigan." *Science* (1992): vol. 257; pg. 232-235.

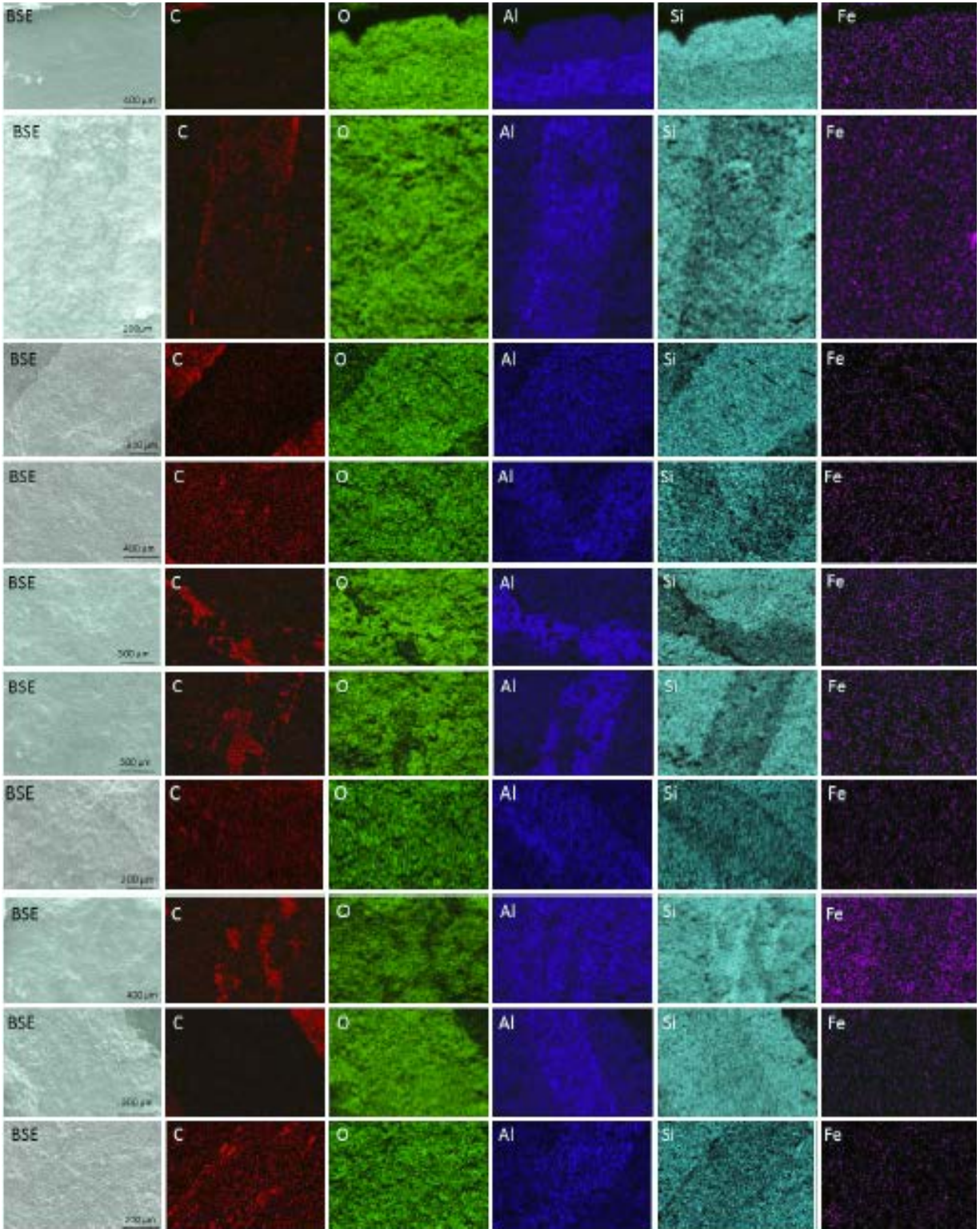
- Huggett, J., Gale, A., Evans, A. "Carbonate concretions from the London Clay (Ypresian, Eocene) of southern England and the exceptional preservation of wood-boring communities." *Journal of the Geological Society, London* (2000): v. 157, pg. 187-200.
- Iken, K. "Grazers on benthic seaweeds." Wiencke C., Bischof K. *Seaweed Biology: novel insights into ecophysiology, ecology and utilization*. Berlin: Springer, 2012. 157-176.
- Kroner A., Lehmann J., Schulmann K., Demoux A., Lexa O., Tomurhuu D., Stipska P., Liu D., Wingate D.T.M. "Lithostratigraphic and Geochronological Constraints on the Evolution of the Central Asian Orogenic Belt in SW Mongolia: Early Paleozoic Rifting Followed by Late Proterozoic Accretion." *American Journal of Science* (2010): vol. 310, 523-574.
- Littler M., Littler D. "The evolution of thallus form survival strategies in benthic marine macroalgae: field and laboratory tests of a functional form model." *The American Naturalist* (1980): vol. 116:1; pg. 25-44.
- Littler, M. "Morphological form and photosynthetic performances of marine macroalgae: tests of a functional/form hypothesis." *Botanica Marina* (1979): vol. 22; pg. 161-165.
- LoDuca S., Behtinger E. "Functional morphology and evolution of early Paleozoic Dasycladalean algae (Chlorophyta)." *Paleobiology* (2009): vol. 35:1: pg. 63-76.
- LoDuca, S., Bykova, N., Wu, M., Zhao, Y. "Seaweed morphology and ecology during the great animal diversification events of the early Paleozoic: A tale of two floras." *Geobiology* (2017): v. 15, pg. 588-616.
- Loydell, D., Orr, P., Kearns, S. "Preservation of soft tissues in Silurian graptolites from Latvia." *Palaeontology* (2004): v. 47, pg. 503-213.
- Macdonald A.F., Jones S.D., Schrag P.D. "Stratigraphic and Tectonic Implications of a Newly Discovered Glacial Diamictite-Cap Carbonate Couplet in Southwestern Mongolia." *Geology* (2009): vol. 37, no. 2, 123-126.
- Macdonald, F. "The geological record of Neoproterozoic glaciations." Arnaud, E., Halverson, G., Shields-Zhou, G. *Geological Society Memoirs*. London, 2011. pg. 331-337.
- Marshall, K.C. *Interfaces in microbial ecology*. Cambridge: Harvard University Press, 1976.
- Meyer, M., Schiffbauer, J., Xiao, S. Cai, Y., Hue, H. "Taphonomy of the upper Ediacaran enigmatic fossil shaanxilithes." *PALAIOS* (2012): v. 27,pg. 354-372.
- Miller, W. *Trace fossils: concepts, problems, prospects*. Amsterdam: Elsevier, 2007.
- Moore, D., Reynolds, R. *X-ray diffraction and the identification and analysis of clay minerals second edition*. Oxford, New York: Oxford University Press, 1997.

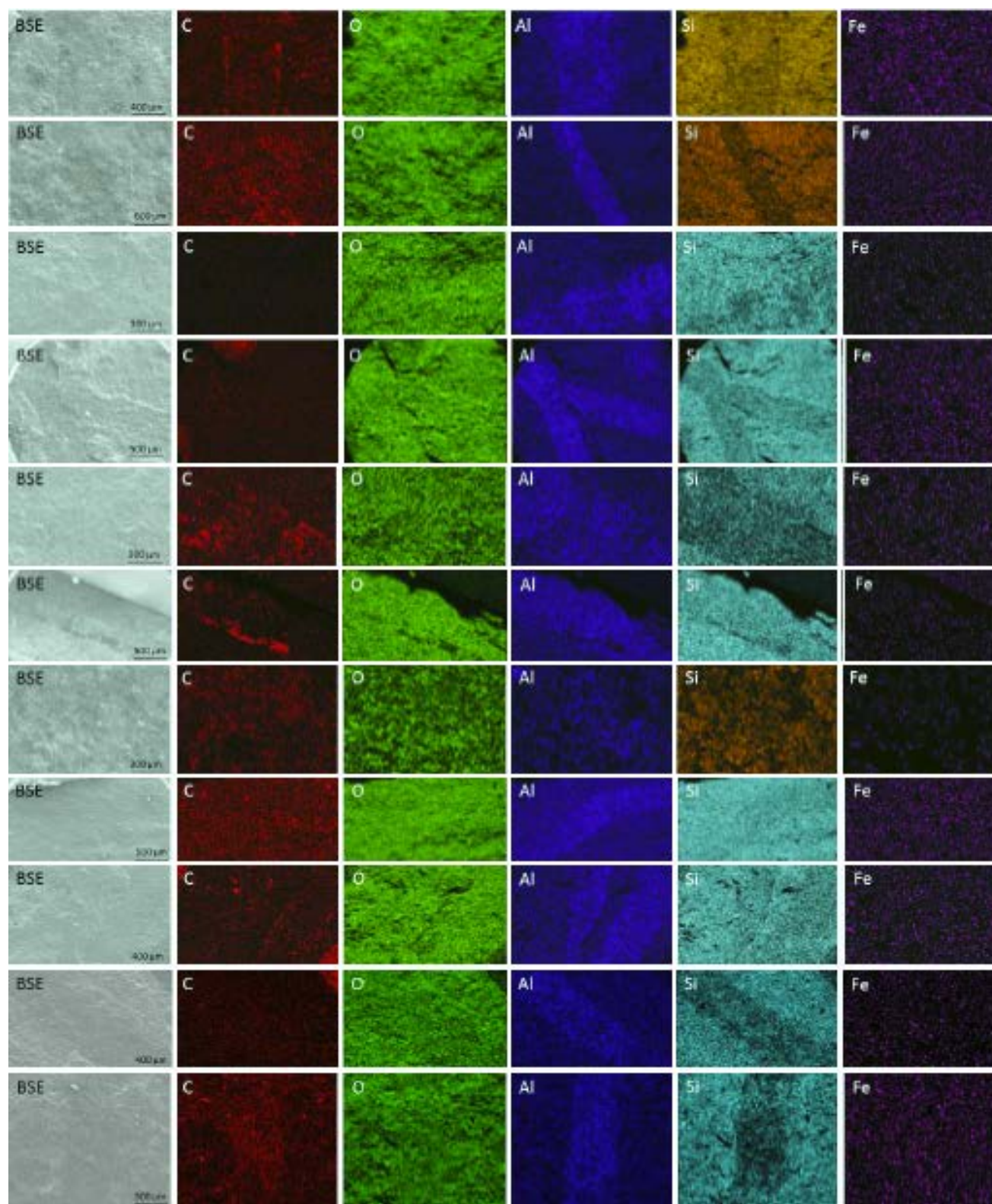
- Moore, R. Lieberman, B. "Preservation of Early and Middle Cambrian soft-bodied arthropods from the Pioche Shale, Nevada, USA." *Palaeogeography, Palaeoclimatology, Palaeoecology* (2009): v. 277, pg. 57-62.
- Muscente, A.D., Xiao, S. "Resolving the three-dimensional and sunsurficial features of carbonaceous compressions and shelly fossils using backscattered electron scanning electron microscopy (SEM-BSE)." *Palaios* (2015): v. 30, pg. 462-481.
- Narbonne M.G. "The Ediacara Biota: Neoproterozoic Origin of Animals and Their Ecosystems." *Annual Review of Earth and Planetary Science* (2005): vol. 33, 421-442.
- Orr, P.J., Briggs, D.E.G., Kearns, S.L. "Cambrian Burgess Shale animals replicated in clay minerals." *Science* (1998): v. 281, p. 1173-1175.
- Orr, P.J., Kearns, S. L., Briggs, D.E.G. "Elemental mapping of exceptionally preserved 'carbonaceous compression' fossils." *Palaeogeography, palaeoclimatology, palaeoecology* (2009): v. 277, p. 1-8.
- Osgoos, R. "Trace fossils of the Cincinnati area." *Palaeontographica Americana* (1970): v. 6:41, pg. 276-439.
- Seilacher, A. "Vendobionta and Psammocorallia: Lost Constructions of Precambrian Evolution." *Journal of the Geological Society, London* (1992): vol. 149, 607-613.
- Smith E.F., MacDonald F.A, Petach A.T., Bold U., Schrag P.D. "Integrated Stratigraphic, Geochemical, and Paleontological Late Ediacaran to Early Cambrian Records from Southwestern Mongolia." *GSA Bulletin* (2016): vol. 128, no. 3/4, 442-462.
- Tang, G., Pang, K., Yuan, X., Xiao, S. "Electron microscopy reveals evidence for simple multicellularity in the Proterozoic fossil Churia." *Geology* (2017): v. 45, pg. 75-78.
- Thang, B. *Formation of clay-polymer complexes*. Amsterdam; New York: Elsevier Scientific Publishing Company, 1979.
- Underwood, C. "Graptolite preservation and deformation." *PALAIOS* (1992): v. 7, pg. 178-186.
- Van Alstyne K. "Adventitious branching as a herbivore-induced defense in the intertidal brown algae *Fucus distichus*." *Marine Ecology Progress Series* (1989): vol. 56; 169-176.
- Van Roy, P., Orr, P.J., Botting J.P., Muir, L.A., Vinther, J., Lefebvre, B., Hariri, K., Briggs, D.E.G. "Ordovician faunas of Bruggess Shale type." *Nature Letters* (2010): v. 465, p. 215- 218.
- Wang W., Guan C., Zhou C., Wan B., Tang Q., Chen X., Chen Z., Yuan X. "Exceptional Preservation of Macrofossils from the Ediacaran Lantian and Miaohu Biotas, South China." *Society for Sedimentary Geology* (2014): 29(3), 129-136.

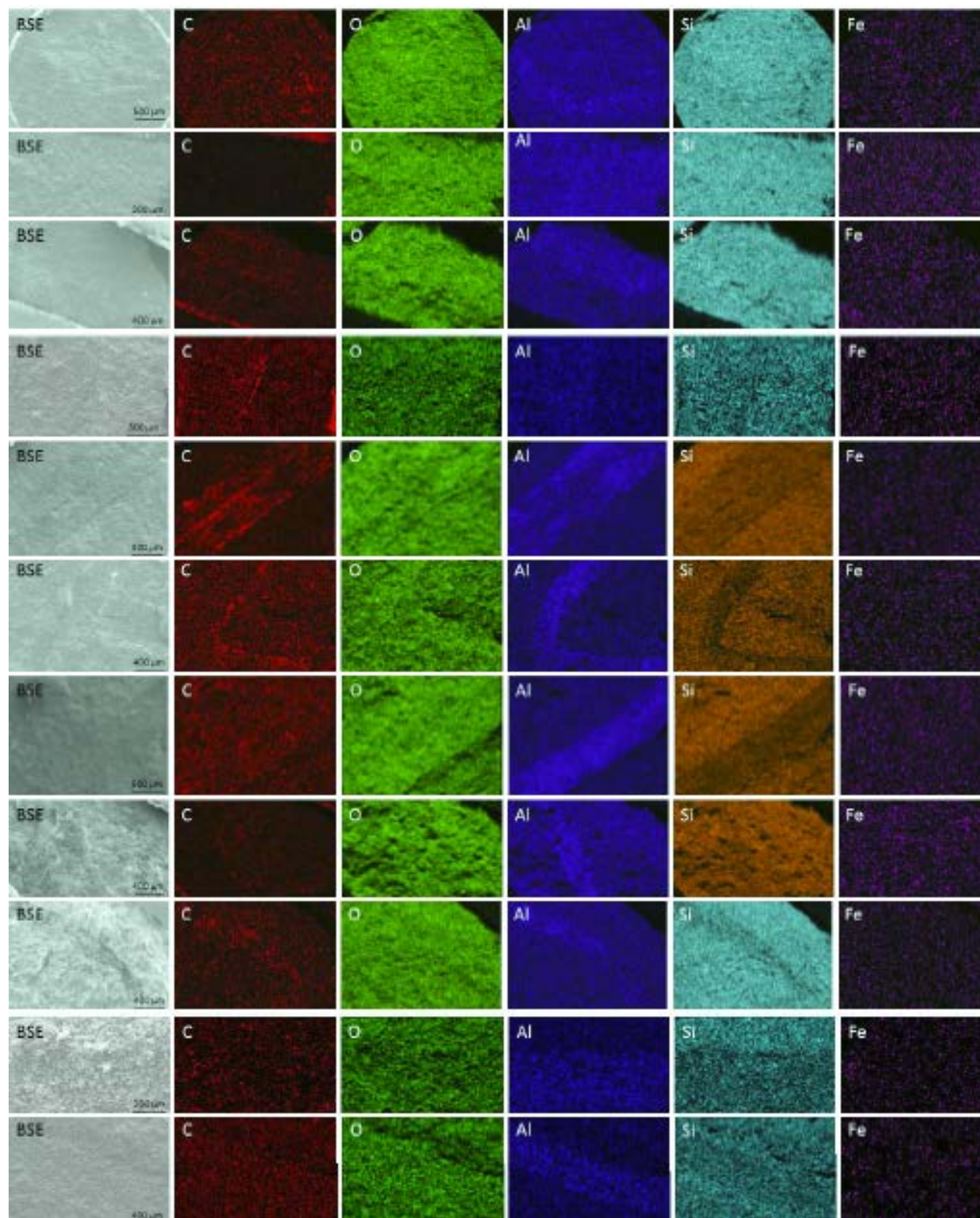
- Wang X., Bernd-D E., Chen X., Mao X. "Integrated Sequence-bio- and chemo-stratigraphy of the Terminal Proterozoic to Lowermost Cambrian "Black Rock Series" from Central South China." *Episodes* (1998): vol. 21, no. 3, 178-189.
- Xiao s., dong L. "POn the morphological and ecological history of Proterozoic macroalgae." Xiao S., Kaufman A. *Neoproterozoic geobiology and paleobiology*. Dordrecht: Springer, 2006. 57-90.
- Xiao S., Laflamme M. "On the eve of Animal Radiation: Phylogeny, Ecology and Evolution of the Ediacara Biota." *Trends in Ecology and Evolution* (2008): vol. 24 no. 1, 31-40.
- Xiao S., Yuan X., Steiner M., Knoll A. "Macroscopic Carbonaceous Compressions in a Terminal Proterozoic Shale: a Systematic Reassessment of the Miaohu Biota, South China." *Journal of Paleontology* (2002): 76(2), 347-376.
- Xunlai Yuan, Jun Li, Ruiji Cao. "A Diverse Metaphyte Assemblage from the Neoproterozoic Black Shales of South China." *Lethaia* (1999): vol. 32, 143-155.
- Yuan X., Chen Z., Xiao S., Zhou C., Hua H. "An early Ediacaran Assemblage of Macroscopic and Morphologically Differentiated Eukaryotes." *Nature* (2011): vol. 470, 390-393.
- Yuan X., Xiao S., Parsley L.R., Zhou C., Chen Z., Hu J. "Towering Sponges in an Early Cambrian Lagerstätte: Disparity Between Nonbilaterian and Bilaterian Epifaunal Tierers at the Neoproterozoic-Cambrian Transition." *Geology* (2002): vol. 30, no. 4, 363-366.
- Yuan, X., Chen, Z., Xiao, S., Zhou, C., Hua, H. "An early Ediacaran assemblage of macroscopic and morphologically differentiated eukaryotes." *Nature* (2011): v. 140, pg. 390-393.
- Zhang, Y. "Multicellular Thallophytes with Differentiated Tissues from late Proterozoic Phosphate rocks of South China." *Lethaia* (1989): vol. 22, 113-132.
- Zhu B., Becker H., Jiang S., Pi D., Fischer-Godde M., Yang J. "Re-Os Geochronology of Black Shales from the Neoproterozoic Doushantuo Formation, Yangtze Platform, South China." *Precambrian Research* (2013): vol. 225, 67-76.
- Zhu, S., Chen, H. "Megascopic multicellular organisms from the 1700-million-year-old Tuanshanzi Formation in the Jixian area, north China." *Science* (1995): v. 270, pg. 620-622.

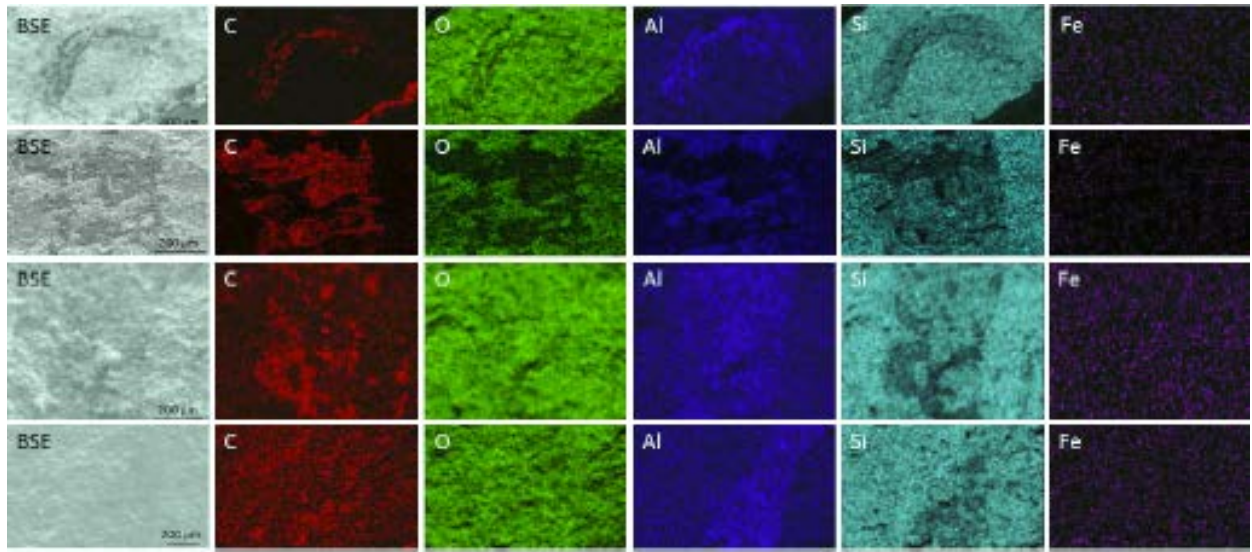
Appendix A:

SEM-EDS maps



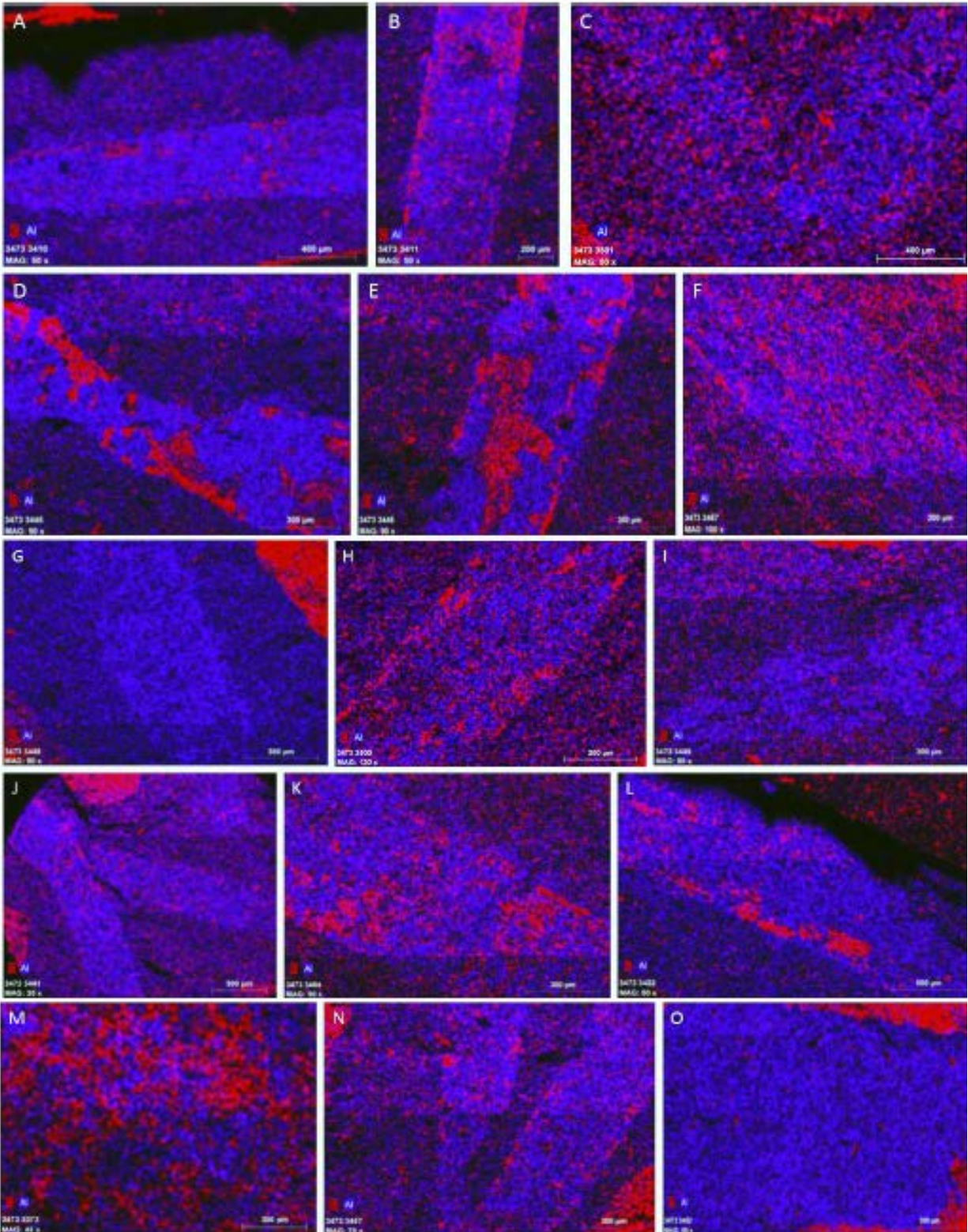


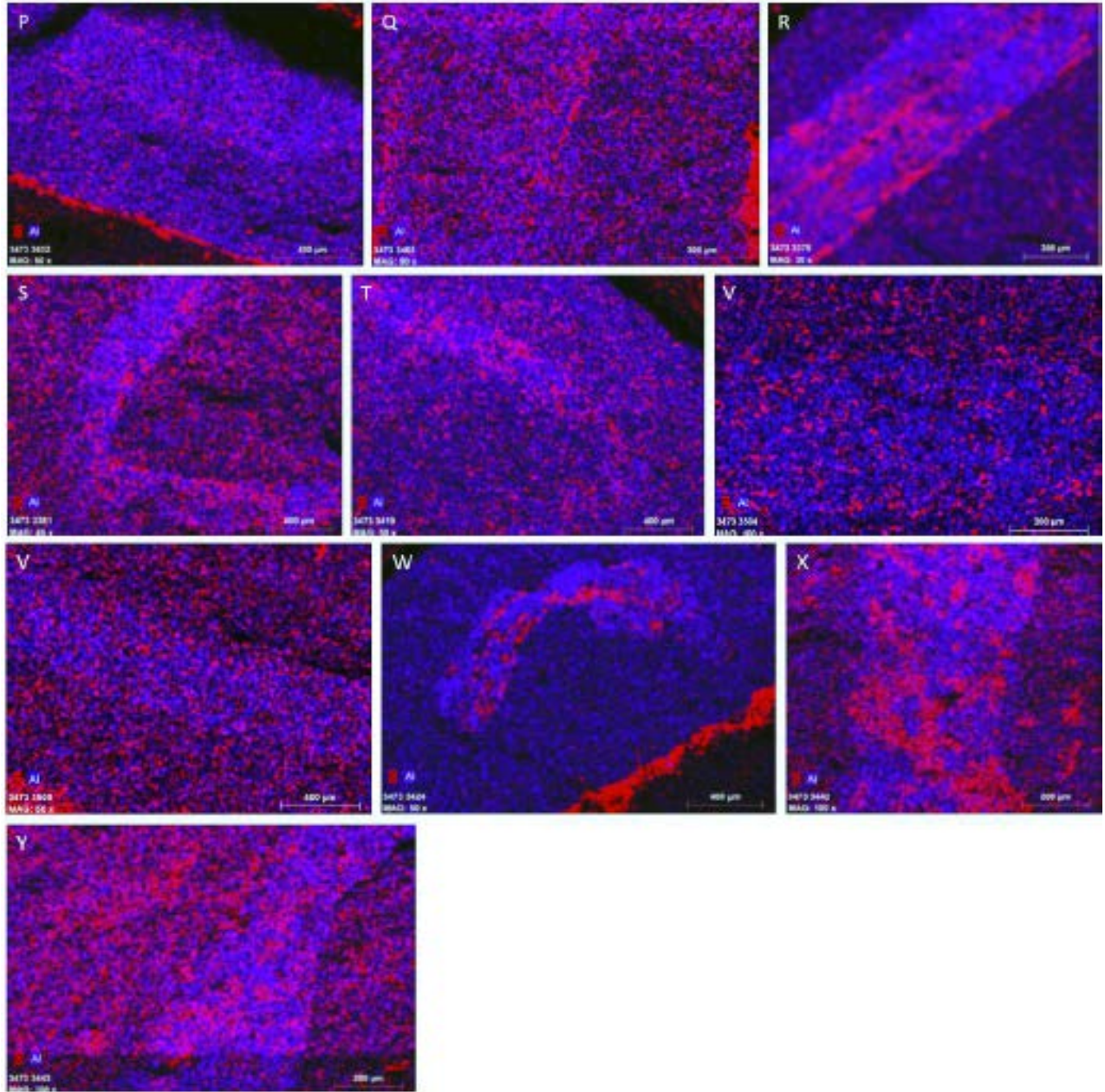




Appendix B:

SEM-EDS map, C and Al overlay





Appendix C:

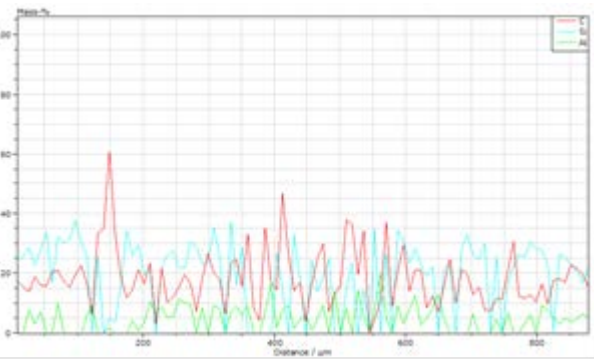
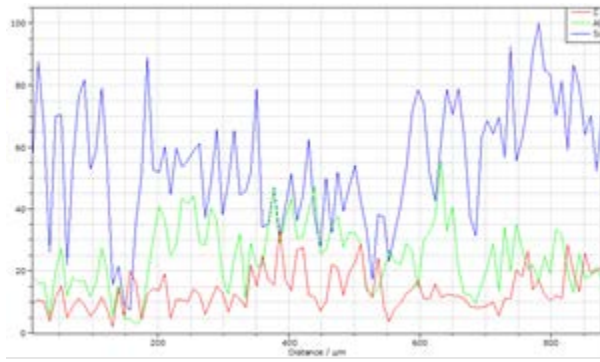
SEM-EDS line scans











Appendix D:

Morphological measurements, non-branching

Specimen	Canopy Height (mm)			Primary Elements						Total						
	Number	Avg. Length (mm)	Avg. Width (mm)	SA (mm ²)	V (mm ³)	SA/V (mm ⁻¹)	Avg. Length (mm)	Avg. Width (mm)	SA (mm ²)	V (mm ³)	SA/V (mm ⁻¹)	Avg. Length (mm)	Avg. Width (mm)	SA (mm ²)	V (mm ³)	SA/V (mm ⁻¹)
ZA_1B	1.00	23.38	0.56	41.23	5.65	7.29	23.38	0.56	41.23	5.65	7.29	23.38	0.56	41.23	5.65	7.29
ZA_1C	1.00	35.54	0.58	65.13	9.35	6.96	35.54	0.58	65.13	9.35	6.96	35.54	0.58	65.13	9.35	6.96
ZA_1D	1.00	32.80	0.73	75.80	13.64	5.56	32.80	0.73	75.80	13.64	5.56	32.80	0.73	75.80	13.64	5.56
ZA_1E	1.00	7.78	0.39	9.84	0.94	10.44	7.78	0.39	9.84	0.94	10.44	7.78	0.39	9.84	0.94	10.44
ZA_2	1.00	15.74	0.72	36.19	6.33	5.71	15.74	0.72	36.19	6.33	5.71	15.74	0.72	36.19	6.33	5.71
ZA_3A	1.00	11.66	0.63	23.50	3.58	6.57	11.66	0.63	23.50	3.58	6.57	11.66	0.63	23.50	3.58	6.57
ZA_3B	1.00	32.62	0.75	77.18	14.21	5.43	32.62	0.75	77.18	14.21	5.43	32.62	0.75	77.18	14.21	5.43
ZA_3C	1.00	24.24	0.35	26.60	2.29	11.61	24.24	0.35	26.60	2.29	11.61	24.24	0.35	26.60	2.29	11.61
ZA_3D	1.00	8.77	0.49	13.87	1.65	8.39	8.77	0.49	13.87	1.65	8.39	8.77	0.49	13.87	1.65	8.39
ZA_3E	1.00	11.63	0.44	16.44	1.78	9.22	11.63	0.44	16.44	1.78	9.22	11.63	0.44	16.44	1.78	9.22
ZA_3F	1.00	10.33	0.44	14.64	1.58	9.24	10.33	0.44	14.64	1.58	9.24	10.33	0.44	14.64	1.58	9.24
ZA_3G	1.00	25.08	0.43	34.39	3.69	9.32	25.08	0.43	34.39	3.69	9.32	25.08	0.43	34.39	3.69	9.32
ZA_3H	1.00	8.76	0.17	4.80	0.21	23.35	8.76	0.17	4.80	0.21	23.35	8.76	0.17	4.80	0.21	23.35
ZA_3I	1.00	15.61	0.70	35.02	5.99	5.85	15.61	0.70	35.02	5.99	5.85	15.61	0.70	35.02	5.99	5.85
ZA_3J	1.00	11.13	0.39	13.79	1.31	10.49	11.13	0.39	13.79	1.31	10.49	11.13	0.39	13.79	1.31	10.49
ZA_3K	1.00	18.64	0.35	20.50	1.76	11.63	18.64	0.35	20.50	1.76	11.63	18.64	0.35	20.50	1.76	11.63
ZA_3L	1.00	7.77	0.35	8.66	0.73	11.78	7.77	0.35	8.66	0.73	11.78	7.77	0.35	8.66	0.73	11.78
ZA_3M	1.00	7.34	0.35	8.18	0.69	11.80	7.34	0.35	8.18	0.69	11.80	7.34	0.35	8.18	0.69	11.80
ZA_4B	1.00	15.14	0.67	32.55	5.33	6.10	15.14	0.67	32.55	5.33	6.10	15.14	0.67	32.55	5.33	6.10
ZA_5A	1.00	37.99	0.37	44.23	4.06	10.89	37.99	0.37	44.23	4.06	10.89	37.99	0.37	44.23	4.06	10.89
ZA_5B	1.00	13.03	0.35	14.43	1.24	11.65	13.03	0.35	14.43	1.24	11.65	13.03	0.35	14.43	1.24	11.65
ZA_5C	1.00	10.40	0.28	9.10	0.62	14.74	10.40	0.28	9.10	0.62	14.74	10.40	0.28	9.10	0.62	14.74
ZA_7A	1.00	19.45	0.52	32.25	4.15	7.78	19.45	0.52	32.25	4.15	7.78	19.45	0.52	32.25	4.15	7.78
ZA_7C	1.00	16.19	0.99	51.91	12.48	4.16	16.19	0.99	51.91	12.48	4.16	16.19	0.99	51.91	12.48	4.16
ZA_7D	1.00	16.28	0.58	30.28	4.33	7.00	16.28	0.58	30.28	4.33	7.00	16.28	0.58	30.28	4.33	7.00
ZA_7E	1.00	82.26	0.66	172.21	28.47	6.05	82.26	0.66	172.21	28.47	6.05	82.26	0.66	172.21	28.47	6.05
ZA_7I	1.00	16.40	0.74	38.75	6.97	5.56	16.40	0.74	38.75	6.97	5.56	16.40	0.74	38.75	6.97	5.56
ZA_7J	1.00	14.83	0.41	19.45	1.98	9.84	14.83	0.41	19.45	1.98	9.84	14.83	0.41	19.45	1.98	9.84
ZA_8A	1.11	29.02	1.11	102.90	27.97	3.68	29.02	1.11	102.90	27.97	3.68	29.02	1.11	102.90	27.97	3.68
ZA_8B	1.00	20.61	0.78	51.71	9.95	5.20	20.61	0.78	51.71	9.95	5.20	20.61	0.78	51.71	9.95	5.20
ZA_8C	1.00	49.90	0.60	94.74	14.15	6.70	49.90	0.60	94.74	14.15	6.70	49.90	0.60	94.74	14.15	6.70
ZA_8D	1.00	25.77	0.38	30.98	2.92	10.60	25.77	0.38	30.98	2.92	10.60	25.77	0.38	30.98	2.92	10.60
ZA_8E	1.00	28.58	0.38	34.33	3.24	10.60	28.58	0.38	34.33	3.24	10.60	28.58	0.38	34.33	3.24	10.60
ZA_8F	1.00	32.90	0.69	71.50	12.12	5.90	32.90	0.69	71.50	12.12	5.90	32.90	0.69	71.50	12.12	5.90
ZA_8G	1.00	23.77	0.60	45.43	6.74	6.74	23.77	0.60	45.43	6.74	6.74	23.77	0.60	45.43	6.74	6.74
ZA_8H	1.00	39.85	0.76	96.01	18.07	5.31	39.85	0.76	96.01	18.07	5.31	39.85	0.76	96.01	18.07	5.31
ZA_9A	1.00	14.53	0.60	27.85	4.08	6.83	14.53	0.60	27.85	4.08	6.83	14.53	0.60	27.85	4.08	6.83
ZA_9B	1.00	39.24	0.75	93.04	17.24	5.40	39.24	0.75	93.04	17.24	5.40	39.24	0.75	93.04	17.24	5.40
ZA_9C	1.00	22.23	0.33	23.48	1.95	12.07	22.23	0.33	23.48	1.95	12.07	22.23	0.33	23.48	1.95	12.07
ZA_9D	1.00	31.72	0.62	61.95	9.45	6.56	31.72	0.62	61.95	9.45	6.56	31.72	0.62	61.95	9.45	6.56
ZA_9E	1.00	27.42	0.62	53.63	8.17	6.57	27.42	0.62	53.63	8.17	6.57	27.42	0.62	53.63	8.17	6.57
ZA_9F	1.00	35.65	0.63	71.59	11.25	6.37	35.65	0.63	71.59	11.25	6.37	35.65	0.63	71.59	11.25	6.37
ZA_10A	1.00	38.32	0.50	60.68	7.55	8.04	38.32	0.50	60.68	7.55	8.04	38.32	0.50	60.68	7.55	8.04
ZA_10B	1.00	21.42	0.33	22.64	1.88	12.07	21.42	0.33	22.64	1.88	12.07	21.42	0.33	22.64	1.88	12.07
ZA_10C	1.00	18.07	0.53	30.40	3.95	7.69	18.07	0.53	30.40	3.95	7.69	18.07	0.53	30.40	3.95	7.69
ZA_10D	1.00	18.29	0.33	19.35	1.60	12.09	18.29	0.33	19.35	1.60	12.09	18.29	0.33	19.35	1.60	12.09
ZA_10E	1.00	19.68	0.60	37.78	5.60	6.75	19.68	0.60	37.78	5.60	6.75	19.68	0.60	37.78	5.60	6.75
ZA_11A	1.00	185.10	0.82	478.23	97.94	4.88	185.10	0.82	478.23	97.94	4.88	185.10	0.82	478.23	97.94	4.88
ZA_11B	1.00	31.00	1.18	116.63	33.65	3.47	31.00	1.18	116.63	33.65	3.47	31.00	1.18	116.63	33.65	3.47
ZA_12A	1.00	100.83	0.56	177.78	24.82	7.16	100.83	0.56	177.78	24.82	7.16	100.83	0.56	177.78	24.82	7.16

Specimen	Canopy Height (mm)	Primary Elements						Total						
		Number	Avg. Length (mm)	Avg. Width (mm)	SA (mm ²)	V (mm ³)	SA/V (mm ⁻¹)	Number	Avg. Length (mm)	Avg. Width (mm)	SA (mm ²)	V (mm ³)	SA/V (mm ⁻¹)	
ZA_12B	0.26	1.00	33.26	0.26	27.68	1.82	15.21	33.26	0.26	27.68	1.82	15.21	1.82	15.21
ZA_12C	0.79	1.00	50.16	0.79	125.72	24.70	5.09	50.16	0.79	125.72	24.70	5.09	5.09	5.09
ZA_12D	0.26	1.00	21.71	0.26	18.10	1.19	15.24	21.71	0.26	18.10	1.19	15.24	1.19	15.24
ZA_12E	0.37	1.00	29.85	0.37	35.28	3.28	10.76	29.85	0.37	35.28	3.28	10.76	3.28	10.76
ZA_12F	0.37	1.00	37.30	0.37	44.02	4.10	10.75	37.30	0.37	44.02	4.10	10.75	4.10	10.75
ZA_12G	0.75	1.00	41.77	0.75	98.85	18.30	5.40	41.77	0.75	98.85	18.30	5.40	5.40	5.40
ZA_12H	0.75	1.00	38.40	0.75	90.95	16.82	5.41	38.40	0.75	90.95	16.82	5.41	5.41	5.41
ZA_12I	0.26	1.00	27.48	0.26	22.89	1.50	15.22	27.48	0.26	22.89	1.50	15.22	1.50	15.22
ZA_14	0.50	1.00	25.82	0.50	41.25	5.15	8.01	25.82	0.50	41.25	5.15	8.01	5.15	8.01
ZA_15A	0.58	1.00	64.24	0.58	116.71	16.73	6.98	64.24	0.58	116.71	16.73	6.98	6.98	6.98
ZA_15B	0.74	1.00	24.70	0.74	57.85	10.47	5.52	24.70	0.74	57.85	10.47	5.52	5.52	5.52
ZA_15C	0.43	1.00	51.85	0.43	70.63	7.60	9.30	51.85	0.43	70.63	7.60	9.30	7.60	9.30
ZA_16A	0.76	1.00	24.66	0.76	59.67	11.15	5.35	24.66	0.76	59.67	11.15	5.35	5.35	5.35
ZA_16B	0.81	1.00	34.22	0.81	88.07	17.63	5.00	34.22	0.81	88.07	17.63	5.00	5.00	5.00
ZA_18	0.42	1.00	26.59	0.42	35.68	3.75	9.51	26.59	0.42	35.68	3.75	9.51	3.75	9.51
ZA_19	0.37	1.00	39.77	0.37	45.79	4.16	11.01	39.77	0.37	45.79	4.16	11.01	4.16	11.01
ZA_21A	0.57	1.00	34.58	0.57	62.07	8.73	7.11	34.58	0.57	62.07	8.73	7.11	7.11	7.11
ZA_21B	0.50	1.00	41.38	0.50	64.71	7.96	8.13	41.38	0.50	64.71	7.96	8.13	7.96	8.13
ZA_22	0.58	1.00	37.52	0.58	68.37	9.77	7.00	37.52	0.58	68.37	9.77	7.00	9.77	7.00
ZA_23A	0.38	1.00	10.95	0.38	13.14	1.21	10.82	10.95	0.38	13.14	1.21	10.82	1.21	10.82
ZA_23B	0.48	1.00	11.98	0.48	18.22	2.12	8.59	11.98	0.48	18.22	2.12	8.59	2.12	8.59
ZA_23D	0.38	1.00	12.31	0.38	14.75	1.37	10.80	12.31	0.38	14.75	1.37	10.80	1.37	10.80
ZA_23E	0.62	1.00	14.70	0.62	29.22	4.43	6.59	14.70	0.62	29.22	4.43	6.59	4.43	6.59
ZA_26	0.56	1.00	23.94	0.56	42.66	5.91	7.21	23.94	0.56	42.66	5.91	7.21	5.91	7.21
ZA_27B	0.65	1.00	5.69	0.65	12.22	1.87	6.53	5.69	0.65	12.22	1.87	6.53	1.87	6.53
ZA_28A	0.34	1.00	15.71	0.34	17.11	1.45	11.79	15.71	0.34	17.11	1.45	11.79	1.45	11.79
ZA_28B	0.50	1.00	15.34	0.50	24.47	3.01	8.13	15.34	0.50	24.47	3.01	8.13	3.01	8.13
ZA_28C	0.49	1.00	22.41	0.49	34.50	4.14	8.34	22.41	0.49	34.50	4.14	8.34	4.14	8.34
ZA_29	0.48	1.00	9.41	0.48	14.57	1.71	8.53	9.41	0.48	14.57	1.71	8.53	1.71	8.53
ZA_30A	0.70	1.00	30.15	0.70	67.43	11.73	5.75	30.15	0.70	67.43	11.73	5.75	5.75	5.75
ZA_30B	0.41	1.00	14.50	0.41	19.03	1.93	9.85	14.50	0.41	19.03	1.93	9.85	1.93	9.85
ZA_30C	0.48	1.00	23.10	0.48	35.25	4.20	8.40	23.10	0.48	35.25	4.20	8.40	4.20	8.40
ZA_30D	0.58	1.00	23.92	0.58	44.32	6.38	6.94	23.92	0.58	44.32	6.38	6.94	6.38	6.94
ZA_30E	0.55	1.00	20.05	0.55	35.29	4.81	7.33	20.05	0.55	35.29	4.81	7.33	4.81	7.33
ZA_30F	0.52	1.00	16.04	0.52	26.66	3.42	7.80	16.04	0.52	26.66	3.42	7.80	3.42	7.80
ZA_30G	0.41	1.00	10.69	0.41	14.10	1.42	9.90	10.69	0.41	14.10	1.42	9.90	1.42	9.90
ZA_30H	0.41	1.00	10.71	0.41	14.12	1.43	9.90	10.71	0.41	14.12	1.43	9.90	1.43	9.90
ZA_30I	0.55	1.00	7.31	0.55	13.17	1.75	7.51	7.31	0.55	13.17	1.75	7.51	1.75	7.51
ZA_30J	0.60	1.00	12.21	0.60	23.57	3.45	6.83	12.21	0.60	23.57	3.45	6.83	3.45	6.83
ZA_30K	0.64	1.00	10.03	0.64	20.93	3.26	6.41	10.03	0.64	20.93	3.26	6.41	3.26	6.41
ZA_30L	0.42	1.00	26.47	0.42	35.18	3.66	9.60	26.47	0.42	35.18	3.66	9.60	3.66	9.60
ZA_30M	0.48	1.00	15.13	0.48	23.21	2.75	8.45	15.13	0.48	23.21	2.75	8.45	2.75	8.45
ZA_31A	0.52	1.00	14.74	0.52	24.53	3.14	7.81	14.74	0.52	24.53	3.14	7.81	3.14	7.81
ZA_31B	0.73	1.00	23.15	0.73	54.06	9.74	5.55	23.15	0.73	54.06	9.74	5.55	5.55	5.55
ZA_32A	0.64	1.00	36.52	0.64	74.27	11.82	6.29	36.52	0.64	74.27	11.82	6.29	6.29	6.29
ZA_32C	0.36	1.00	13.17	0.36	14.93	1.31	11.39	13.17	0.36	14.93	1.31	11.39	1.31	11.39
ZA_33A	0.46	1.00	25.46	0.46	37.03	4.21	8.79	25.46	0.46	37.03	4.21	8.79	4.21	8.79
ZA_33B	0.78	1.00	35.58	0.78	88.20	17.03	5.18	35.58	0.78	88.20	17.03	5.18	5.18	5.18
ZA_33C	0.72	1.00	16.27	0.72	37.33	6.53	5.72	16.27	0.72	37.33	6.53	5.72	6.53	5.72
ZA_34A	0.63	1.00	33.68	0.63	67.56	10.59	6.38	33.68	0.63	67.56	10.59	6.38	6.38	6.38
ZA_34B	0.51	1.00	19.87	0.51	32.22	4.06	7.94	19.87	0.51	32.22	4.06	7.94	4.06	7.94
ZA_34C	0.46	1.00	9.46	0.46	14.02	1.58	8.89	9.46	0.46	14.02	1.58	8.89	1.58	8.89

Specimen	Canopy Height (mm)	Primary Elements						Total					
		Number	Avg. Length (mm)	Avg. Width (mm)	SA (mm ²)	V (mm ³)	SA/V (mm ⁻¹)	Number	Avg. Length (mm)	Avg. Width (mm)	SA (mm ²)	V (mm ³)	SA/V (mm ⁻¹)
ZA_34D	0.68	1.00	36.49	0.68	78.76	13.28	5.93	36.49	0.68	78.76	13.28	5.93	
ZA_35A	0.62	1.00	23.41	0.62	45.94	6.99	6.57	23.41	0.62	45.94	6.99	6.57	
ZA_35B	0.39	1.00	42.48	0.39	51.72	4.97	10.41	42.48	0.39	51.72	4.97	10.41	
ZA_35C	0.65	1.00	46.84	0.65	95.51	15.30	6.24	46.84	0.65	95.51	15.30	6.24	
ZA_36A	1.07	1.00	30.96	1.07	105.32	27.57	3.82	30.96	1.07	105.32	27.57	3.82	
ZA_36B	0.86	1.00	22.27	0.86	61.02	12.81	4.76	22.27	0.86	61.02	12.81	4.76	
ZA_37A	0.44	1.00	32.12	0.44	44.88	4.93	9.11	32.12	0.44	44.88	4.93	9.11	
ZA_37B	0.60	1.00	25.08	0.60	47.58	7.02	6.78	25.08	0.60	47.58	7.02	6.78	
ZA_38A	0.97	1.00	43.44	0.97	133.24	31.82	4.19	43.44	0.97	133.24	31.82	4.19	
ZA_38B	0.67	1.00	22.24	0.67	47.70	7.91	6.03	22.24	0.67	47.70	7.91	6.03	
ZA_38C	0.65	1.00	19.41	0.65	39.96	6.34	6.30	19.41	0.65	39.96	6.34	6.30	
ZA_39A	0.22	1.00	9.44	0.22	6.66	0.37	18.23	9.44	0.22	6.66	0.37	18.23	
ZA_39B	0.35	1.00	12.18	0.35	13.65	1.18	11.53	12.18	0.35	13.65	1.18	11.53	
ZA_39C	0.42	1.00	9.41	0.42	12.78	1.32	9.67	9.41	0.42	12.78	1.32	9.67	
ZA_40A	0.51	1.00	16.83	0.51	27.19	3.40	8.01	16.83	0.51	27.19	3.40	8.01	
ZA_40B	0.48	1.00	28.16	0.48	42.99	5.14	8.37	28.16	0.48	42.99	5.14	8.37	
ZA_40C	0.50	1.00	8.12	0.50	13.16	1.60	8.23	8.12	0.50	13.16	1.60	8.23	
ZA_40D	0.34	1.00	9.17	0.34	9.85	0.81	12.12	9.17	0.34	9.85	0.81	12.12	
ZA_41A	0.83	1.00	14.71	0.83	39.42	7.95	4.96	14.71	0.83	39.42	7.95	4.96	
ZA_41B	0.49	1.00	10.21	0.49	15.91	1.88	8.44	10.21	0.49	15.91	1.88	8.44	
ZA_42A	0.64	1.00	18.22	0.64	36.97	5.77	6.41	18.22	0.64	36.97	5.77	6.41	
ZA_42C	0.61	1.00	22.77	0.61	44.05	6.61	6.67	22.77	0.61	44.05	6.61	6.67	
ZA_42A	0.32	1.00	7.01	0.32	7.18	0.56	12.82	7.01	0.32	7.18	0.56	12.82	
ZA_42B	0.28	1.00	14.28	0.28	12.67	0.88	14.43	14.28	0.28	12.67	0.88	14.43	
ZA_42C	0.63	1.00	50.51	0.63	99.89	15.54	6.43	50.51	0.63	99.89	15.54	6.43	
ZA_42D	0.62	1.00	35.79	0.62	70.29	10.80	6.51	35.79	0.62	70.29	10.80	6.51	
ZA_42E	0.56	1.00	20.21	0.56	36.03	4.98	7.24	20.21	0.56	36.03	4.98	7.24	
ZA_42F	0.32	1.00	11.53	0.32	11.71	0.92	12.71	11.53	0.32	11.71	0.92	12.71	
ZA_42G	0.09	1.00	9.40	0.09	2.64	0.06	45.16	9.40	0.09	2.64	0.06	45.16	
ZA_42H	0.20	1.00	34.11	0.20	21.27	1.05	20.26	34.11	0.20	21.27	1.05	20.26	
ZA_45A	0.78	1.00	19.19	0.78	47.76	9.09	5.25	19.19	0.78	47.76	9.09	5.25	
ZA_45B	0.31	1.00	24.52	0.31	24.25	1.89	12.86	24.52	0.31	24.25	1.89	12.86	
ZA_45C	0.52	1.00	28.42	0.52	46.92	6.06	7.75	28.42	0.52	46.92	6.06	7.75	
ZA_45D	0.43	1.00	7.48	0.43	10.48	1.11	9.48	7.48	0.43	10.48	1.11	9.48	
ZA_45E	0.63	1.00	7.08	0.63	14.68	2.22	6.61	7.08	0.63	14.68	2.22	6.61	
ZA_47A	0.31	1.00	17.45	0.31	17.19	1.32	12.98	17.45	0.31	17.19	1.32	12.98	
ZA_47B	0.41	1.00	17.70	0.41	23.00	2.32	9.89	17.70	0.41	23.00	2.32	9.89	
ZA_47C	0.67	1.00	8.13	0.67	17.80	2.86	6.22	8.13	0.67	17.80	2.86	6.22	
ZA_48A	0.42	1.00	22.63	0.42	29.75	3.06	9.73	22.63	0.42	29.75	3.06	9.73	
ZA_48B	0.44	1.00	7.49	0.44	10.62	1.13	9.38	7.49	0.44	10.62	1.13	9.38	
ZA_48C	0.48	1.00	18.90	0.48	28.54	3.35	8.53	18.90	0.48	28.54	3.35	8.53	
ZA_48D	0.62	1.00	15.45	0.62	30.67	4.66	6.58	15.45	0.62	30.67	4.66	6.58	
ZA_49A	0.45	1.00	14.13	0.45	20.23	2.24	9.05	14.13	0.45	20.23	2.24	9.05	
ZA_49C	0.50	1.00	6.49	0.50	10.63	1.28	8.28	6.49	0.50	10.63	1.28	8.28	
ZA_50A	0.83	1.00	27.60	0.83	73.10	14.96	4.89	27.60	0.83	73.10	14.96	4.89	
ZA_50B	0.38	1.00	22.82	0.38	27.38	2.57	10.64	22.82	0.38	27.38	2.57	10.64	
ZA_50C	0.74	1.00	23.60	0.74	55.93	10.23	5.47	23.60	0.74	55.93	10.23	5.47	
ZA_50D	0.32	1.00	32.73	0.32	32.53	2.55	12.76	32.73	0.32	32.53	2.55	12.76	
ZA_50E	0.64	1.00	19.67	0.64	39.85	6.23	6.40	19.67	0.64	39.85	6.23	6.40	
ZA_50F	0.67	1.00	14.13	0.67	30.38	4.96	6.12	14.13	0.67	30.38	4.96	6.12	
ZA_50G	0.47	1.00	22.31	0.47	33.27	3.87	8.60	22.31	0.47	33.27	3.87	8.60	

Specimen	Canopy Height (mm)	Primary Elements						Total					
		Number	Avg. Length (mm)	Avg. Width (mm)	SA (mm ²)	V (mm ³)	SA/V (mm ⁻¹)	Number	Avg. Length (mm)	Avg. Width (mm)	SA (mm ²)	V (mm ³)	SA/V (mm ⁻¹)
ZA_50H	0.70	1.00	7.85	0.70	18.06	3.03	5.96	7.85	0.70	18.06	3.03	5.96	
ZA_50I	0.80	1.00	19.88	0.80	50.94	9.99	5.10	19.88	0.80	50.94	9.99	5.10	
ZA_50K	0.53	1.00	7.77	0.53	13.25	1.68	7.88	7.77	0.53	13.25	1.68	7.88	
ZA_50L	0.58	1.00	20.73	0.58	38.27	5.47	6.99	20.73	0.58	38.27	5.47	6.99	
ZA_51A	0.75	1.00	8.85	0.75	21.85	3.95	5.53	8.85	0.75	21.85	3.95	5.53	
ZA_51B	0.65	1.00	10.88	0.65	22.84	3.60	6.35	10.88	0.65	22.84	3.60	6.35	
ZA_51C	0.44	1.00	5.05	0.44	7.28	0.77	9.49	5.05	0.44	7.28	0.77	9.49	
ZA_52A	0.86	1.00	54.55	0.86	148.13	31.53	4.70	54.55	0.86	148.13	31.53	4.70	
ZA_52B	0.59	1.00	13.44	0.59	25.54	3.70	6.91	13.44	0.59	25.54	3.70	6.91	
ZA_53A	0.47	1.00	74.12	0.47	110.20	12.96	8.50	74.12	0.47	110.20	12.96	8.50	
ZA_53C	0.42	1.00	15.58	0.42	20.92	2.18	9.61	15.58	0.42	20.92	2.18	9.61	
ZA_53D	0.75	1.00	21.03	0.75	50.14	9.19	5.46	21.03	0.75	50.14	9.19	5.46	
ZA_54	0.54	1.00	14.48	0.54	25.19	3.36	7.49	14.48	0.54	25.19	3.36	7.49	
ZA_55B	0.33	1.00	4.62	0.33	5.02	0.40	12.41	4.62	0.33	5.02	0.40	12.41	
ZA_55C	0.32	1.00	8.44	0.32	8.56	0.67	12.86	8.44	0.32	8.56	0.67	12.86	
ZA_55D	0.66	1.00	15.93	0.66	33.70	5.45	6.19	15.93	0.66	33.70	5.45	6.19	
ZA_55E	0.53	1.00	19.60	0.53	33.31	4.39	7.59	19.60	0.53	33.31	4.39	7.59	
ZA_55F	0.42	1.00	4.84	0.42	6.61	0.66	10.01	4.84	0.42	6.61	0.66	10.01	
ZA_56A	0.84	1.00	35.88	0.84	95.64	19.83	4.82	35.88	0.84	95.64	19.83	4.82	
ZA_56B	0.54	1.00	13.73	0.54	23.75	3.14	7.55	13.73	0.54	23.75	3.14	7.55	
ZA_56C	0.52	1.00	14.16	0.52	23.73	3.05	7.77	14.16	0.52	23.73	3.05	7.77	
ZA_57A	0.78	1.00	48.36	0.78	119.24	23.04	5.18	48.36	0.78	119.24	23.04	5.18	
ZA_57B	0.53	1.00	41.07	0.53	68.53	8.99	7.62	41.07	0.53	68.53	8.99	7.62	
ZA_57C	0.33	1.00	19.24	0.33	19.80	1.60	12.41	19.24	0.33	19.80	1.60	12.41	
ZA_57D	0.35	1.00	16.33	0.35	18.25	1.59	11.49	16.33	0.35	18.25	1.59	11.49	
ZA_57E	0.45	1.00	12.35	0.45	17.56	1.92	9.15	12.35	0.45	17.56	1.92	9.15	
ZA_58A	0.36	1.00	6.17	0.36	7.24	0.64	11.34	6.17	0.36	7.24	0.64	11.34	
ZA_58B	0.73	1.00	18.39	0.73	43.12	7.74	5.57	18.39	0.73	43.12	7.74	5.57	
ZA_58C	0.33	1.00	19.71	0.33	20.41	1.65	12.33	19.71	0.33	20.41	1.65	12.33	
ZA_58D	0.41	1.00	10.98	0.41	14.25	1.42	10.03	10.98	0.41	14.25	1.42	10.03	
ZA_58E	0.09	1.00	10.71	0.09	3.07	0.07	44.14	10.71	0.09	3.07	0.07	44.14	
ZA_58F	0.39	1.00	7.23	0.39	8.97	0.84	10.67	7.23	0.39	8.97	0.84	10.67	
ZA_58G	0.39	1.00	9.24	0.39	11.41	1.08	10.61	9.24	0.39	11.41	1.08	10.61	
ZA_59A	1.34	1.00	11.40	1.34	50.78	16.07	3.16	11.40	1.34	50.78	16.07	3.16	
ZA_59B	0.99	1.00	14.56	0.99	47.00	11.29	4.16	14.56	0.99	47.00	11.29	4.16	
ZA_60	0.78	1.00	27.40	0.78	68.41	13.22	5.18	27.40	0.78	68.41	13.22	5.18	
ZA_61A	0.66	1.00	4.74	0.66	10.52	1.63	6.47	4.74	0.66	10.52	1.63	6.47	
ZA_61B	0.53	1.00	13.20	0.53	22.53	2.94	7.66	13.20	0.53	22.53	2.94	7.66	
ZA_61D	0.76	1.00	4.48	0.76	11.60	2.03	5.71	4.48	0.76	11.60	2.03	5.71	
ZA_62A	0.48	1.00	22.16	0.48	33.84	4.03	8.41	22.16	0.48	33.84	4.03	8.41	
ZA_62B	0.49	1.00	14.14	0.49	22.00	2.63	8.35	14.14	0.49	22.00	2.63	8.35	
ZA_63A	0.77	1.00	75.28	0.77	181.74	34.58	5.26	75.28	0.77	181.74	34.58	5.26	
ZA_63B	0.51	1.00	13.94	0.51	22.86	2.88	7.94	13.94	0.51	22.86	2.88	7.94	
ZA_63C	0.43	1.00	21.00	0.43	28.44	3.01	9.46	21.00	0.43	28.44	3.01	9.46	
ZA_63D	0.62	1.00	22.71	0.62	44.53	6.77	6.58	22.71	0.62	44.53	6.77	6.58	
ZA_64A	0.49	1.00	71.60	0.49	110.54	13.50	8.19	71.60	0.49	110.54	13.50	8.19	
ZA_64B	0.53	1.00	45.13	0.53	75.69	9.99	7.58	45.13	0.53	75.69	9.99	7.58	
ZA_65A	0.42	1.00	12.10	0.42	16.31	1.69	9.64	12.10	0.42	16.31	1.69	9.64	
ZA_65B	0.57	1.00	28.50	0.57	51.15	7.17	7.14	28.50	0.57	51.15	7.17	7.14	
ZA_65C	0.56	1.00	31.66	0.56	55.75	7.68	7.26	31.66	0.56	55.75	7.68	7.26	
ZA_65D	0.66	1.00	45.93	0.66	95.87	15.70	6.10	45.93	0.66	95.87	15.70	6.10	

Specimen	Canopy Height (mm)	Primary Elements						Total					
		Number	Avg. Length (mm)	Avg. Width (mm)	SA (mm ²)	V (mm ³)	SA/V (mm ⁻¹)	Number	Avg. Length (mm)	Avg. Width (mm)	SA (mm ²)	V (mm ³)	SA/V (mm ⁻¹)
ZA_66B	0.58	1.00	19.34	0.58	35.63	5.07	7.02	19.34	0.58	35.63	5.07	7.02	
ZA_67A	0.67	1.00	37.38	0.67	79.22	13.13	6.03	37.38	0.67	79.22	13.13	6.03	
ZA_67B	0.68	1.00	14.11	0.68	30.85	5.12	6.02	14.11	0.68	30.85	5.12	6.02	
ZA_67C	0.68	1.00	24.76	0.68	53.60	8.99	5.96	24.76	0.68	53.60	8.99	5.96	
ZA_68A	0.50	1.00	25.62	0.50	40.87	5.09	8.03	25.62	0.50	40.87	5.09	8.03	
ZA_68B	0.46	1.00	43.82	0.46	64.18	7.41	8.67	43.82	0.46	64.18	7.41	8.67	
ZA_68C	0.37	1.00	11.06	0.37	13.14	1.20	10.93	11.06	0.37	13.14	1.20	10.93	
ZA_69A	0.47	1.00	36.23	0.47	53.47	6.20	8.62	36.23	0.47	53.47	6.20	8.62	
ZA_69B	0.43	1.00	13.67	0.43	18.88	2.01	9.38	13.67	0.43	18.88	2.01	9.38	
ZA_69C	0.43	1.00	26.14	0.43	35.83	3.85	9.31	26.14	0.43	35.83	3.85	9.31	
ZA_69D	0.49	1.00	13.75	0.49	21.71	2.63	8.24	13.75	0.49	21.71	2.63	8.24	
ZA_69E	0.37	1.00	20.11	0.37	23.45	2.14	10.97	20.11	0.37	23.45	2.14	10.97	
ZA_69F	0.31	1.00	12.68	0.31	12.57	0.97	12.98	12.68	0.31	12.57	0.97	12.98	
ZA_69G	0.58	1.00	29.35	0.58	53.79	7.70	6.99	29.35	0.58	53.79	7.70	6.99	
ZA_69H	0.41	1.00	27.07	0.41	35.20	3.59	9.81	27.07	0.41	35.20	3.59	9.81	
ZA_69I	0.76	1.00	11.49	0.76	28.25	5.18	5.45	11.49	0.76	28.25	5.18	5.45	
ZA_69J	0.43	1.00	12.62	0.43	17.45	1.86	9.40	12.62	0.43	17.45	1.86	9.40	
ZA_69K	0.51	1.00	8.04	0.51	13.16	1.61	8.17	8.04	0.51	13.16	1.61	8.17	
ZA_69L	0.25	1.00	6.77	0.25	5.30	0.32	16.62	6.77	0.25	5.30	0.32	16.62	
ZA_69M	0.43	1.00	8.16	0.43	11.39	1.20	9.48	8.16	0.43	11.39	1.20	9.48	
ZA_70A	0.26	1.00	8.27	0.26	6.72	0.42	15.93	8.27	0.26	6.72	0.42	15.93	
ZA_70B	0.51	1.00	27.99	0.51	45.24	5.72	7.91	27.99	0.51	45.24	5.72	7.91	
ZA_70C	0.74	1.00	16.38	0.74	39.14	7.12	5.50	16.38	0.74	39.14	7.12	5.50	
ZA_70D	0.32	1.00	10.49	0.32	10.80	0.86	12.57	10.49	0.32	10.80	0.86	12.57	
ZA_70E	0.49	1.00	40.82	0.49	63.31	7.72	8.20	40.82	0.49	63.31	7.72	8.20	
ZA_70F	0.43	1.00	46.89	0.43	64.20	6.93	9.26	46.89	0.43	64.20	6.93	9.26	
ZA_71A	0.67	1.00	29.16	0.67	62.33	10.37	6.01	29.16	0.67	62.33	10.37	6.01	
ZA_71B	0.73	1.00	17.65	0.73	41.00	7.28	5.63	17.65	0.73	41.00	7.28	5.63	
ZA_71C	0.48	1.00	13.89	0.48	21.12	2.47	8.55	13.89	0.48	21.12	2.47	8.55	
ZA_72A	0.87	1.00	24.61	0.87	68.59	14.69	4.67	24.61	0.87	68.59	14.69	4.67	
ZA_72B	0.63	1.00	23.42	0.63	46.88	7.27	6.44	23.42	0.63	46.88	7.27	6.44	
ZA_72C	0.39	1.00	36.53	0.39	44.97	4.36	10.31	36.53	0.39	44.97	4.36	10.31	
ZA_72D	0.45	1.00	16.76	0.45	23.73	2.61	9.11	16.76	0.45	23.73	2.61	9.11	
ZA_72E	0.39	1.00	8.90	0.39	11.14	1.06	10.48	8.90	0.39	11.14	1.06	10.48	
ZA_72F	0.62	1.00	8.31	0.62	16.70	2.48	8.31	8.31	0.62	16.70	2.48	8.31	
ZA_73A	0.50	1.00	61.69	0.50	96.86	12.01	8.06	61.69	0.50	96.86	12.01	8.06	
ZA_73C	0.98	1.00	19.37	0.98	60.91	14.51	4.20	19.37	0.98	60.91	14.51	4.20	
ZA_74	0.94	1.00	40.65	0.94	121.24	28.14	4.31	40.65	0.94	121.24	28.14	4.31	
ZA_75	0.33	1.00	17.44	0.33	18.07	1.46	12.35	17.44	0.33	18.07	1.46	12.35	
ZA_76A	0.31	1.00	25.33	0.31	24.57	1.87	13.11	25.33	0.31	24.57	1.87	13.11	
ZA_76B	0.35	1.00	17.54	0.35	19.47	1.69	11.54	17.54	0.35	19.47	1.69	11.54	
ZA_76C	0.14	1.00	6.74	0.14	2.93	0.10	29.49	6.74	0.14	2.93	0.10	29.49	
ZA_76D	0.52	1.00	6.32	0.52	10.79	1.35	7.98	6.32	0.52	10.79	1.35	7.98	
ZA_76E	0.31	1.00	24.75	0.31	24.01	1.83	13.11	24.75	0.31	24.01	1.83	13.11	
ZA_77A	0.45	1.00	21.95	0.45	31.47	3.52	8.94	21.95	0.45	31.47	3.52	8.94	
ZA_78A	0.78	1.00	14.25	0.78	35.81	6.79	5.28	14.25	0.78	35.81	6.79	5.28	
ZA_79A	0.69	1.00	17.84	0.69	39.63	6.74	5.88	17.84	0.69	39.63	6.74	5.88	
ZA_79C	0.58	1.00	29.89	0.58	55.05	7.92	6.95	29.89	0.58	55.05	7.92	6.95	
ZA_80A	0.70	1.00	65.91	0.70	145.02	25.14	5.77	65.91	0.70	145.02	25.14	5.77	
ZA_80B	0.70	1.00	62.95	0.70	139.93	24.49	5.71	62.95	0.70	139.93	24.49	5.71	
ZA_80C	0.56	1.00	17.65	0.56	31.75	4.41	7.21	17.65	0.56	31.75	4.41	7.21	

Specimen	Canopy Height (mm)	Primary Elements						Total					
		Number	Avg. Length (mm)	Avg. Width (mm)	SA (mm ²)	V (mm ³)	SA/V (mm ⁻¹)	Number	Avg. Length (mm)	Avg. Width (mm)	SA (mm ²)	V (mm ³)	SA/V (mm ⁻¹)
ZA_81	0.52	1.00	94.86	0.52	156.50	20.45	7.65	94.86	0.52	156.50	20.45	7.65	
ZA_82A	0.48	1.00	53.56	0.48	81.59	9.81	8.32	53.56	0.48	81.59	9.81	8.32	
ZA_82B	0.82	1.00	24.79	0.82	64.88	13.08	4.96	24.79	0.82	64.88	13.08	4.96	
ZA_82C	0.59	1.00	25.39	0.59	47.26	6.85	6.90	25.39	0.59	47.26	6.85	6.90	
ZA_82D	0.52	1.00	34.50	0.52	57.20	7.44	7.69	34.50	0.52	57.20	7.44	7.69	
ZA_82E	0.50	1.00	12.03	0.50	19.17	2.33	8.21	12.03	0.50	19.17	2.33	8.21	
ZA_82F	0.60	1.00	20.71	0.60	39.37	5.79	6.80	20.71	0.60	39.37	5.79	6.80	
ZA_82G	0.35	1.00	12.12	0.35	13.55	1.17	11.56	12.12	0.35	13.55	1.17	11.56	
ZA_82H	0.59	1.00	32.33	0.59	60.03	8.72	6.89	32.33	0.59	60.03	8.72	6.89	
ZA_82I	0.35	1.00	24.35	0.35	27.03	2.35	11.48	24.35	0.35	27.03	2.35	11.48	
ZA_83A	0.48	1.00	29.69	0.48	45.20	5.39	8.38	29.69	0.48	45.20	5.39	8.38	
ZA_83B	0.34	1.00	30.09	0.34	32.31	2.73	11.83	30.09	0.34	32.31	2.73	11.83	
ZA_83C	0.60	1.00	16.12	0.60	30.99	4.57	6.78	16.12	0.60	30.99	4.57	6.78	
ZA_83D	0.38	1.00	13.12	0.38	15.89	1.49	10.68	13.12	0.38	15.89	1.49	10.68	
ZA_83E	0.77	1.00	29.49	0.77	72.14	13.69	5.27	29.49	0.77	72.14	13.69	5.27	
ZA_83F	0.36	1.00	15.19	0.36	17.37	1.55	11.24	15.19	0.36	17.37	1.55	11.24	
ZA_83G	0.34	1.00	16.75	0.34	18.06	1.52	11.88	16.75	0.34	18.06	1.52	11.88	
ZA_84	0.85	1.00	64.39	0.85	172.98	36.52	4.74	64.39	0.85	172.98	36.52	4.74	
ZA_85A	0.73	1.00	40.11	0.73	92.65	16.73	5.54	40.11	0.73	92.65	16.73	5.54	
ZA_85B	0.48	1.00	8.62	0.48	13.39	1.57	8.55	8.62	0.48	13.39	1.57	8.55	
ZA_85C	0.22	1.00	9.12	0.22	6.50	0.36	18.08	9.12	0.22	6.50	0.36	18.08	
ZA_86	0.89	1.00	18.15	0.89	51.65	11.16	4.63	18.15	0.89	51.65	11.16	4.63	
ZA_87A	0.83	1.00	43.96	0.83	116.06	23.94	4.85	43.96	0.83	116.06	23.94	4.85	
ZA_87B	0.59	1.00	39.25	0.59	73.13	10.69	6.84	39.25	0.59	73.13	10.69	6.84	
ZA_87C	0.51	1.00	30.57	0.51	49.07	6.17	7.95	30.57	0.51	49.07	6.17	7.95	
ZA_87D	0.33	1.00	9.51	0.33	10.11	0.83	12.22	9.51	0.33	10.11	0.83	12.22	
ZA_87E	0.53	1.00	15.81	0.53	26.59	3.45	7.72	15.81	0.53	26.59	3.45	7.72	
ZA_88A	0.32	1.00	10.68	0.32	10.85	0.85	12.73	10.68	0.32	10.85	0.85	12.73	
ZA_88B	0.75	1.00	10.20	0.75	24.94	4.52	5.52	10.20	0.75	24.94	4.52	5.52	
ZA_88C	0.32	1.00	34.43	0.32	34.65	2.75	12.60	34.43	0.32	34.65	2.75	12.60	
ZA_88D	0.53	1.00	11.83	0.53	20.17	2.62	7.70	11.83	0.53	20.17	2.62	7.70	
ZA_89A	0.73	1.00	19.25	0.73	44.89	8.03	5.59	19.25	0.73	44.89	8.03	5.59	
ZA_89B	0.48	1.00	8.71	0.48	13.37	1.55	8.63	8.71	0.48	13.37	1.55	8.63	
ZA_89C	0.40	1.00	13.16	0.40	16.57	1.61	10.28	13.16	0.40	16.57	1.61	10.28	
ZA_89D	0.44	1.00	15.26	0.44	21.49	2.34	9.18	15.26	0.44	21.49	2.34	9.18	
ZA_90	0.69	1.00	17.84	0.69	39.51	6.71	5.89	17.84	0.69	39.51	6.71	5.89	
ZA_91	0.53	1.00	23.84	0.53	40.12	5.26	7.63	23.84	0.53	40.12	5.26	7.63	
ZA_92	0.29	1.00	26.49	0.29	24.26	1.75	13.87	26.49	0.29	24.26	1.75	13.87	
ZA_94A	0.60	1.00	19.28	0.60	36.58	5.36	6.83	19.28	0.60	36.58	5.36	6.83	
ZA_94B	0.60	1.00	8.59	0.60	16.61	2.39	6.96	8.59	0.60	16.61	2.39	6.96	
ZA_94C	0.37	1.00	14.00	0.37	16.38	1.49	11.01	14.00	0.37	16.38	1.49	11.01	
ZA_94D	0.65	1.00	19.76	0.65	40.67	6.45	6.30	19.76	0.65	40.67	6.45	6.30	
ZA_95	0.52	1.00	22.24	0.52	36.46	4.65	7.84	22.24	0.52	36.46	4.65	7.84	
ZA_96A	0.30	1.00	9.15	0.30	8.67	0.63	13.69	9.15	0.30	8.67	0.63	13.69	
ZA_96B	0.53	1.00	19.31	0.53	32.32	4.19	7.71	19.31	0.53	32.32	4.19	7.71	
ZA_97	0.44	1.00	11.44	0.44	16.04	1.72	9.31	11.44	0.44	16.04	1.72	9.31	
ZA_98	0.66	1.00	12.79	0.66	27.28	4.40	6.66	12.79	0.66	27.28	4.40	6.20	
ZA_99A	0.30	1.00	21.08	0.30	20.27	1.53	13.25	21.08	0.30	20.27	1.53	13.25	
ZA_99B	0.89	1.00	13.44	0.89	38.66	8.30	4.66	13.44	0.89	38.66	8.30	4.66	
ZA_100	0.72	1.00	56.55	0.72	128.29	22.88	5.61	56.55	0.72	128.29	22.88	5.61	
ZA_101A	0.72	1.00	30.87	0.72	70.70	12.60	5.61	30.87	0.72	70.70	12.60	5.61	

Specimen	Canopy Height (mm)	Primary Elements						Total					
		Number	Avg. Length (mm)	Avg. Width (mm)	SA (mm ²)	V (mm ³)	SA/V (mm ⁻¹)	Number	Avg. Length (mm)	Avg. Width (mm)	SA (mm ²)	V (mm ³)	SA/V (mm ⁻¹)
ZA_101B	0.45	1.00	9.32	0.45	13.48	1.48	9.10	9.32	0.45	13.48	1.48	9.10	
ZA_102A	0.73	1.00	10.69	0.73	25.37	4.48	5.66	10.69	0.73	25.37	4.48	5.66	
ZA_102B	0.57	1.00	26.24	0.57	47.73	6.76	7.06	26.24	0.57	47.73	6.76	7.06	
ZA_102C	0.45	1.00	18.65	0.45	26.85	3.00	8.94	18.65	0.45	26.85	3.00	8.94	
ZA_103A	0.44	1.00	27.41	0.44	38.08	4.15	9.18	27.41	0.44	38.08	4.15	9.18	
ZA_103B	0.20	1.00	18.29	0.20	11.32	0.55	20.52	18.29	0.20	11.32	0.55	20.52	
ZA_104	0.60	1.00	40.89	0.60	78.00	11.67	6.68	40.89	0.60	78.00	11.67	6.68	
ZA_105A	0.73	1.00	15.21	0.73	35.71	6.36	5.61	15.21	0.73	35.71	6.36	5.61	
ZA_105B	0.58	1.00	13.35	0.58	24.84	3.53	7.05	13.35	0.58	24.84	3.53	7.05	
ZA_106	0.56	1.00	18.89	0.56	33.95	4.72	7.20	18.89	0.56	33.95	4.72	7.20	
ZA_107B	0.55	1.00	19.51	0.55	34.17	4.63	7.38	19.51	0.55	34.17	4.63	7.38	
ZA_107C	0.46	1.00	9.71	0.46	14.32	1.61	8.92	9.71	0.46	14.32	1.61	8.92	
ZA_108A	0.19	1.00	2.98	0.19	1.78	0.08	22.29	2.98	0.19	1.78	0.08	22.29	
ZA_108B	0.58	1.00	5.07	0.58	9.69	1.32	7.34	5.07	0.58	9.69	1.32	7.34	
ZA_108C	0.30	1.00	5.81	0.30	5.58	0.41	13.77	5.81	0.30	5.58	0.41	13.77	
ZA_110	0.83	1.00	22.37	0.83	59.17	12.01	4.93	22.37	0.83	59.17	12.01	4.93	
ZA_112	0.77	1.00	16.01	0.77	39.53	7.41	5.33	16.01	0.77	39.53	7.41	5.33	
ZA_114	0.31	1.00	17.07	0.31	16.61	1.26	13.15	17.07	0.31	16.61	1.26	13.15	
ZA_117A	0.14	1.00	9.64	0.14	4.31	0.15	28.50	9.64	0.14	4.31	0.15	28.50	
ZA_117B	0.40	1.00	14.39	0.40	18.23	1.79	10.19	14.39	0.40	18.23	1.79	10.19	
ZA_118A	0.22	1.00	13.54	0.22	9.39	0.51	18.41	13.54	0.22	9.39	0.51	18.41	
ZA_118B	0.25	1.00	6.47	0.25	5.07	0.30	16.64	6.47	0.25	5.07	0.30	16.64	
ZA_119A	0.35	1.00	29.90	0.35	33.43	2.94	11.37	29.90	0.35	33.43	2.94	11.37	
ZA_119B	0.28	1.00	6.80	0.28	6.10	0.42	14.58	6.80	0.28	6.10	0.42	14.58	
ZA_119C	0.32	1.00	20.86	0.32	21.05	1.67	12.64	20.86	0.32	21.05	1.67	12.64	
ZA_119D	0.38	1.00	8.82	0.38	10.61	0.97	10.89	8.82	0.38	10.61	0.97	10.89	
ZA_121A	0.26	1.00	15.52	0.26	12.92	0.84	15.34	15.52	0.26	12.92	0.84	15.34	
ZA_121B	0.61	1.00	19.13	0.61	37.47	5.66	6.62	19.13	0.61	37.47	5.66	6.62	
ZA_122A	0.48	1.00	13.94	0.48	21.19	2.48	8.55	13.94	0.48	21.19	2.48	8.55	
ZA_122B	0.85	1.00	6.78	0.85	19.28	3.86	4.99	6.78	0.85	19.28	3.86	4.99	
ZA_122C	0.67	1.00	23.92	0.67	50.80	8.35	6.08	23.92	0.67	50.80	8.35	6.08	
ZA_123A	0.68	1.00	15.33	0.68	33.60	5.61	5.99	15.33	0.68	33.60	5.61	5.99	
ZA_123B	0.62	1.00	25.80	0.62	50.74	7.76	6.54	25.80	0.62	50.74	7.76	6.54	
ZA_124A	0.93	1.00	53.98	0.93	158.63	36.49	4.35	53.98	0.93	158.63	36.49	4.35	
ZA_124B	0.32	1.00	10.09	0.32	10.43	0.83	12.54	10.09	0.32	10.43	0.83	12.54	
ZA_125	1.17	1.00	14.80	1.17	56.33	15.80	3.57	14.80	1.17	56.33	15.80	3.57	
ZA_126A	1.16	1.00	31.41	1.16	116.63	33.24	3.51	31.41	1.16	116.63	33.24	3.51	
ZA_126B	1.19	1.00	11.55	1.19	45.34	12.82	3.54	11.55	1.19	45.34	12.82	3.54	
ZA_127A	0.51	1.00	35.37	0.51	56.83	7.17	7.93	35.37	0.51	56.83	7.17	7.93	
ZA_127B	0.51	1.00	18.39	0.51	29.74	3.73	7.98	18.39	0.51	29.74	3.73	7.98	
ZA_128A	0.22	1.00	8.21	0.22	5.85	0.32	18.10	8.21	0.22	5.85	0.32	18.10	
ZA_128B	0.50	1.00	7.65	0.50	12.42	1.51	8.25	7.65	0.50	12.42	1.51	8.25	
ZA_128C	0.45	1.00	21.39	0.45	30.41	3.37	9.02	21.39	0.45	30.41	3.37	9.02	
ZA_128D	0.30	1.00	17.72	0.30	16.89	1.26	13.40	17.72	0.30	16.89	1.26	13.40	
ZA_128E	0.43	1.00	24.56	0.43	33.06	3.48	9.49	24.56	0.43	33.06	3.48	9.49	
ZA_129A	0.83	1.00	60.98	0.83	160.41	33.14	4.84	60.98	0.83	160.41	33.14	4.84	
ZA_129B	0.82	1.00	45.55	0.82	118.63	24.16	4.91	45.55	0.82	118.63	24.16	4.91	
ZA_129C	1.11	1.00	14.07	1.11	50.84	13.54	3.76	14.07	1.11	50.84	13.54	3.76	
ZA_129D	0.78	1.00	17.86	0.78	44.52	8.46	5.26	17.86	0.78	44.52	8.46	5.26	
ZA_130B	0.21	1.00	3.69	0.21	2.44	0.12	20.05	3.69	0.21	2.44	0.12	20.05	
ZA_131	0.54	1.00	8.58	0.54	14.93	1.94	7.68	8.58	0.54	14.93	1.94	7.68	

Specimen	Canopy Height (mm)	Primary Elements						Total					
		Number	Avg. Length (mm)	Avg. Width (mm)	SA (mm ²)	V (mm ³)	SA/V (mm ⁻¹)	Number	Avg. Length (mm)	Avg. Width (mm)	SA (mm ²)	V (mm ³)	SA/V (mm ⁻¹)
ZA_133	0.54	1.00	10.98	0.54	18.90	2.47	7.66	10.98	0.54	18.90	2.47	7.66	
ZA_134A	0.70	1.00	13.79	0.70	31.17	5.34	5.84	13.79	0.70	31.17	5.34	5.84	
ZA_134B	0.28	1.00	10.31	0.28	9.22	0.64	14.43	10.31	0.28	9.22	0.64	14.43	
ZA_134C	0.31	1.00	8.63	0.31	8.67	0.67	12.97	8.63	0.31	8.67	0.67	12.97	
ZA_135	0.90	1.00	103.98	0.90	294.78	65.97	4.47	103.98	0.90	294.78	65.97	4.47	
ZA_136B	0.47	1.00	26.10	0.47	38.62	4.47	8.64	26.10	0.47	38.62	4.47	8.64	
ZA_137A	0.49	1.00	16.04	0.49	24.89	2.99	8.34	16.04	0.49	24.89	2.99	8.34	
ZA_137B	1.03	1.00	30.85	1.03	101.75	25.85	3.94	30.85	1.03	101.75	25.85	3.94	
ZA_139A	0.39	1.00	23.20	0.39	28.35	2.71	10.45	23.20	0.39	28.35	2.71	10.45	
ZA_139B	0.17	1.00	48.60	0.17	26.45	1.14	23.16	48.60	0.17	26.45	1.14	23.16	
ZA_139C	0.71	1.00	96.08	0.71	215.30	38.13	5.65	96.08	0.71	215.30	38.13	5.65	
ZA_140A	0.60	1.00	38.29	0.60	73.18	10.96	6.67	38.29	0.60	73.18	10.96	6.67	
ZA_140B	0.74	1.00	34.54	0.74	81.35	14.93	5.45	34.54	0.74	81.35	14.93	5.45	
ZA_140C	0.63	1.00	8.05	0.63	16.61	2.52	6.58	8.05	0.63	16.61	2.52	6.58	
ZA_141	0.66	1.00	14.00	0.66	29.79	4.82	6.19	14.00	0.66	29.79	4.82	6.19	
ZA_144A	0.61	1.00	21.94	0.61	42.60	6.41	6.65	21.94	0.61	42.60	6.41	6.65	
ZA_144B	0.39	1.00	13.97	0.39	17.30	1.66	10.43	13.97	0.39	17.30	1.66	10.43	
ZA_144C	0.22	1.00	11.40	0.22	8.02	0.44	18.19	11.40	0.22	8.02	0.44	18.19	
ZA_144D	0.14	1.00	8.33	0.14	3.64	0.12	29.23	8.33	0.14	3.64	0.12	29.23	
ZA_144E	0.22	1.00	8.17	0.22	5.77	0.32	18.26	8.17	0.22	5.77	0.32	18.26	
ZA_146A	0.37	1.00	21.81	0.37	25.83	2.39	10.79	21.81	0.37	25.83	2.39	10.79	
ZA_146B	0.33	1.00	12.64	0.33	13.31	1.09	12.24	12.64	0.33	13.31	1.09	12.24	
ZA_146C	0.37	1.00	12.46	0.37	14.85	1.37	10.86	12.46	0.37	14.85	1.37	10.86	
ZA_147A	0.49	1.00	5.71	0.49	9.16	1.08	8.51	5.71	0.49	9.16	1.08	8.51	
ZA_147B	0.65	1.00	9.24	0.65	19.65	3.10	6.33	9.24	0.65	19.65	3.10	6.33	
ZA_149	0.77	1.00	23.13	0.77	56.92	10.79	5.27	23.13	0.77	56.92	10.79	5.27	
ZA_150	0.37	1.00	8.04	0.37	9.66	0.88	10.94	8.04	0.37	9.66	0.88	10.94	
ZA_151A	0.68	1.00	8.35	0.68	18.67	3.07	6.09	8.35	0.68	18.67	3.07	6.09	
ZA_151B	0.65	1.00	23.40	0.65	48.42	7.76	6.24	23.40	0.65	48.42	7.76	6.24	
ZA_151C	0.23	1.00	7.87	0.23	5.69	0.32	17.88	7.87	0.23	5.69	0.32	17.88	
ZA_152A	0.48	1.00	18.15	0.48	27.48	3.23	8.51	18.15	0.48	27.48	3.23	8.51	
ZA_152B	0.08	1.00	10.14	0.08	2.62	0.05	48.98	10.14	0.08	2.62	0.05	48.98	
ZA_152C	0.65	1.00	8.33	0.65	17.73	2.78	6.38	8.33	0.65	17.73	2.78	6.38	
ZA_152D	0.62	1.00	5.09	0.62	10.53	1.54	6.83	5.09	0.62	10.53	1.54	6.83	
ZA_152E	0.55	1.00	21.39	0.55	37.21	5.02	7.41	21.39	0.55	37.21	5.02	7.41	
ZA_154A	0.30	1.00	6.26	0.30	6.08	0.45	13.56	6.26	0.30	6.08	0.45	13.56	
ZA_154B	0.17	1.00	4.15	0.17	2.22	0.09	24.43	4.15	0.17	2.22	0.09	24.43	
ZA_155A	0.38	1.00	13.21	0.38	15.95	1.49	10.71	13.21	0.38	15.95	1.49	10.71	
ZA_155B	0.35	1.00	7.47	0.35	8.38	0.71	11.73	7.47	0.35	8.38	0.71	11.73	
ZA_155C	0.34	1.00	12.87	0.34	13.88	1.16	11.95	12.87	0.34	13.88	1.16	11.95	
ZA_156	0.63	1.00	6.90	0.63	14.32	2.16	6.62	6.90	0.63	14.32	2.16	6.62	
ZA_157A	0.18	1.00	16.33	0.18	9.49	0.43	21.86	16.33	0.18	9.49	0.43	21.86	
ZA_157B	0.40	1.00	7.63	0.40	9.76	0.94	10.34	7.63	0.40	9.76	0.94	10.34	
ZA_157C	0.24	1.00	12.33	0.24	9.19	0.53	17.18	12.33	0.24	9.19	0.53	17.18	
ZA_157D	0.09	1.00	5.88	0.09	1.71	0.04	43.82	5.88	0.09	1.71	0.04	43.82	
ZA_157E	0.40	1.00	8.01	0.40	10.23	0.99	10.33	8.01	0.40	10.23	0.99	10.33	
ZA_159A	0.44	1.00	28.86	0.44	40.18	4.39	9.16	28.86	0.44	40.18	4.39	9.16	
ZA_159B	0.37	1.00	12.23	0.37	14.26	1.29	11.09	12.23	0.37	14.26	1.29	11.09	
ZA_160	0.48	1.00	22.32	0.48	34.07	4.05	8.41	22.32	0.48	34.07	4.05	8.41	
ZA_162	0.52	1.00	12.07	0.52	20.18	2.57	7.84	12.07	0.52	20.18	2.57	7.84	
ZA_163A	0.38	1.00	12.68	0.38	15.44	1.45	10.63	12.68	0.38	15.44	1.45	10.63	

Specimen	Canopy Height (mm)	Primary Elements						Total					
		Number	Avg. Length (mm)	Avg. Width (mm)	SA (mm ²)	V (mm ³)	SA/V (mm ⁻¹)	Number	Avg. Length (mm)	Avg. Width (mm)	SA (mm ²)	V (mm ³)	SA/V (mm ⁻¹)
ZA_163B	0.44	1.00	6.93	0.44	9.78	1.03	9.46	6.93	0.44	9.78	1.03	9.46	
ZA_163C	0.50	1.00	17.86	0.50	28.32	3.48	8.14	17.86	0.50	28.32	3.48	8.14	
ZA_163D	0.48	1.00	19.20	0.48	29.49	3.52	8.39	19.20	0.48	29.49	3.52	8.39	
ZA_166	0.49	1.00	59.13	0.49	91.72	11.24	8.16	59.13	0.49	91.72	11.24	8.16	
ZA_167A	0.22	1.00	6.93	0.22	4.84	0.26	18.55	6.93	0.22	4.84	0.26	18.55	
ZA_167B	0.17	1.00	13.26	0.17	7.25	0.31	23.27	13.26	0.17	7.25	0.31	23.27	
ZA_167C	0.47	1.00	8.33	0.47	12.67	1.45	8.73	8.33	0.47	12.67	1.45	8.73	
ZA_167D	0.17	1.00	9.09	0.17	4.98	0.21	23.34	9.09	0.17	4.98	0.21	23.34	
ZA_167E	0.08	1.00	7.04	0.08	1.71	0.03	52.23	7.04	0.08	1.71	0.03	52.23	
ZA_169	0.51	1.00	51.80	0.51	83.36	10.58	7.88	51.80	0.51	83.36	10.58	7.88	
ZA_170A	0.25	1.00	8.59	0.25	6.84	0.42	16.23	8.59	0.25	6.84	0.42	16.23	
ZA_170B	0.44	1.00	4.43	0.44	6.45	0.68	9.50	4.43	0.44	6.45	0.68	9.50	
ZA_170C	0.09	1.00	4.29	0.09	22.28	2.47	45.92	4.29	0.09	22.28	2.47	45.92	
ZA_171A	0.45	1.00	15.54	0.45	9.28	1.16	7.99	15.54	0.45	9.28	1.16	7.99	
ZA_171B	0.53	1.00	5.37	0.53	8.10	0.58	14.02	5.37	0.53	8.10	0.58	14.02	
ZA_172B	0.29	1.00	8.75	0.29	8.10	0.58	14.02	8.75	0.29	8.10	0.58	14.02	
ZA_173A	0.54	1.00	17.92	0.54	31.08	4.16	7.46	17.92	0.54	31.08	4.16	7.46	
ZA_173B	0.56	1.00	20.32	0.56	36.29	5.02	7.23	20.32	0.56	36.29	5.02	7.23	
ZA_175	0.78	1.00	17.60	0.78	44.06	8.41	5.24	17.60	0.78	44.06	8.41	5.24	
ZA_177	0.53	1.00	22.33	0.53	37.67	4.94	7.62	22.33	0.53	37.67	4.94	7.62	
ZA_178	0.75	1.00	10.32	0.75	25.21	4.57	5.52	10.32	0.75	25.21	4.57	5.52	
ZA_179A	0.15	1.00	7.20	0.15	3.31	0.12	27.86	7.20	0.15	3.31	0.12	27.86	
ZA_179B	0.15	1.00	8.21	0.15	3.77	0.14	27.83	8.21	0.15	3.77	0.14	27.83	
ZA_179C	0.46	1.00	10.55	0.46	15.56	1.75	8.89	10.55	0.46	15.56	1.75	8.89	
ZA_179D	0.52	1.00	8.35	0.52	14.16	1.80	7.87	8.35	0.52	14.16	1.80	7.87	
ZA_179E	0.46	1.00	10.47	0.46	15.45	1.74	8.89	10.47	0.46	15.45	1.74	8.89	
ZA_182A	0.27	1.00	11.41	0.27	9.64	0.63	15.21	11.41	0.27	9.64	0.63	15.21	
ZA_182B	0.31	1.00	9.74	0.31	9.73	0.75	12.98	9.74	0.31	9.73	0.75	12.98	
ZA_182C	0.27	1.00	7.47	0.27	6.35	0.42	15.31	7.47	0.27	6.35	0.42	15.31	
ZA_182D	0.37	1.00	8.07	0.37	9.57	0.86	11.09	8.07	0.37	9.57	0.86	11.09	
ZA_183	0.44	1.00	11.20	0.44	15.74	1.69	9.29	11.20	0.44	15.74	1.69	9.29	
ZA_184A	0.18	1.00	9.45	0.18	5.45	0.25	22.19	9.45	0.18	5.45	0.25	22.19	
ZA_184B	0.18	1.00	15.58	0.18	8.95	0.41	22.11	15.58	0.18	8.95	0.41	22.11	
ZA_186C	0.28	1.00	7.48	0.28	6.72	0.46	14.50	7.48	0.28	6.72	0.46	14.50	
ZA_186D	0.31	1.00	12.50	0.31	12.48	0.97	12.90	12.50	0.31	12.48	0.97	12.90	
ZA_187B	0.38	1.00	68.59	0.38	82.71	7.90	10.47	68.59	0.38	82.71	7.90	10.47	
ZA_187C	0.30	1.00	9.93	0.30	9.56	0.71	13.45	9.93	0.30	9.56	0.71	13.45	
ZA_187D	0.10	1.00	7.64	0.10	2.32	0.06	41.93	7.64	0.10	2.32	0.06	41.93	
ZA_189A	0.70	1.00	28.55	0.70	63.06	10.83	5.83	28.55	0.70	63.06	10.83	5.83	
ZA_189B	0.38	1.00	11.59	0.38	13.90	1.29	10.81	11.59	0.38	13.90	1.29	10.81	
ZA_190	0.47	1.00	39.34	0.47	58.03	6.73	8.62	39.34	0.47	58.03	6.73	8.62	
ZA_191A	0.49	1.00	27.08	0.49	42.22	5.15	8.20	27.08	0.49	42.22	5.15	8.20	
ZA_191B	0.26	1.00	45.60	0.26	37.33	2.42	15.43	45.60	0.26	37.33	2.42	15.43	
ZA_192A	0.74	1.00	11.74	0.74	28.15	5.05	5.58	11.74	0.74	28.15	5.05	5.58	
ZA_192B	0.70	1.00	14.61	0.70	32.98	5.65	5.83	14.61	0.70	32.98	5.65	5.83	
ZA_192C	0.42	1.00	8.87	0.42	12.06	1.25	9.68	8.87	0.42	12.06	1.25	9.68	
ZA_192D	0.42	1.00	10.79	0.42	14.62	1.52	9.64	10.79	0.42	14.62	1.52	9.64	
ZA_193	0.52	1.00	27.05	0.52	44.68	5.76	7.75	27.05	0.52	44.68	5.76	7.75	
ZA_194	0.97	1.00	21.55	0.97	67.18	15.95	4.21	21.55	0.97	67.18	15.95	4.21	
ZA_195B	0.35	1.00	19.72	0.35	21.61	1.85	11.66	19.72	0.35	21.61	1.85	11.66	
ZA_196A	0.46	1.00	31.09	0.46	44.84	5.07	8.84	31.09	0.46	44.84	5.07	8.84	

Specimen	Canopy Height (mm)	Primary Elements						Total					
		Number	Avg. Length (mm)	Avg. Width (mm)	SA (mm ²)	V (mm ³)	SA/V (mm ⁻¹)	Number	Avg. Length (mm)	Avg. Width (mm)	SA (mm ²)	V (mm ³)	SA/V (mm ⁻¹)
ZA_196B	0.52	1.00	28.78	0.52	47.32	6.08	7.78	28.78	0.52	47.32	6.08	7.78	
ZA_196C	0.46	1.00	22.43	0.46	32.44	3.66	8.86	22.43	0.46	32.44	3.66	8.86	
ZA_196D	0.29	1.00	16.63	0.29	15.17	1.08	14.01	16.63	0.29	15.17	1.08	14.01	
ZA_196E	0.42	1.00	8.46	0.42	11.43	1.17	9.76	8.46	0.42	11.43	1.17	9.76	
ZA_196F	0.37	1.00	6.46	0.37	7.66	1.11	11.21	6.46	0.37	7.66	1.11	11.21	
ZA_197A	0.65	1.00	56.01	0.65	114.63	18.46	6.21	56.01	0.65	114.63	18.46	6.21	
ZA_197B	0.43	1.00	22.11	0.43	29.85	3.15	9.48	22.11	0.43	29.85	3.15	9.48	
ZA_200A	0.56	1.00	87.20	0.56	152.72	21.16	7.22	87.20	0.56	152.72	21.16	7.22	
ZA_200B	0.56	1.00	10.81	0.56	19.36	2.62	7.38	10.81	0.56	19.36	2.62	7.38	
ZA_200C	0.22	1.00	20.25	0.22	14.19	0.78	18.12	20.25	0.22	14.19	0.78	18.12	
ZA_201	0.78	1.00	8.60	0.78	21.99	4.10	5.37	8.60	0.78	21.99	4.10	5.37	
ZA_202	0.75	1.00	36.59	0.75	87.41	16.29	5.37	36.59	0.75	87.41	16.29	5.37	
ZA_203	0.58	1.00	10.47	0.58	19.53	2.75	7.11	10.47	0.58	19.53	2.75	7.11	
ZA_204	0.82	1.00	9.90	0.82	26.67	5.27	5.06	9.90	0.82	26.67	5.27	5.06	
ZA_205	0.68	1.00	10.42	0.68	22.80	3.73	6.12	10.42	0.68	22.80	3.73	6.12	
ZA_206A	0.41	1.00	34.44	0.41	45.04	4.63	9.72	34.44	0.41	45.04	4.63	9.72	
ZA_206B	0.37	1.00	11.13	0.37	13.25	1.22	10.90	11.13	0.37	13.25	1.22	10.90	
ZA_206C	0.53	3.00	25.51	0.53	43.23	5.71	7.57	25.51	0.53	43.23	5.71	7.57	
ZA_206D	0.44	1.00	68.88	0.44	95.25	10.42	9.14	68.88	0.44	95.25	10.42	9.14	
ZA_206E	0.60	1.00	25.52	0.60	48.98	7.31	6.70	25.52	0.60	48.98	7.31	6.70	
ZA_208	0.67	1.00	9.73	0.67	21.07	3.40	6.20	9.73	0.67	21.07	3.40	6.20	
ZA_209	0.56	1.00	28.50	0.56	50.42	6.97	7.24	28.50	0.56	50.42	6.97	7.24	
ZA_210	0.57	1.00	15.72	0.57	28.44	3.95	7.19	15.72	0.57	28.44	3.95	7.19	
ZA_211	0.79	1.00	7.26	0.79	18.89	3.52	5.36	7.26	0.79	18.89	3.52	5.36	
ZA_212A	0.68	1.00	52.25	0.68	112.61	19.08	5.90	52.25	0.68	112.61	19.08	5.90	
ZA_212B	0.52	1.00	18.57	0.52	30.62	3.91	7.83	18.57	0.52	30.62	3.91	7.83	
ZA_212C	0.51	1.00	22.80	0.51	36.77	4.62	7.96	22.80	0.51	36.77	4.62	7.96	
ZA_212D	0.41	1.00	26.48	0.41	34.09	3.44	9.90	26.48	0.41	34.09	3.44	9.90	
ZA_212E	0.32	1.00	10.34	0.32	10.58	0.84	12.65	10.34	0.32	10.58	0.84	12.65	
ZA_214A	0.78	1.00	36.62	0.78	90.76	17.53	5.18	36.62	0.78	90.76	17.53	5.18	
ZA_214B	0.20	1.00	11.40	0.20	7.11	0.35	20.48	11.40	0.20	7.11	0.35	20.48	
ZA_217A	0.09	1.00	4.05	0.09	1.14	0.03	45.44	4.05	0.09	1.14	0.03	45.44	
ZA_217B	0.25	1.00	5.25	0.25	4.26	0.26	16.25	5.25	0.25	4.26	0.26	16.25	
ZA_217E	0.28	1.00	2.50	0.28	2.34	0.16	14.99	2.50	0.28	2.34	0.16	14.99	
ZA_217F	0.23	1.00	2.99	0.23	2.20	0.12	18.37	2.99	0.23	2.20	0.12	18.37	
ZA_218A	0.50	1.00	21.03	0.50	33.42	4.13	8.10	21.03	0.50	33.42	4.13	8.10	
ZA_218B	0.49	1.00	16.28	0.49	25.43	3.07	8.29	16.28	0.49	25.43	3.07	8.29	
ZA_218C	0.71	1.00	18.31	0.71	41.79	7.31	5.72	18.31	0.71	41.79	7.31	5.72	
ZA_218D	0.14	1.00	4.13	0.14	1.83	0.06	29.26	4.13	0.14	1.83	0.06	29.26	
ZA_219	0.29	1.00	25.23	0.29	23.19	1.68	13.82	25.23	0.29	23.19	1.68	13.82	
ZA_220A	0.25	1.00	37.81	0.25	29.90	1.87	15.99	37.81	0.25	29.90	1.87	15.99	
ZA_220B	0.16	1.00	6.99	0.16	3.53	0.14	25.44	6.99	0.16	3.53	0.14	25.44	
ZA_220C	0.41	1.00	8.40	0.41	10.93	1.08	10.11	8.40	0.41	10.93	1.08	10.11	
ZA_220D	0.34	1.00	8.18	0.34	8.84	0.73	12.11	8.18	0.34	8.84	0.73	12.11	
ZA_221A	0.31	1.00	20.63	0.31	20.49	1.60	12.84	20.63	0.31	20.49	1.60	12.84	
ZA_221B	0.12	1.00	8.12	0.12	3.16	0.10	32.77	8.12	0.12	3.16	0.10	32.77	
ZA_221C	0.31	1.00	20.67	0.31	20.54	1.60	12.84	20.67	0.31	20.54	1.60	12.84	
ZA_221D	1.17	1.00	6.03	1.17	24.37	6.51	3.74	6.03	1.17	24.37	6.51	3.74	
ZA_222	0.47	1.00	6.82	0.47	10.34	1.17	8.86	6.82	0.47	10.34	1.17	8.86	
ZA_223A	0.34	1.00	10.99	0.34	12.02	1.02	11.84	10.99	0.34	12.02	1.02	11.84	
ZA_233B	0.67	1.00	6.30	0.67	13.86	2.19	6.32	6.30	0.67	13.86	2.19	6.32	

Specimen	Canopy Height (mm)	Primary Elements						Total					
		Number	Avg. Length (mm)	Avg. Width (mm)	SA (mm ²)	V (mm ³)	SA/V (mm ⁻¹)	Number	Avg. Length (mm)	Avg. Width (mm)	SA (mm ²)	V (mm ³)	SA/V (mm ⁻¹)
ZA_224A	0.94	1.00	10.54	0.94	32.50	7.31	4.45	10.54	0.94	32.50	7.31	4.45	
ZA_224B	0.25	1.00	12.04	0.25	9.39	0.57	16.43	12.04	0.25	9.39	0.57	16.43	
ZA_244C	0.25	1.00	10.39	0.25	8.12	0.49	16.45	10.39	0.25	8.12	0.49	16.45	
ZA_224D	0.28	1.00	4.55	0.28	4.05	0.27	14.99	4.55	0.28	4.05	0.27	14.99	
ZA_224E	0.28	1.00	11.44	0.28	9.99	0.68	14.72	11.44	0.28	9.99	0.68	14.72	
ZA_224F	0.28	1.00	5.45	0.28	4.82	0.32	14.91	5.45	0.28	4.82	0.32	14.91	
ZA_224G	0.35	1.00	4.97	0.35	5.60	0.47	11.93	4.97	0.35	5.60	0.47	11.93	
ZA_225	0.42	1.00	21.51	0.42	28.57	2.96	9.64	21.51	0.42	28.57	2.96	9.64	
ZA_226	0.97	1.00	23.27	0.97	72.11	17.08	4.22	23.27	0.97	72.11	17.08	4.22	
ZA_227	0.81	1.00	23.23	0.81	59.81	11.85	5.05	23.23	0.81	59.81	11.85	5.05	
ZA_228A	0.45	1.00	9.60	0.45	13.88	1.53	9.10	9.60	0.45	13.88	1.53	9.10	
ZA_228C	0.32	1.00	29.91	0.32	30.59	2.46	12.41	29.91	0.32	30.59	2.46	12.41	
ZA_229	0.47	1.00	33.81	0.47	50.46	5.91	8.53	33.81	0.47	50.46	5.91	8.53	
ZA_230	0.47	1.00	20.34	0.47	30.17	3.48	8.66	20.34	0.47	30.17	3.48	8.66	
ZA_231A	0.81	1.00	44.40	0.81	114.25	22.98	4.97	44.40	0.81	114.25	22.98	4.97	
ZA_231B	0.68	1.00	9.25	0.68	20.47	3.36	6.10	9.25	0.68	20.47	3.36	6.10	
ZA_231C	0.34	1.00	18.49	0.34	19.92	1.68	11.87	18.49	0.34	19.92	1.68	11.87	
ZA_232C	0.16	1.00	27.11	0.16	14.00	0.57	24.46	27.11	0.16	14.00	0.57	24.46	
ZA_233	0.50	1.00	40.71	0.50	63.79	7.86	8.11	40.71	0.50	63.79	7.86	8.11	
ZA_234B	0.69	1.00	44.79	0.69	97.64	16.69	5.85	44.79	0.69	97.64	16.69	5.85	
ZA_235A	0.37	1.00	30.38	0.37	35.32	3.23	10.94	30.38	0.37	35.32	3.23	10.94	
ZA_235B	0.43	1.00	19.98	0.43	27.20	2.89	9.42	19.98	0.43	27.20	2.89	9.42	
ZA_235C	0.63	1.00	20.27	0.63	40.92	6.38	6.42	20.27	0.63	40.92	6.38	6.42	
ZA_236	0.75	1.00	7.06	0.75	17.47	3.10	5.63	7.06	0.75	17.47	3.10	5.63	
ZA_238A	0.52	1.00	21.75	0.52	36.01	4.63	7.77	21.75	0.52	36.01	4.63	7.77	
ZA_238B	0.39	1.00	11.57	0.39	14.34	1.37	10.48	11.57	0.39	14.34	1.37	10.48	
ZA_238C	0.39	1.00	32.98	0.39	40.41	3.90	10.37	32.98	0.39	40.41	3.90	10.37	
ZA_238D	0.37	3.00	17.88	0.37	20.94	1.91	10.95	17.88	0.37	20.94	1.91	10.95	
ZA_238E	1.33	1.00	37.45	1.33	158.83	51.77	3.07	37.45	1.33	158.83	51.77	3.07	
ZA_240B	3.42	1.00	5.93	3.42	81.99	54.40	1.51	5.93	3.42	81.99	54.40	1.51	
ZA_240C	0.32	1.00	8.49	0.32	8.75	0.69	12.66	8.49	0.32	8.75	0.69	12.66	
ZA_241A	0.79	1.00	42.71	0.79	107.48	21.14	5.08	42.71	0.79	107.48	21.14	5.08	
ZA_241C	0.31	1.00	13.42	0.31	13.26	1.02	13.01	13.42	0.31	13.26	1.02	13.01	
ZA_243A	0.56	1.00	25.91	0.56	46.13	6.40	7.21	25.91	0.56	46.13	6.40	7.21	
ZA_243B	0.37	1.00	9.01	0.37	10.54	0.94	11.18	9.01	0.37	10.54	0.94	11.18	
ZA_246A	0.40	1.00	15.94	0.40	20.17	1.98	10.18	15.94	0.40	20.17	1.98	10.18	
ZA_246B	0.68	1.00	29.40	0.68	63.30	10.61	5.97	29.40	0.68	63.30	10.61	5.97	
ZA_249	0.41	1.00	37.35	0.41	48.59	4.98	9.76	37.35	0.41	48.59	4.98	9.76	
ZA_250	0.50	1.00	10.99	0.50	17.54	2.13	8.23	10.99	0.50	17.54	2.13	8.23	
ZA_251A	0.31	1.00	34.97	0.31	33.97	2.60	13.04	34.97	0.31	33.97	2.60	13.04	
ZA_251B	0.39	1.00	48.01	0.39	59.04	5.73	10.30	48.01	0.39	59.04	5.73	10.30	
ZA_251C	0.14	1.00	7.91	0.14	3.46	0.12	29.24	7.91	0.14	3.46	0.12	29.24	
ZA_251D	0.31	1.00	7.36	0.31	7.27	0.55	13.26	7.36	0.31	7.27	0.55	13.26	
ZA_251E	0.14	1.00	22.32	0.14	9.70	0.33	29.08	22.32	0.14	9.70	0.33	29.08	
ZA_252B	0.31	1.00	12.02	0.31	11.89	0.91	13.03	12.02	0.31	11.89	0.91	13.03	
ZA_252C	0.56	1.00	4.53	0.56	8.48	1.12	7.57	4.53	0.56	8.48	1.12	7.57	
ZA_252D	0.37	1.00	6.28	0.37	7.40	0.66	11.28	6.28	0.37	7.40	0.66	11.28	
ZA_253B	0.32	1.00	33.73	0.32	34.37	2.76	12.44	33.73	0.32	34.37	2.76	12.44	
ZA_253C	0.45	1.00	13.21	0.45	18.90	2.08	9.08	13.21	0.45	18.90	2.08	9.08	
ZA_254A	0.12	3.00	9.50	0.12	3.69	0.11	32.73	9.50	0.12	3.69	0.11	32.73	
ZA_254B	0.14	1.00	14.31	0.14	6.19	0.21	29.34	14.31	0.14	6.19	0.21	29.34	

Specimen	Canopy Height (mm)	Primary Elements						Total					
		Number	Avg. Length (mm)	Avg. Width (mm)	SA (mm ²)	V (mm ³)	SA/V (mm ⁻¹)	Number	Avg. Length (mm)	Avg. Width (mm)	SA (mm ²)	V (mm ³)	SA/V (mm ⁻¹)
ZA_256	0.44	1.00	10.05	0.44	14.16	1.52	9.31	10.05	0.44	14.16	1.52	9.31	
ZA_257	1.25	1.00	107.68	1.25	424.05	131.44	3.23	107.68	1.25	424.05	131.44	3.23	
ZA_258A	0.83	1.00	27.61	0.83	73.31	15.04	4.87	27.61	0.83	73.31	15.04	4.87	
ZA_258B	0.23	1.00	9.31	0.23	6.89	0.40	17.38	9.31	0.23	6.89	0.40	17.38	
ZA_261A	0.33	1.00	19.68	0.33	20.37	1.65	12.33	19.68	0.33	20.37	1.65	12.33	
ZA_261B	0.22	1.00	4.69	0.22	3.37	0.18	18.28	4.69	0.22	3.37	0.18	18.28	
ZA_261C	0.46	1.00	5.04	0.46	7.65	0.84	9.05	5.04	0.46	7.65	0.84	9.05	
ZA_262A	0.32	1.00	19.78	0.32	20.23	1.62	12.49	19.78	0.32	20.23	1.62	12.49	
ZA_262B	0.49	1.00	11.76	0.49	18.35	2.19	8.38	11.76	0.49	18.35	2.19	8.38	
ZA_262C	0.51	1.00	13.38	0.51	21.84	2.73	7.99	13.38	0.51	21.84	2.73	7.99	
ZA_263	0.66	1.00	39.86	0.66	83.79	13.79	6.07	39.86	0.66	83.79	13.79	6.07	
ZA_264A	0.16	3.00	4.56	0.16	2.26	0.09	26.24	4.56	0.16	2.26	0.09	26.24	
ZA_264B	0.47	1.00	4.76	0.47	7.37	0.83	8.93	4.76	0.47	7.37	0.83	8.93	
ZA_264C	0.11	1.00	7.01	0.11	2.42	0.07	36.98	7.01	0.11	2.42	0.07	36.98	
ZA_267A	0.27	1.00	20.01	0.27	16.95	1.13	15.03	20.01	0.27	16.95	1.13	15.03	
ZA_267B	0.54	1.00	28.95	0.54	49.17	6.53	7.53	28.95	0.54	49.17	6.53	7.53	
ZA_267C	0.46	1.00	57.36	0.46	82.64	9.40	8.79	57.36	0.46	82.64	9.40	8.79	
ZA_268A	0.40	1.00	7.91	0.40	10.16	0.99	10.28	7.91	0.40	10.16	0.99	10.28	
ZA_268B	0.21	1.00	18.32	0.21	12.15	0.63	19.16	18.32	0.21	12.15	0.63	19.16	
ZA_269	0.22	1.00	32.35	0.22	22.84	1.27	17.92	32.35	0.22	22.84	1.27	17.92	
ZA_270A	0.39	1.00	21.35	0.39	26.39	2.55	10.35	21.35	0.39	26.39	2.55	10.35	
ZA_270B	0.46	1.00	17.87	0.46	26.09	2.96	8.83	17.87	0.46	26.09	2.96	8.83	
ZA_270C	0.21	1.00	16.91	0.21	10.95	0.56	19.63	16.91	0.21	10.95	0.56	19.63	
ZA_270D	0.28	1.00	34.41	0.28	29.94	2.06	14.55	34.41	0.28	29.94	2.06	14.55	
ZA_271C	0.60	1.00	13.13	0.60	25.26	3.70	6.83	13.13	0.60	25.26	3.70	6.83	
ZA_271D	0.40	1.00	22.85	0.40	29.02	2.88	10.06	22.85	0.40	29.02	2.88	10.06	
ZA_271E	0.46	1.00	13.75	0.46	20.11	2.26	8.88	13.75	0.46	20.11	2.26	8.88	
ZA_273A	0.83	1.00	13.22	0.83	35.72	7.22	4.95	13.22	0.83	35.72	7.22	4.95	
ZA_273B	0.87	1.00	16.80	0.87	47.08	9.98	4.72	16.80	0.87	47.08	9.98	4.72	
ZA_274A	0.41	1.00	5.18	0.41	7.98	0.67	10.26	5.18	0.41	7.98	0.67	10.26	
ZA_274B	0.23	1.00	11.19	0.23	7.98	0.44	17.96	11.19	0.23	7.98	0.44	17.96	
ZA_274C	0.32	1.00	5.46	0.32	5.61	0.43	12.94	5.46	0.32	5.61	0.43	12.94	
ZA_274D	0.25	1.00	11.81	0.25	9.40	0.58	16.11	11.81	0.25	9.40	0.58	16.11	
ZA_275	0.48	1.00	9.15	0.48	14.19	1.66	8.53	9.15	0.48	14.19	1.66	8.53	
ZA_276	0.30	1.00	7.00	0.30	6.76	0.50	13.57	7.00	0.30	6.76	0.50	13.57	
ZA_277A	0.59	1.00	4.48	0.59	8.85	1.23	7.23	4.48	0.59	8.85	1.23	7.23	
ZA_277B	0.67	1.00	12.34	0.67	26.80	4.39	6.11	12.34	0.67	26.80	4.39	6.11	
ZA_277C	0.53	1.00	21.26	0.53	36.09	4.76	7.58	21.26	0.53	36.09	4.76	7.58	
ZA_277D	0.51	1.00	11.74	0.51	19.10	2.37	8.06	11.74	0.51	19.10	2.37	8.06	
ZA_278	0.34	1.00	7.53	0.34	8.27	0.69	11.96	7.53	0.34	8.27	0.69	11.96	
ZA_280A	0.37	1.00	22.10	0.37	25.82	2.36	10.93	22.10	0.37	25.82	2.36	10.93	
ZA_280B	0.33	1.00	4.52	0.33	4.90	0.39	12.45	4.52	0.33	4.90	0.39	12.45	
ZA_280C	0.28	1.00	6.36	0.28	5.65	0.38	14.76	6.36	0.28	5.65	0.38	14.76	
ZA_280D	0.38	1.00	14.10	0.38	17.05	1.60	10.67	14.10	0.38	17.05	1.60	10.67	
ZA_281A	0.52	1.00	8.86	0.52	14.84	1.87	7.95	8.86	0.52	14.84	1.87	7.95	
ZA_281B	0.49	1.00	3.88	0.49	6.33	0.73	8.71	3.88	0.49	6.33	0.73	8.71	
ZA_282A	0.51	1.00	12.34	0.51	20.09	2.50	8.04	12.34	0.51	20.09	2.50	8.04	
ZA_282B	0.39	1.00	10.03	0.39	12.49	1.19	10.48	10.03	0.39	12.49	1.19	10.48	
ZA_283A	0.60	1.00	14.64	0.60	28.15	4.14	6.80	14.64	0.60	28.15	4.14	6.80	
ZA_283B	0.53	1.00	15.42	0.53	25.91	3.35	7.73	15.42	0.53	25.91	3.35	7.73	
ZA_283D	0.43	1.00	17.39	0.43	23.99	2.57	9.33	17.39	0.43	23.99	2.57	9.33	

Specimen	Canopy Height (mm)	Primary Elements						Total					
		Number	Avg. Length (mm)	Avg. Width (mm)	SA (mm ²)	V (mm ³)	SA/V (mm ⁻¹)	Number	Avg. Length (mm)	Avg. Width (mm)	SA (mm ²)	V (mm ³)	SA/V (mm ⁻¹)
ZA_283E	0.38	1.00	20.29	0.38	24.38	2.29	10.65	20.29	0.38	24.38	2.29	10.65	
ZA_285B	0.46	1.00	14.94	0.46	22.01	2.50	8.79	14.94	0.46	22.01	2.50	8.79	
ZA_286	0.73	1.00	27.01	0.73	63.09	11.42	5.52	27.01	0.73	63.09	11.42	5.52	
ZA_287	0.66	1.00	12.43	0.66	26.57	4.29	6.19	12.43	0.66	26.57	4.29	6.19	
ZA_289A	0.63	1.00	19.86	0.63	39.60	6.09	6.50	19.86	0.63	39.60	6.09	6.50	
ZA_289B	0.28	1.00	16.46	0.28	14.44	0.99	14.56	16.46	0.28	14.44	0.99	14.56	
ZA_291A	0.34	1.00	18.38	0.34	20.04	1.71	11.74	18.38	0.34	20.04	1.71	11.74	
ZA_291B	0.67	1.00	20.02	0.67	42.70	7.01	6.09	20.02	0.67	42.70	7.01	6.09	
ZA_292A	0.44	1.00	9.24	0.44	13.18	1.43	9.23	9.24	0.44	13.18	1.43	9.23	
ZA_292B	0.17	1.00	15.43	0.17	8.48	0.37	23.12	15.43	0.17	8.48	0.37	23.12	
ZA_292C	0.31	1.00	12.53	0.31	12.47	0.96	12.94	12.53	0.31	12.47	0.96	12.94	
ZA_292D	0.43	1.00	14.89	0.43	20.16	2.11	9.55	14.89	0.43	20.16	2.11	9.55	
ZA_292E	0.37	1.00	9.91	0.37	11.59	1.04	11.13	9.91	0.37	11.59	1.04	11.13	
ZA_293	0.54	1.00	17.18	0.54	29.41	3.89	7.57	17.18	0.54	29.41	3.89	7.57	
ZA_294	0.49	1.00	22.44	0.49	35.04	4.26	8.22	22.44	0.49	35.04	4.26	8.22	
ZA_295	1.02	1.00	86.82	1.02	280.82	71.47	3.93	86.82	1.02	280.82	71.47	3.93	
ZA_296	0.85	1.00	34.22	0.85	92.03	19.23	4.79	34.22	0.85	92.03	19.23	4.79	
ZA_297A	0.92	1.00	160.07	0.92	463.73	106.35	4.36	160.07	0.92	463.73	106.35	4.36	
ZA_297B	0.42	1.00	25.51	0.42	33.76	3.50	9.65	25.51	0.42	33.76	3.50	9.65	
ZA_298	0.98	1.00	36.97	0.98	114.80	27.65	4.15	36.97	0.98	114.80	27.65	4.15	
ZA_299	0.76	1.00	33.13	0.76	79.96	15.02	5.32	33.13	0.76	79.96	15.02	5.32	
ZA_300A	0.57	1.00	29.55	0.57	52.93	7.41	7.15	29.55	0.57	52.93	7.41	7.15	
ZA_300B	0.49	1.00	12.17	0.49	19.25	2.33	8.26	12.17	0.49	19.25	2.33	8.26	
ZA_301A	0.43	1.00	16.03	0.43	21.98	2.34	9.41	16.03	0.43	21.98	2.34	9.41	
ZA_301B	0.43	1.00	15.13	0.43	20.77	2.21	9.41	15.13	0.43	20.77	2.21	9.41	
ZA_302A	0.35	1.00	16.87	0.35	18.89	1.65	11.45	16.87	0.35	18.89	1.65	11.45	
ZA_302B	0.47	1.00	39.11	0.47	58.19	6.81	8.54	39.11	0.47	58.19	6.81	8.54	
ZA_304	0.53	1.00	31.05	0.53	52.41	6.92	7.57	31.05	0.53	52.41	6.92	7.57	
ZA_306A	0.54	1.00	33.60	0.54	57.43	7.69	7.47	33.60	0.54	57.43	7.69	7.47	
ZA_306B	0.36	1.00	8.86	0.36	10.28	0.91	11.28	8.86	0.36	10.28	0.91	11.28	
ZA_306C	0.81	1.00	9.36	0.81	24.81	4.81	5.16	9.36	0.81	24.81	4.81	5.16	
ZA_306D	0.64	1.00	7.96	0.64	16.69	2.57	6.48	7.96	0.64	16.69	2.57	6.48	
ZA_306E	0.10	1.00	17.72	0.10	5.58	0.14	40.11	17.72	0.10	5.58	0.14	40.11	
ZA_306F	0.45	1.00	28.67	0.45	40.73	4.54	8.98	28.67	0.45	40.73	4.54	8.98	
ZA_307	0.90	1.00	108.19	0.90	308.39	69.41	4.44	108.19	0.90	308.39	69.41	4.44	
ZA_310B	0.45	1.00	27.34	0.45	38.86	4.33	8.98	27.34	0.45	38.86	4.33	8.98	
ZA_311	0.96	1.00	33.60	0.96	102.63	24.26	4.23	33.60	0.96	102.63	24.26	4.23	
ZA_313A	0.89	1.00	16.04	0.89	46.11	9.99	4.61	16.04	0.89	46.11	9.99	4.61	
ZA_313B	0.75	1.00	37.41	0.75	89.22	16.61	5.37	37.41	0.75	89.22	16.61	5.37	
ZA_314A	0.48	1.00	46.90	0.48	70.46	8.34	8.45	46.90	0.48	70.46	8.34	8.45	
ZA_314B	0.29	1.00	18.29	0.29	17.02	1.24	13.71	18.29	0.29	17.02	1.24	13.71	
ZA_314C	0.29	1.00	70.20	0.29	64.94	4.76	13.63	70.20	0.29	64.94	4.76	13.63	
ZA_314D	0.65	1.00	14.28	0.65	29.94	4.78	6.27	14.28	0.65	29.94	4.78	6.27	
ZA_314E	0.41	1.00	20.37	0.41	26.36	2.66	9.90	20.37	0.41	26.36	2.66	9.90	
ZA_314F	0.41	1.00	17.87	0.41	23.21	2.35	9.89	17.87	0.41	23.21	2.35	9.89	
ZA_314G	0.42	1.00	24.66	0.42	32.48	3.35	9.70	24.66	0.42	32.48	3.35	9.70	
ZA_314H	0.50	1.00	14.07	0.50	22.29	2.72	8.21	14.07	0.50	22.29	2.72	8.21	
ZA_315A	0.39	1.00	20.35	0.39	24.83	2.37	10.49	20.35	0.39	24.83	2.37	10.49	
ZA_315B	0.34	1.00	23.24	0.34	25.29	2.16	11.71	23.24	0.34	25.29	2.16	11.71	
ZA_315C	0.34	1.00	5.51	0.34	6.14	0.51	11.99	5.51	0.34	6.14	0.51	11.99	
ZA_315D	0.54	1.00	7.92	0.54	13.99	1.84	7.61	7.92	0.54	13.99	1.84	7.61	

Specimen	Canopy Height (mm)	Primary Elements						Total					
		Number	Avg. Length (mm)	Avg. Width (mm)	SA (mm ²)	V (mm ³)	SA/V (mm ⁻¹)	Avg. Length (mm)	Avg. Width (mm)	SA (mm ²)	V (mm ³)	SA/V (mm ⁻¹)	
ZA_316	0.19	1.00	36.92	0.19	22.20	1.06	21.00	36.92	0.19	22.20	1.06	21.00	
ZA_317A	0.51	1.00	28.78	0.51	46.49	5.88	7.91	28.78	0.51	46.49	5.88	7.91	
ZA_317B	0.81	1.00	42.20	0.81	108.64	13.16	8.21	42.20	0.81	108.64	13.16	8.21	
ZA_317C	0.40	1.00	19.00	0.40	23.99	2.36	10.16	19.00	0.40	23.99	2.36	10.16	
ZA_318A	0.63	1.00	32.95	0.63	66.13	10.36	6.38	32.95	0.63	66.13	10.36	6.38	
ZA_318B	0.57	1.00	36.06	0.57	64.60	9.07	7.12	36.06	0.57	64.60	9.07	7.12	
ZA_318C	0.51	1.00	31.28	0.51	50.11	6.29	7.97	31.28	0.51	50.11	6.29	7.97	
ZA_321A	0.57	1.00	12.69	0.57	23.14	3.21	7.20	12.69	0.57	23.14	3.21	7.20	
ZA_321B	0.77	1.00	11.47	0.77	28.60	5.31	5.38	11.47	0.77	28.60	5.31	5.38	
ZA_321C	0.86	1.00	19.06	0.83	50.89	10.36	4.91	19.06	0.83	50.89	10.36	4.91	
ZA_323	0.61	1.00	22.20	0.61	42.83	6.40	6.69	22.20	0.61	42.83	6.40	6.69	
ZA_324	0.52	1.00	15.72	0.52	26.14	3.35	7.80	15.72	0.52	26.14	3.35	7.80	
ZA_325A	0.11	1.00	5.71	0.11	1.94	0.05	37.73	5.71	0.11	1.94	0.05	37.73	
ZA_325B	0.09	1.00	8.69	0.09	2.33	0.05	47.29	8.69	0.09	2.33	0.05	47.29	
ZA_326	0.70	1.00	32.32	0.70	71.39	12.29	5.81	32.32	0.70	71.39	12.29	5.81	
ZA_328A	0.51	1.00	33.32	0.51	53.77	6.80	7.90	33.32	0.51	53.77	6.80	7.90	
ZA_328B	0.43	1.00	18.55	0.43	25.39	2.70	9.39	18.55	0.43	25.39	2.70	9.39	
ZA_329A	0.59	1.00	21.75	0.59	40.56	5.86	6.92	21.75	0.59	40.56	5.86	6.92	
ZA_329B	0.37	1.00	18.25	0.37	21.65	2.00	10.80	18.25	0.37	21.65	2.00	10.80	
ZA_329C	0.48	1.00	13.66	0.48	20.82	2.44	8.53	13.66	0.48	20.82	2.44	8.53	
ZA_330A	0.56	1.00	29.64	0.56	52.13	7.17	7.27	29.64	0.56	52.13	7.17	7.27	
ZA_330B	0.43	1.00	10.55	0.43	14.64	1.55	9.43	10.55	0.43	14.64	1.55	9.43	
ZA_330C	0.43	1.00	38.86	0.43	53.13	5.72	9.29	38.86	0.43	53.13	5.72	9.29	
ZA_331	0.38	1.00	6.18	0.38	7.69	0.72	10.74	6.18	0.38	7.69	0.72	10.74	
ZA_332	0.60	1.00	115.56	0.60	217.92	32.55	6.70	115.56	0.60	217.92	32.55	6.70	
ZA_334	0.83	1.00	42.25	0.83	111.73	23.07	4.84	42.25	0.83	111.73	23.07	4.84	
ZA_335A	0.27	1.00	65.61	0.27	55.74	3.75	14.85	65.61	0.27	55.74	3.75	14.85	
ZA_335B	0.27	1.00	39.65	0.27	33.73	2.27	14.87	39.65	0.27	33.73	2.27	14.87	
ZA_336	0.41	1.00	42.78	0.41	54.93	5.56	9.87	42.78	0.41	54.93	5.56	9.87	
ZA_340	0.51	1.00	26.51	0.51	42.86	5.41	7.92	26.51	0.51	42.86	5.41	7.92	
ZA_343	0.60	1.00	12.43	0.60	23.91	3.49	6.85	12.43	0.60	23.91	3.49	6.85	
ZA_344	0.47	1.00	26.92	0.47	40.34	4.73	8.53	26.92	0.47	40.34	4.73	8.53	
ZA_345A	0.23	1.00	6.59	0.23	4.80	0.72	17.85	6.59	0.23	4.80	0.72	17.85	
ZA_345B	0.41	1.00	3.64	0.41	4.92	0.48	10.35	3.64	0.41	4.92	0.48	10.35	
ZA_345C	0.26	1.00	3.43	0.26	2.91	0.18	15.97	3.43	0.26	2.91	0.18	15.97	
ZA_345D	0.22	1.00	4.34	0.22	3.02	0.16	18.98	4.34	0.22	3.02	0.16	18.98	
ZA_346A	0.52	1.00	12.01	0.52	20.07	2.56	7.84	12.01	0.52	20.07	2.56	7.84	
ZA_349A	0.97	1.00	43.04	0.97	132.84	31.92	4.16	43.04	0.97	132.84	31.92	4.16	
ZA_349B	0.78	1.00	78.01	0.78	191.77	37.16	5.16	78.01	0.78	191.77	37.16	5.16	
ZA_350A	0.58	1.00	61.52	0.58	113.36	16.47	6.88	61.52	0.58	113.36	16.47	6.88	
ZA_350B	0.46	1.00	44.82	0.46	65.21	7.48	8.72	44.82	0.46	65.21	7.48	8.72	
ZA_351	0.50	1.00	67.21	0.50	105.92	13.19	8.03	67.21	0.50	105.92	13.19	8.03	
ZA_353	0.73	1.00	62.46	0.73	144.61	26.35	5.49	62.46	0.73	144.61	26.35	5.49	
ZA_354A	0.53	1.00	48.42	0.53	80.72	10.60	7.62	48.42	0.53	80.72	10.60	7.62	
ZA_354B	0.44	1.00	15.64	0.44	22.11	2.42	9.14	15.64	0.44	22.11	2.42	9.14	
ZA_355	0.74	1.00	18.83	0.74	44.43	8.03	5.53	18.83	0.74	44.43	8.03	5.53	
ZA_356A	0.46	1.00	28.06	0.46	41.04	4.70	8.73	28.06	0.46	41.04	4.70	8.73	
ZA_356B	0.53	1.00	8.65	0.53	14.90	1.92	7.75	8.65	0.53	14.90	1.92	7.75	

Specimen	Canopy Height (mm)	Primary Elements						Total					
		Number	Avg. Length (mm)	Avg. Width (mm)	SA (mm ²)	V (mm ³)	SA/V (mm ⁻¹)	Number	Avg. Length (mm)	Avg. Width (mm)	SA (mm ²)	V (mm ³)	SA/V (mm ⁻¹)
ZA_357A	0.54	1.00	13.91	0.54	24.17	3.22	7.51	13.91	0.54	24.17	3.22	7.51	
ZA_357B	0.73	1.00	15.57	0.73	36.62	6.55	5.59	15.57	0.73	36.62	6.55	5.59	
ZA_357C	0.36	1.00	17.44	0.36	19.91	1.77	11.23	17.44	0.36	19.91	1.77	11.23	
ZA_358	0.46	1.00	23.09	0.46	33.68	3.83	8.78	23.09	0.46	33.68	3.83	8.78	
ZA_359A	0.66	1.00	10.79	0.66	23.01	3.68	6.26	10.79	0.66	23.01	3.68	6.26	
ZA_359B	0.52	1.00	10.51	0.52	17.62	2.24	7.87	10.51	0.52	17.62	2.24	7.87	
ZA_363	0.56	1.00	42.12	0.56	74.41	10.33	7.20	42.12	0.56	74.41	10.33	7.20	
ZA_366A	0.24	1.00	16.00	0.24	12.36	0.75	16.52	16.00	0.24	12.36	0.75	16.52	
ZA_366B	0.36	1.00	21.76	0.36	24.45	2.15	11.36	21.76	0.36	24.45	2.15	11.36	
ZA_367A	0.53	1.00	73.97	0.53	124.48	16.56	7.52	73.97	0.53	124.48	16.56	7.52	
ZA_367B	0.47	1.00	33.24	0.47	49.72	5.84	8.52	33.24	0.47	49.72	5.84	8.52	
ZA_369	0.53	1.00	69.96	0.53	116.86	15.43	7.58	69.96	0.53	116.86	15.43	7.58	
ZA_375A	0.52	1.00	5.50	0.52	9.47	1.18	8.00	5.50	0.52	9.47	1.18	8.00	
ZA_375B	0.53	1.00	13.78	0.53	23.37	3.04	7.69	13.78	0.53	23.37	3.04	7.69	
ZA_375C	0.21	1.00	7.34	0.21	4.96	0.26	19.14	7.34	0.21	4.96	0.26	19.14	
ZA_375D	0.47	1.00	9.14	0.47	13.95	1.61	8.66	9.14	0.47	13.95	1.61	8.66	
ZA_378A	0.69	1.00	32.57	0.69	71.11	12.10	5.88	32.57	0.69	71.11	12.10	5.88	
ZA_378B	0.51	1.00	17.91	0.51	29.15	3.67	7.94	17.91	0.51	29.15	3.67	7.94	
ZA_379A	0.47	1.00	27.65	0.47	40.71	4.69	8.67	27.65	0.47	40.71	4.69	8.67	
ZA_379B	0.56	1.00	22.68	0.56	40.66	5.66	7.18	22.68	0.56	40.66	5.66	7.18	
ZA_380A	0.29	1.00	133.38	0.29	119.48	8.50	14.05	133.38	0.29	119.48	8.50	14.05	
ZA_380B	0.40	1.00	30.47	0.40	38.91	3.90	9.97	30.47	0.40	38.91	3.90	9.97	
ZA_380C	0.40	1.00	28.32	0.40	36.18	3.63	9.97	28.32	0.40	36.18	3.63	9.97	
ZA_381A	0.47	1.00	25.15	0.47	37.54	4.38	8.57	25.15	0.47	37.54	4.38	8.57	
ZA_381B	0.42	1.00	21.27	0.42	28.40	2.96	9.60	21.27	0.42	28.40	2.96	9.60	
ZA_381C	0.21	1.00	23.73	0.21	15.72	0.82	19.13	23.73	0.21	15.72	0.82	19.13	
ZA_384	0.51	1.00	34.86	0.51	56.34	7.15	7.89	34.86	0.51	56.34	7.15	7.89	
ZA_388A	0.53	1.00	81.11	0.53	135.69	17.95	7.56	81.11	0.53	135.69	17.95	7.56	
ZA_388B	0.50	1.00	76.10	0.50	119.87	14.94	8.03	76.10	0.50	119.87	14.94	8.03	
ZA_388C	0.18	1.00	33.36	0.18	18.59	0.82	22.66	33.36	0.18	18.59	0.82	22.66	
ZA_392A	0.47	1.00	71.18	0.47	106.30	12.55	8.47	71.18	0.47	106.30	12.55	8.47	
ZA_392B	0.47	1.00	60.84	0.47	90.90	10.73	8.47	60.84	0.47	90.90	10.73	8.47	
ZA_392C	0.47	1.00	61.46	0.47	91.82	10.84	8.47	61.46	0.47	91.82	10.84	8.47	
ZA_392D	0.47	1.00	76.70	0.47	114.51	13.53	8.46	76.70	0.47	114.51	13.53	8.46	
ZA_392E	0.47	1.00	30.41	0.47	45.61	5.36	8.50	30.41	0.47	45.61	5.36	8.50	
ZA_392F	0.47	1.00	18.89	0.47	28.47	3.33	8.54	18.89	0.47	28.47	3.33	8.54	
ZA_394	0.56	1.00	17.37	0.56	31.20	4.32	7.22	17.37	0.56	31.20	4.32	7.22	
ZA_397A	0.39	1.00	51.61	0.39	62.79	6.04	10.40	51.61	0.39	62.79	6.04	10.40	
ZA_397B	0.13	1.00	18.47	0.13	7.51	0.24	31.12	18.47	0.13	7.51	0.24	31.12	
ZA_397C	0.13	1.00	26.54	0.13	10.78	0.35	31.08	26.54	0.13	10.78	0.35	31.08	
ZA_398A	0.57	1.00	9.83	0.57	18.10	2.51	7.22	9.83	0.57	18.10	2.51	7.22	
ZA_398B	0.43	1.00	45.16	0.43	61.83	6.68	9.26	45.16	0.43	61.83	6.68	9.26	
ZA_398C	0.16	1.00	16.37	0.16	8.32	0.33	24.97	16.37	0.16	8.32	0.33	24.97	
ZA_398D	0.16	1.00	28.10	0.16	14.25	0.57	24.92	28.10	0.16	14.25	0.57	24.92	
ZA_402A	0.27	1.00	44.56	0.27	37.33	2.48	15.08	44.56	0.27	37.33	2.48	15.08	
ZA_402B	0.48	1.00	16.59	0.48	25.32	2.99	8.47	16.59	0.48	25.32	2.99	8.47	
ZA_402C	0.42	1.00	20.27	0.42	27.01	2.81	9.62	20.27	0.42	27.01	2.81	9.62	
ZA_402D	0.27	1.00	27.61	0.27	23.18	1.53	15.11	27.61	0.27	23.18	1.53	15.11	
ZA_403B	0.63	1.00	21.31	0.63	42.85	6.66	6.43	21.31	0.63	42.85	6.66	6.43	
ZA_404A	0.48	1.00	14.57	0.48	22.42	2.66	8.44	14.57	0.48	22.42	2.66	8.44	
ZA_404B	0.37	1.00	17.07	0.37	20.00	1.82	10.96	17.07	0.37	20.00	1.82	10.96	

Appendix E: Morphological measurements, dichotomous branching

Specimen	Canopy Height (mm)				Primary Elements							Secondary Elements						
	Number	Avg. Length (mm)	Avg. Width (mm)	SA (mm ²)	V (mm ³)	SA/V (mm ⁻¹)	Number	Avg. Length (mm)	Avg. Width (mm)	SA (mm ²)	V (mm ³)	SA/V (mm ⁻¹)	Number	Avg. Length (mm)	Avg. Width (mm)	SA (mm ²)	V (mm ³)	SA/V (mm ⁻¹)
ZA_32B	1.00	12.42	0.56	22.46	3.09	7.27	2.00	4.45	0.65	9.69	1.46	6.64	2.00	4.45	0.65	9.69	1.46	6.64
ZA_42B	1.00	19.04	0.65	39.76	6.39	6.22	2.00	7.42	0.66	15.99	2.51	6.36	2.00	7.42	0.66	15.99	2.51	6.36
ZA_53B	1.00	12.42	0.434	26.71	4.34	6.16	2.00	4.15	0.65	9.14	1.38	6.64	2.00	4.15	0.65	9.14	1.38	6.64
ZA_55A	1.00	5.99	0.45	8.74	0.94	9.26	2.00	16.03	0.59	30.19	4.37	6.92	2.00	16.03	0.59	30.19	4.37	6.92
ZA_61C	1.00	6.56	0.48	10.31	1.20	8.59	2.00	14.17	0.56	25.54	3.53	7.25	2.00	14.17	0.56	25.54	3.53	7.25
ZA_73B	1.00	17.63	0.14	7.67	0.26	29.10	2.00	4.94	0.14	2.17	0.07	29.39	2.00	4.94	0.14	2.17	0.07	29.39
ZA_77B	1.00	22.82	0.43	31.32	3.36	9.33	2.00	16.79	0.50	26.96	3.35	8.06	2.00	16.79	0.50	26.96	3.35	8.06
ZA_78B	1.00	13.93	0.55	24.72	3.36	7.36	2.00	13.40	0.64	27.67	4.34	6.38	2.00	13.40	0.64	27.67	4.34	6.38
ZA_78C	1.00	11.83	0.58	22.23	3.17	7.02	2.00	21.38	0.58	39.61	5.69	6.97	2.00	21.38	0.58	39.61	5.69	6.97
ZA_79B	1.00	20.12	0.73	46.96	8.42	5.58	2.00	6.68	0.69	15.32	2.53	6.06	2.00	6.68	0.69	15.32	2.53	6.06
ZA_82J	1.00	3.78	0.26	3.22	0.01	15.80	2.00	12.34	0.27	10.50	0.70	15.09	2.00	12.34	0.27	10.50	0.70	15.09
ZA_111	1.00	1.25	0.09	0.36	0.01	47.05	2.00	3.81	0.09	1.06	0.02	45.98	2.00	3.81	0.09	1.06	0.02	45.98
ZA_115	1.00	8.17	0.61	16.32	2.41	6.77	2.00	37.67	0.70	83.20	14.37	5.79	2.00	37.67	0.70	83.20	14.37	5.79
ZA_136A	1.00	15.23	0.48	23.16	2.72	8.52	2.00	5.59	0.34	6.10	0.50	12.23	2.00	5.59	0.34	6.10	0.50	12.23
ZA_172A	1.00	19.40	0.26	15.88	1.02	15.55	2.00	3.59	0.21	2.44	0.12	19.61	2.00	3.59	0.21	2.44	0.12	19.61
ZA_186A	1.00	13.70	0.31	13.66	1.06	12.88	2.00	9.39	0.54	16.32	2.13	7.65	2.00	9.39	0.54	16.32	2.13	7.65
ZA_186B	1.00	6.60	0.40	8.48	0.82	10.38	2.00	8.33	0.23	6.07	0.34	17.71	2.00	8.33	0.23	6.07	0.34	17.71
ZA_187A	1.00	10.25	0.27	8.83	0.59	14.96	2.00	8.47	0.20	5.35	0.26	20.34	2.00	8.47	0.20	5.35	0.26	20.34
ZA_196G	1.00	20.98	0.43	28.75	3.07	9.35	2.00	3.92	0.30	3.81	0.27	13.93	2.00	3.92	0.30	3.81	0.27	13.93
ZA_216	1.00	30.54	0.92	89.26	20.16	4.43	2.00	56.76	0.83	149.36	30.84	4.84	2.00	56.76	0.83	149.36	30.84	4.84
ZA_217C	1.00	10.13	0.13	1.84	0.06	32.18	2.00	4.91	0.19	2.97	0.14	21.57	2.00	4.91	0.19	2.97	0.14	21.57
ZA_234A	1.00	30.44	1.25	121.72	37.21	3.27	2.00	17.84	0.92	52.63	11.75	4.48	2.00	17.84	0.92	52.63	11.75	4.48
ZA_239A	1.00	6.89	0.08	1.70	0.03	51.57	2.00	2.59	0.34	2.93	0.23	12.61	2.00	2.59	0.34	2.93	0.23	12.61
ZA_239B	1.00	6.26	0.16	1.37	0.05	26.37	2.00	9.21	0.30	8.84	0.65	13.51	2.00	9.21	0.30	8.84	0.65	13.51
ZA_240A	1.00	42.83	0.40	42.76	4.23	10.11	2.00	10.60	0.30	10.06	0.74	13.61	2.00	10.60	0.30	10.06	0.74	13.61
ZA_241B	1.00	0.93	1.05	4.80	0.81	5.96	2.00	16.41	0.58	30.25	4.29	7.05	2.00	16.41	0.58	30.25	4.29	7.05
ZA_252A	1.00	14.75	0.17	1.22	0.05	24.38	2.00	5.22	0.22	3.63	0.19	18.82	2.00	5.22	0.22	3.63	0.19	18.82
ZA_253A	1.00	60.26	0.68	41.28	6.91	5.97	2.00	30.08	0.64	61.27	9.73	6.30	2.00	30.08	0.64	61.27	9.73	6.30
ZA_265	1.00	20.20	0.42	13.38	1.36	9.84	2.00	7.69	0.25	6.11	0.37	16.32	2.00	7.69	0.25	6.11	0.37	16.32
ZA_271A	1.00	31.27	0.40	14.27	1.41	10.15	2.00	18.30	0.30	17.38	1.29	13.44	2.00	18.30	0.30	17.38	1.29	13.44
ZA_271B	1.00	19.00	0.35	13.87	1.70	11.53	2.00	4.12	0.52	7.17	0.88	8.15	2.00	4.12	0.52	7.17	0.88	8.15
ZA_283C	1.00	9.65	0.47	14.61	1.68	8.70	2.00	9.19	0.53	15.64	2.00	7.81	2.00	9.19	0.53	15.64	2.00	7.81
ZA_342A	1.00	8.97	0.24	2.62	0.15	17.40	2.00	4.84	0.48	7.65	0.87	8.76	2.00	4.84	0.48	7.65	0.87	8.76
ZA_342B	1.00	9.77	0.53	8.16	1.03	7.94	2.00	3.77	0.61	7.77	1.09	7.11	2.00	3.77	0.61	7.77	1.09	7.11
ZA_346B	1.00	34.00	0.74	79.86	14.62	5.46	2.00	6.42	0.27	5.64	0.38	14.91	2.00	6.42	0.27	5.64	0.38	14.91
ZA_368	1.00	25.49	0.97	8.53	1.71	4.99	2.00	11.72	0.30	11.18	0.83	13.50	2.00	11.72	0.30	11.18	0.83	13.50
ZA_373	1.00	60.49	0.49	71.68	8.77	8.17	2.00	8.85	0.39	10.96	1.04	10.59	2.00	8.85	0.39	10.96	1.04	10.59
ZA_385	1.00	11.39	0.42	8.21	0.84	9.79	2.00	5.98	0.29	5.65	0.41	13.94	2.00	5.98	0.29	5.65	0.41	13.94
ZA_403A	1.00	27.78	0.85	22.55	4.53	4.98	2.00	14.42	0.47	21.68	2.51	8.63	2.00	14.42	0.47	21.68	2.51	8.63
ZA_195A	1.00	6.52	0.31	6.47	0.49	13.25	2.00	29.14	0.42	38.52	4.00	9.64	2.00	29.14	0.42	38.52	4.00	9.64

Specimen	Total					
	Branching angle (deg)	Length (mm)	Width (mm)	SA(mm ²)	V (mm ³)	SA/V (mm ⁻¹)
ZA_32B	64.14	16.88	0.60	32.15	4.55	7.06
ZA_42B	82.39	26.46	0.66	55.75	8.91	6.26
ZA_53B	55.62	16.57	0.66	35.85	5.71	6.27
ZA_55A	56.43	22.02	0.52	38.94	5.31	7.33
ZA_61C	53.39	20.72	0.52	35.85	4.73	7.59
ZA_73B	64.79	22.57	0.14	9.84	0.34	29.16
ZA_77B	41.67	39.60	0.47	58.28	6.71	8.69
ZA_78B	69.57	27.34	0.60	52.38	7.69	6.81
ZA_78C	76.87	33.21	0.58	61.84	8.85	6.98
ZA_79B	76.11	26.80	0.71	62.27	10.94	5.69
ZA_82J	70.74	16.12	0.27	13.72	0.90	15.25
ZA_111	54.09	5.06	0.09	1.42	0.03	46.24
ZA_115	63.12	45.84	0.66	99.52	16.78	5.93
ZA_136A	77.11	20.82	0.41	29.26	3.22	9.09
ZA_172A	96.34	22.99	0.23	18.32	1.15	15.99
ZA_186A	42.34	23.09	0.43	29.98	3.19	9.39
ZA_186B	48.46	14.94	0.31	14.55	1.16	12.55
ZA_187A	76.71	18.71	0.24	14.19	0.85	16.61
ZA_196G	52.77	24.90	0.37	32.56	3.35	9.73
ZA_216	42.60	87.30	0.87	238.62	51.00	4.68
ZA_217C	51.40	9.50	0.16	4.81	0.19	24.69
ZA_234A	50.41	48.28	1.08	174.34	48.96	3.56
ZA_239A	59.20	9.48	0.21	4.62	0.27	17.44
ZA_239B	69.15	11.93	0.23	10.22	0.71	14.45
ZA_240A	15.36	44.61	0.35	52.81	4.97	10.63
ZA_241B	61.93	17.34	0.81	35.05	5.09	6.88
ZA_252A	58.52	7.39	0.19	4.85	0.24	19.92
ZA_253A	56.98	49.01	0.66	102.55	16.64	6.16
ZA_265	22.84	17.75	0.33	19.49	1.73	11.24
ZA_271A	76.74	29.44	0.35	31.65	2.70	11.73
ZA_271B	61.56	16.49	0.44	21.04	2.08	10.10
ZA_283C	66.67	18.83	0.50	30.25	3.68	8.21
ZA_342A	38.11	8.23	0.36	10.26	1.02	10.03
ZA_342B	85.43	8.38	0.57	15.93	2.12	7.51
ZA_346B	36.44	40.42	0.51	85.50	14.99	5.70
ZA_368	42.35	14.04	0.63	19.71	2.54	7.77
ZA_373	72.25	55.01	0.44	82.64	9.81	8.43
ZA_385	53.68	11.95	0.36	13.87	1.24	11.14
ZA_403A	57.67	22.50	0.66	44.22	7.04	6.28
ZA_195A	78.45	35.66	0.36	44.99	4.49	10.03

Appendix F: Morphological measurements, single monopodial

Specimen	Canopy Height (mm)	Number	Primary Elements				
			Length (mm)	Width (mm)	SA (mm ²)	V (mm ³)	SA/V (mm ⁻¹)
ZA_7B	22.40	1.00	22.40	0.18	12.99	0.60	21.83
ZA_7F	46.49	1.00	46.49	1.04	153.65	39.54	3.89
ZA_7G	58.50	1.00	58.50	0.99	183.56	45.10	4.07
ZA_7H	57.56	1.00	57.56	0.78	142.12	27.56	5.16
ZA_23C	23.63	1.00	23.63	0.55	41.05	5.55	7.40
ZA_49B	17.84	1.00	17.84	0.56	31.92	4.41	7.24
ZA_50I	12.94	1.00	12.94	0.37	15.29	1.40	10.94
ZA_66A	29.78	1.00	29.78	0.71	67.28	11.82	5.69
ZA_107A	8.04	1.00	8.04	0.70	18.41	3.08	5.97
ZA_158	11.87	1.00	11.87	0.57	21.91	3.07	7.14
ZA_285A	16.08	1.00	16.08	0.45	22.99	2.54	9.03
ZA_310A	5.26	1.00	5.26	0.80	14.19	2.64	5.39

Specimen	Secondary Elements						Total					
	Number	Length (mm)	Width (mm)	SA (mm ²)	V (mm ³)	SA/V (mm ⁻¹)	Branching angle (deg)	Length (mm)	Width (mm)	SA (mm ²)	V (mm ³)	SA/V (mm ⁻¹)
ZA_7B	1.00	4.22	0.37	5.08	0.45	11.34	66.27	26.61	0.28	18.08	1.04	17.33
ZA_7F	1.00	11.69	0.58	21.89	3.11	7.04	98.31	58.17	0.81	175.54	42.65	4.12
ZA_7G	1.00	12.08	0.37	14.17	1.28	11.04	22.40	70.58	0.68	197.74	46.38	4.26
ZA_7H	1.00	3.72	0.78	10.08	1.78	5.66	49.12	61.28	0.78	152.20	29.34	5.19
ZA_23C	1.00	7.63	0.60	14.96	2.16	6.92	36.70	31.25	0.57	56.01	7.71	7.26
ZA_49B	1.00	13.57	0.36	15.33	1.34	11.41	78.62	31.41	0.46	47.25	5.75	8.22
ZA_50I	1.00	8.08	0.37	9.63	0.87	11.03	28.64	21.02	0.37	24.91	2.27	10.97
ZA_66A	1.00	5.01	0.61	10.17	1.46	6.97	40.92	34.79	0.66	77.45	13.28	5.83
ZA_107A	1.00	1.05	0.41	1.61	0.14	11.67	50.86	9.09	0.55	20.02	3.22	6.22
ZA_158	1.00	9.60	0.57	17.59	2.42	7.26	85.48	21.47	0.57	39.50	5.49	7.19
ZA_285A	1.00	5.19	0.23	3.85	0.22	17.70	80.67	21.27	0.34	26.84	2.76	9.72
ZA_310A	1.00	3.14	0.50	5.26	0.60	8.72	42.18	8.40	0.65	19.45	3.24	6.01

**Appendix G:
Morphological measurements, fan-shaped**

Specimen	Total Length (mm)	Total Average Width (mm)	Total Surface Area (mm ²)	Total Volume (mm ³)	SA/V (mm [^] -1)
ZA_232A	12.925	0.311	12.77363147	0.981343356	13.01647521
ZA_232B	8.084	0.332	8.60046	0.699474891	12.29559505
ZA_365	6.761	0.193	4.15578215	0.197694784	21.02120283

Specimen	Location	Morphotype	Canopy Height (mm)	Primary Elements					
				Number	Average Length (mm)	Average Width (mm)	Surface Area (mm ²)	Volume (mm ³)	SA/V (mm [^] -1)
ZA_232A	Zuun-Arts Fm, Zavkhan Province, Mongolia	fan	0.311	3	12.925	0.311	12.77363147	0.981343356	13.01647521
ZA_232B	Zuun-Arts Fm, Zavkhan Province, Mongolia	fan	0.332	2	8.084	0.332	8.60046	0.699474891	12.29559505
ZA_365	Zuun-Arts Fm, Zavkhan Province, Mongolia	fan	7.803	3	6.761	0.193	4.15578215	0.197694784	21.02120283

Appendix H:

Morphological measurements, small non-branching

Specimen	Total Length (mm)	Total Average Width (mm)	Total Surface Area (mm ²)	Total Volume (mm ³)	SA/V (mm ^{^2} -1)
ZA_213B	3.741	0.128	1.5293056	0.048114647	31.78461641
ZA_213C	2.004	0.181	1.19038813	0.05153764	23.09745151

Specimen	Location	Morphotype	Canopy Height (mm)	Primary Elements					
				Number	Average Length (mm)	Average Width (mm)	Surface Area (mm ²)	Volume (mm ³)	SA/V (mm ^{^2} -1)
ZA_213B	Zuun-Arts Fm, Zavkhan Province, Mongolia	small	0.128	1	3.741	0.128	1.5293056	0.048114647	31.78461641
ZA_213C	Zuun-Arts Fm, Zavkhan Province, Mongolia	small	0.181	1	2.004	0.181	1.19038813	0.05153764	23.09745151

Appendix I:

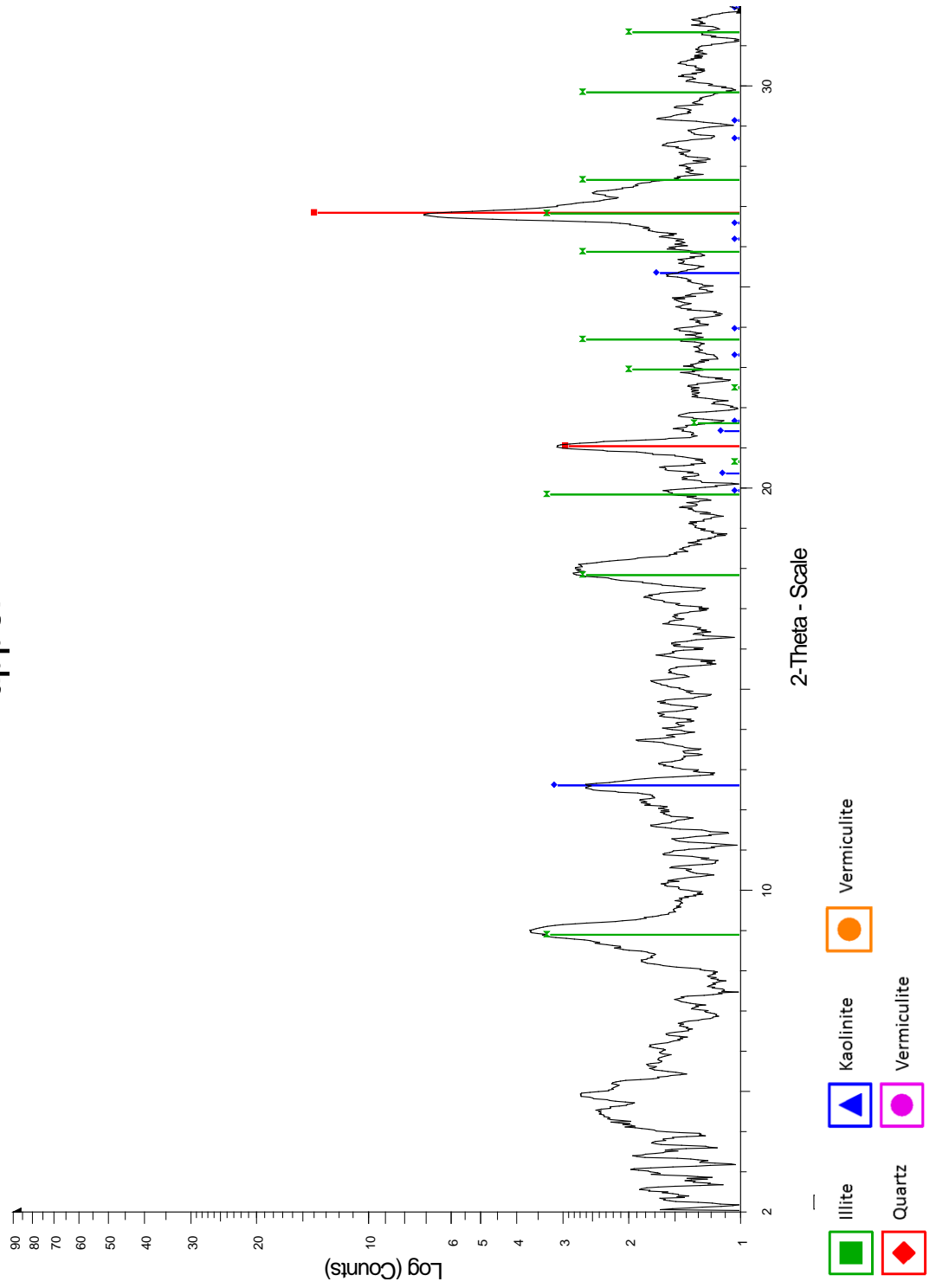
Morphological measurements, shrub-like

Specimen	Total Length (mm)	Total Average Width (mm)	Total Surface Area (mm ²)	Total Volume (mm ³)	SA/V (mm ² ·l ⁻¹)
ZA_130A	3.2	0.22	2.286548	0.1215808	18.80681818
ZA_245	4.398	0.31	4.4318902	0.331778523	13.35797797

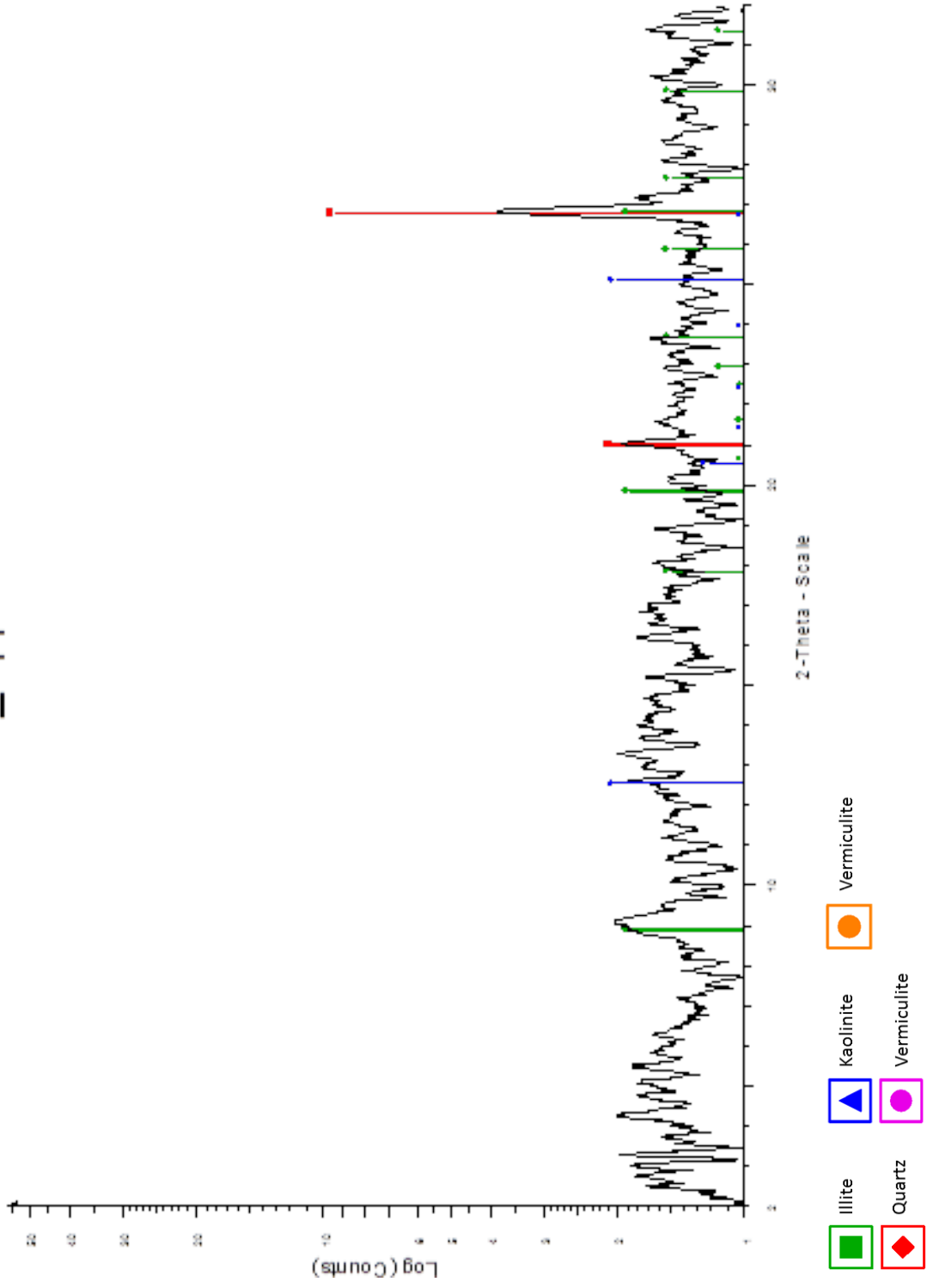
Location	Morphotype	Canopy Height (mm)	Primary Elements					
			Number	Average Length (mm)	Average Width (mm)	Surface Area (mm ²)	Volume (mm ³)	SA/V (mm ² ·l ⁻¹)
Zuun-Arts Fm, Zavkhan Province, Mongolia	shrub	0.22	1	3.2	0.22	2.286548	0.1215808	18.80681818
Zuun-Arts Fm, Zavkhan Province, Mongolia	shrub	0.31	6	4.398	0.31	4.4318902	0.331778523	13.35797797

Appendix J: XRD patterns

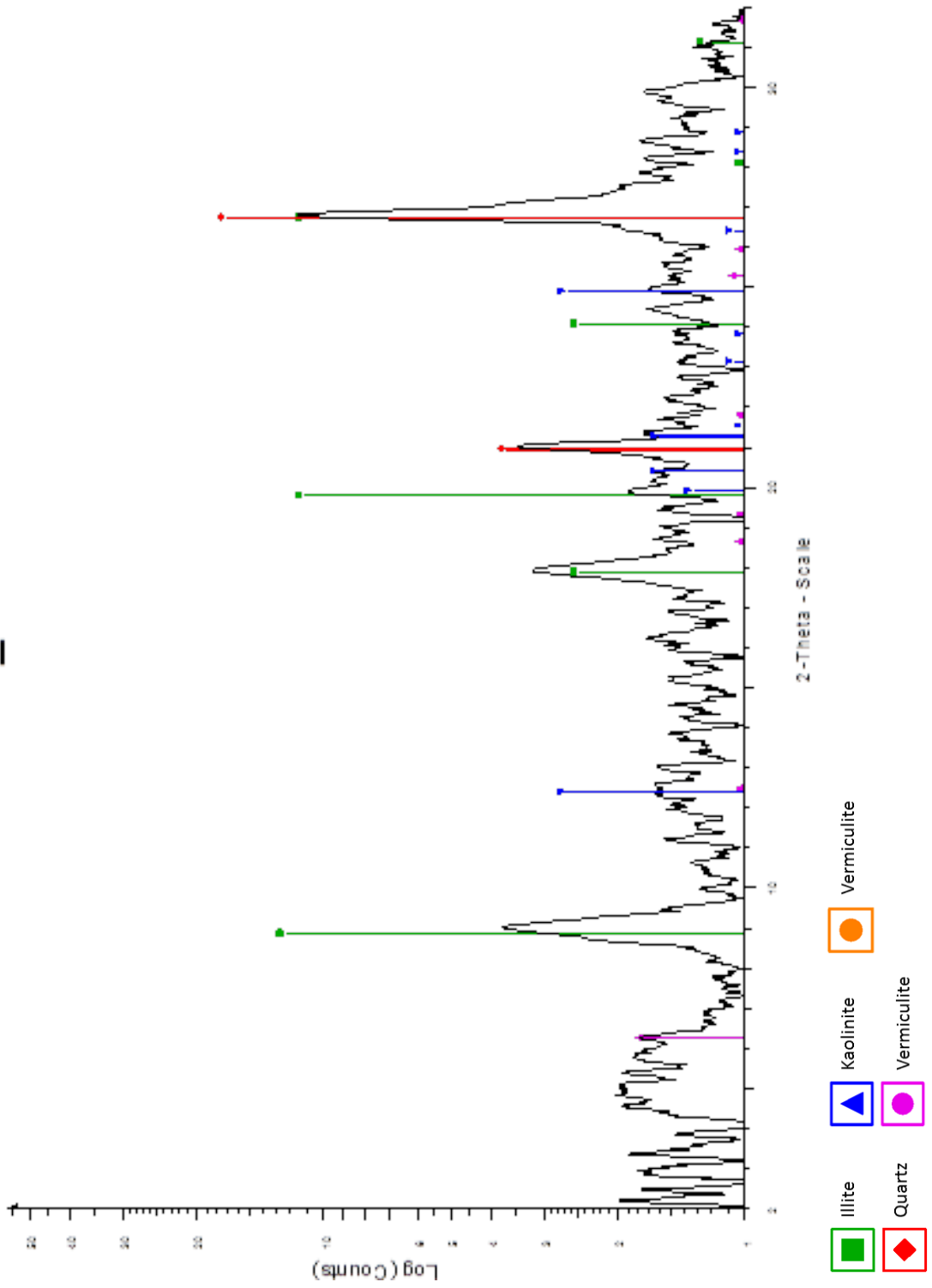
upper



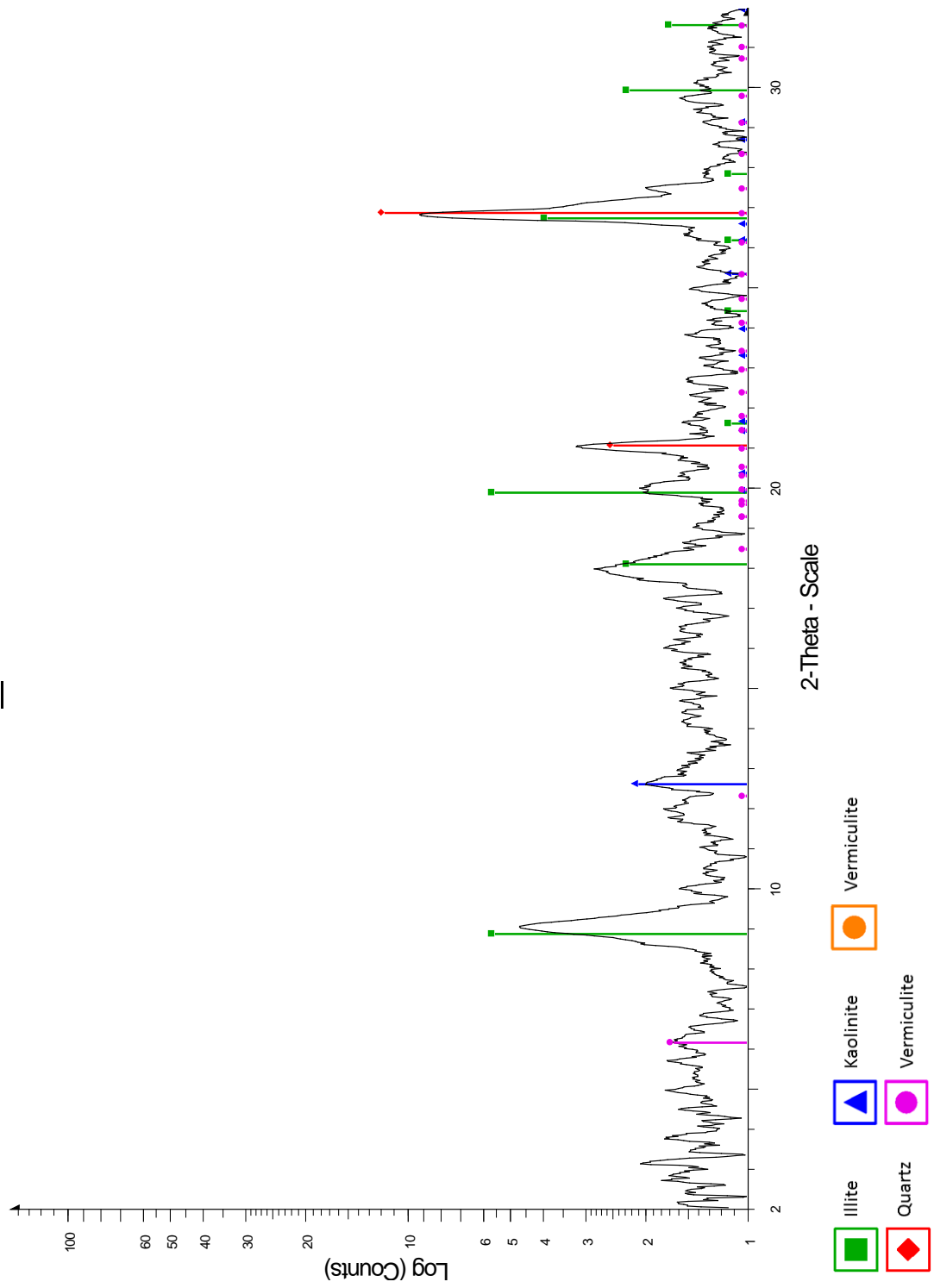
ZA_UpperEG



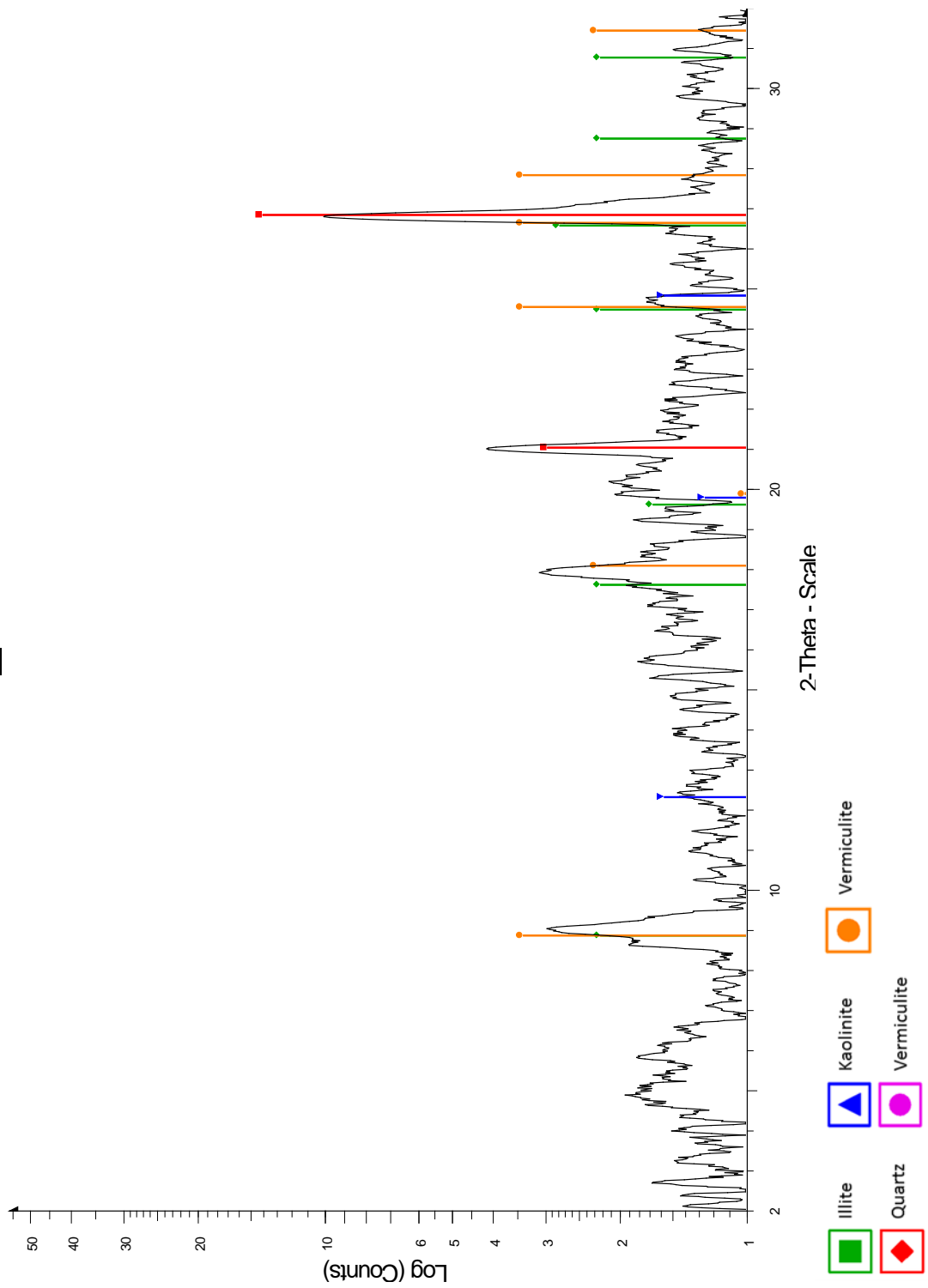
ZA_378



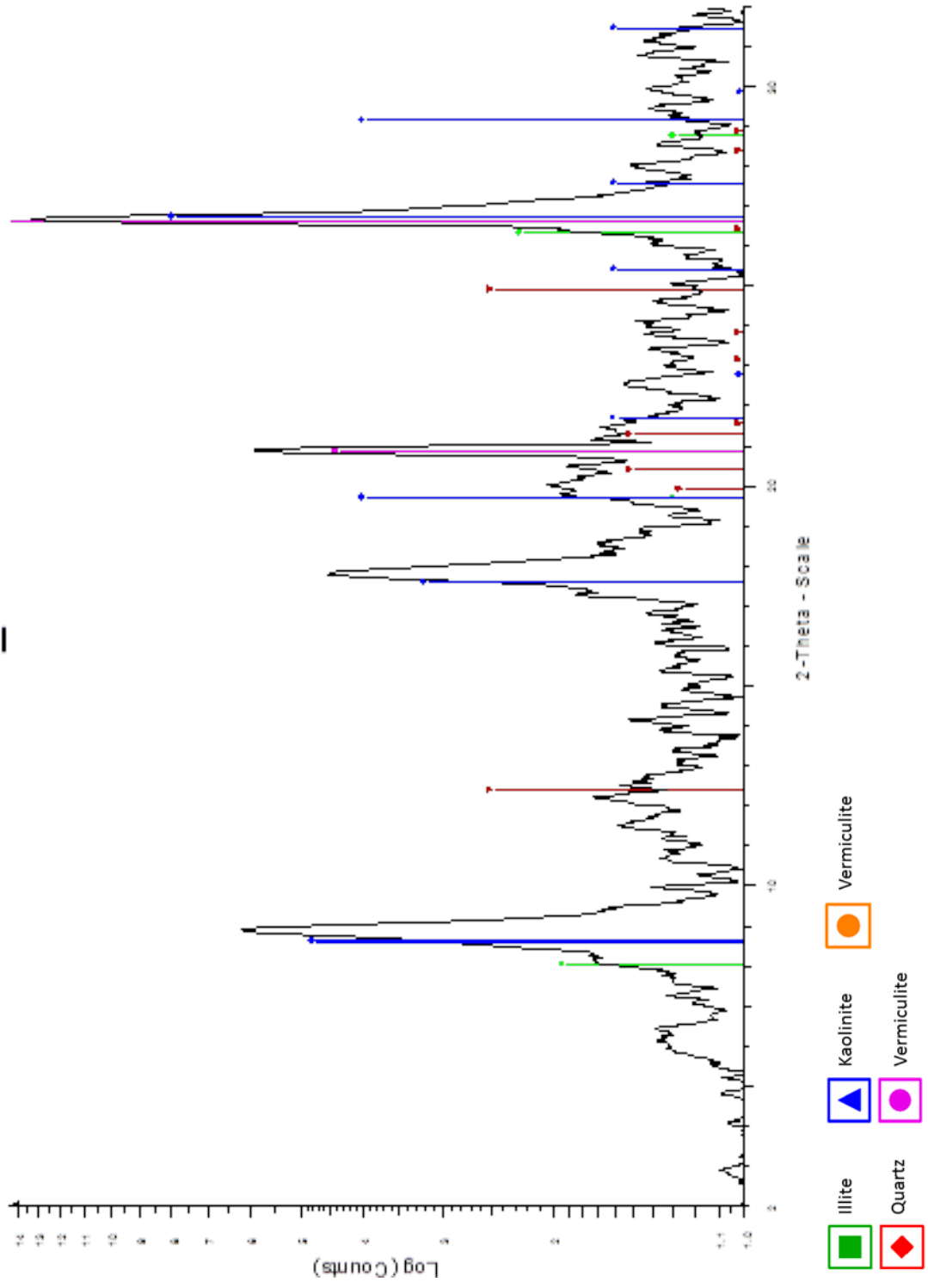
ZA_378EG



ZA_173



ZA_17



ZA_22

